NASA CR-134865
PWA-5263

FINAL REPORT
EVALUATION OF POWDER METALLURGY SUPERALLOY DISK MATERIALS

by

D. J. Evans

August 1975

PRATT & WHITNEY AIRCRAFT
DIVISION OF
UNITED TECHNOLOGIES CORPORATION

prepared for

NATIONAL AERONAUTICS AND SPACE ADMINISTRATION

NASA Lewis Research Center
Contract NAS 3-15841

1. Report No.	2. Government Accession No.	3. Recipient's Catalog No.
NASA CR-134865		

4. Title and Subtitle	5. Report Date
EVALUATION OF POWDER METALLURGY SUPERALLOY DISK MATERIALS	August 1975
	6. Performing Organization Code

7. Author(s)	8. Performing Organization Report No.
D. J. Evans	PWA-5263
	10. Work Unit No.

9. Performing Organization Name and Address	11. Contract or Grant No.
United Technologies Corporation Pratt & Whitney Aircraft Division East Hartford, Connecticut 06108	NAS3-15841
	13. Type of Report and Period Covered Contractor Report

12. Sponsoring Agency Name and Address	14. Sponsoring Agency Code
National Aeronautics and Space Administration Washington, D.C. 20546	

15. Supplementary Notes

Project Manager, Fredric H. Harf, Research Advisor, Robert L. Dreshfield, Materials and Structures Division, NASA Lewis Research Center, Cleveland, Ohio 44135

16. Abstract

A program was conducted to develop nickel-base superalloy disk material using prealloyed powder metallurgy techniques. The program included fabrication of test specimens and subscale turbine disks from four different prealloyed powders (NASA-TRW-VIA, AF2-1DA, Mar-M-432 and MERL 80). Based on evaluation of these specimens and disks, two alloys (AF2-1DA and Mar-M-432) were selected for scale-up evaluation. Using fabricating experience gained in the subscale turbine disk effort, test specimens and full scale turbine disks were formed from the selected alloys. These specimens and disks were then subjected to a rigorous test program to evaluate their physical properties and determine their suitability for use in advanced performance turbine engines. A major objective of the program was to develop processes which would yield alloy properties that would be repeatable in producing jet engine disks from the same powder metallurgy alloys. The feasibility of manufacturing full scale gas turbine engine disks by thermomechanical processing of pre-alloyed metal powders was demonstrated. AF2-1DA was shown to possess tensile and creep-rupture properties in excess of those of Astroloy, one of the highest temperature capability disk alloys now in production. It was further determined that metallographic evaluation after post-HIP elevated temperature exposure should be used to verify the effectiveness of consolidation of hot isostatically pressed billets.

17. Key Words (Suggested by Author(s))	18. Distribution Statement
Powder metallurgy, Hot isostatic pressing Superalloys, Thermomechanical processing, High temperature alloys, Turbine disk, prealloyed powder, Nickel base alloys.	Unclassified

19. Security Classif. (of this report)	20. Security Classif. (of this page)	21. No. of Pages	22. Price*
Unclassified	Unclassified	121	$5.25

* For sale by the National Technical Information Service, Springfield, Virginia 22151

FOREWORD

This report, was prepared for the National Aeronautics and Space Administration Lewis Research Center under Contract NAS3-15841. It presents the results of a program conducted to develop nickel-base superalloy disk material using prealloyed powder metallurgy techniques.

Appreciation is expressed for the contributions made by Mr. Frederic H. Harf Project Manager and Mr. Robert L. Dreshfield, Research Advisor of the Materials and Structures Division of the NASA Lewis Research Center.

TABLE OF CONTENTS

LIST OF ILLUSTRATIONS

LIST OF ILLUSTRATIONS (Cont'd)

LIST OF ILLUSTRATIONS (Cont'd)

LIST OF ILLUSTRATIONS (Cont'd)

LIST OF ILLUSTRATIONS (Cont'd)

LIST OF TABLES

LIST OF TABLES (Cont'd)

LIST OF TABLES (Cont'd)

1.0 SUMMARY

The objective of this program was to produce a high strength, high temperature disk material, suitable for operation in a gas turbine engine at temperatures up to 760°C (1400°F) using suitable thermomechanical processing (TMP) of prealloyed, nickel-base superalloy powders. The goals of this program were 1700 MN/m^2 (250,000 psi) yield strength and 2150 MN/m^2 (312,000 psi) ultimate tensile strength at room temperature, and 1550 MN/m^2 (225,000 psi) yield strength and 1850 MN/m^2 (268,000 psi) ultimate tensile strength at 650°C (1200°F). In addition, creep and creep-rupture goals of less than 0.2 percent creep in 100 hours and rupture in 1000 hours at 650°C (1200°F) at a stress of 1035 MN/m^2 (150,000 psi) were established. The program was divided into two tasks: Task I included qualification and selection of alloys, and Task II was a scale-up study and evaluation of the selected alloys.

Four alloys were selected for screening evaluation in Task I. Two, Mar-M-432 and NASA-TRW-VIA, are very high strength cast alloys which showed potential for fabrication into powder metallurgy wrought products. The third alloy, AF2-1DA, was the highest strength wrought alloy available at the time, and the fourth alloy, designated MERL 80, is an experimental, high tantalum content (ten percent, by weight) alloy developed by Pratt & Whitney Aircraft, and showed potential in subscale tests for meeting program goals. Production powder heats of each of the four alloys were produced by vacuum atomization, and were subsequently screened to -60 +400 mesh particle size range.

Powder consolidation was accomplished by hot isostatic pressing (HIP) at 1150°C (2100°F) and 103.5 MN/m^2 (15,000 psi). Subscale sections of the consolidated billets were upset forged isothermally on heated dies, using a variety of temperatures and strain rates of 0.1 and 0.5 min^{-1} to establish TMP conditions for the 0.152 m (six inches) diameter by 0.152m (six inches) high Task I billet forgings. One billet for each alloy was forged at 0.1 and at 0.5 min^{-1} at temperatures selected to retain as much work as possible. Mechanical property screening tests consisted of tensile tests at room temperature and 650°C (1200°F), and creep-rupture tests conducted at 650°C (1200°F) at a stress of 1035 MN/m^2 (150,000 psi). Results of these tests showed that none of the alloy/process combinations evaluated met the program goals.

A series of subscale TMP studies were conducted to improve tensile and creep-rupture properties. These subscale pieces were forged on heated dies at strain rates to 5.0 min^{-1}, and included partial solution treatments to increase creep-rupture properties by coarsening grain size. Both tensile and creep properties showed improvement; however, forging stresses increased greatly with the increase in strain rate. There was also an increased tendency for cracking at the higher strain rates. Based on the best combination of tensile and creep strengths plus better ductility, AF2-1DA and Mar-M-432 were selected for the Task II scale-up study and evaluation.

In Task II, one full scale forging billet of each alloy was produced by HIP vacuum-atomized powder at 1177°C (2150°F) and 103.5 MN/m^2 (15,000 psi). These billets were then isothermally forged at 0.1 min^{-1} strain rate, at 1093°C (2000°F) for Mar-M-432 and 1135°C (2075°F) for AF2-1DA. The latter alloy yielded a sound forging, while severe cracking

occurred in the Mar-M-432 disk, and that disk was not, therefore, evaluated for mechanical properties. Comparison of the Mar-M-432 billet slices removed prior to forging with sections taken after forging led to a significant finding. The microstructure as-consolidated appeared fully dense, while that of the forging was very porous. This difference may be explained by assuming that a minor container leak during the initial cold pressurization in the HIP cycle caused a small volume of helium to be admitted to the container. This did not prevent initial densification, but upon subsequent thermal exposure created porosity which led to cracking during forging.

Microstructural and mechanical property evaluation of the partial solution treated and aged AF2-1DA disk was performed. Evaluation included sections of the disk exposed for 1500 hours at temperatures of 650 and 705°C (1200 and 1300°F). No evidence of phase instability was noted either microstructurally or in mechanical property tests.

Mechanical property evaluation of the full scale AF2-1DA disk included tensile (smooth and notched), creep and creep-rupture, low cycle fatigue, and fatigue crack growth rate. Results indicated an improvement in strength relative to Task I properties, although strengths remained below program goals. The tensile and creep strengths of TMP AF2-1DA are better, however, than the currently employed, high temperature nickel-base disk alloy, Astroloy.

2.0 INTRODUCTION

The objective of this program was to develop nickel-base superalloys, produced by prealloyed powder techniques, for use in turbine engine disks operating between room temperature and 760°C (1400°F) and having properties considerably exceeding those of conventional, wrought superalloys presently used.

2.1 BACKGROUND INFORMATION

The increased performance requirements of advanced gas turbine engines will demand improved strength disk materials capable of operating at higher temperatures. These superior disk alloys must possess sufficient stability to retain their improved properties after extended operation under more stringent conditions. Specifically, higher engine performance requirements can be translated into higher burst or tensile strengths in the relatively cooler disk bore, and higher creep strength at the hotter disk rim. After accomplishing improvements in bore tensile strengths and rim creep strengths, it is also imperative that reasonable levels of ductility, low cycle fatigue (LCF) resistance, and fracture toughness be maintained.

The increased performance and uniform property levels in ultra-high strength nickel-base superalloys are functions of the alloy composition, the uniformity of the alloying constituents, and the dislocation substructure present in the alloy. Physical metallurgy principles and state-of-the-art knowledge allow the selection of appropriate alloying additions which will improve solid solution strengthening and precipitation hardening. Uniform properties can be achieved by the use of prealloyed metal powders which contain more uniformly distributed alloying constituents. Further property improvements can be obtained through the addition of a stabilized dislocation substructure achieved through thermomechanical processing and precipitation heat treatment.

The use of metal powders to obtain chemically and metallurgically uniform structures for critical rotating gas turbine hardware has been gaining acceptance with the advent of high purity, prealloyed superalloy powders, and the development of suitable consolidation techniques, such as hot isostatic pressing (HIP), (a densification process combining simultaneous application of high temperature and isostatic gas pressure), and extrusion, which can achieve 100 percent theoretical densities. Advanced gas turbine disk designs are requiring property levels well in excess of present material properties, thus necessitating the development of new alloys; however, conventional casting and forging practice, when applied to these alloys, has not been fully successful in achieving the required improvements. Gross casting segregation and inconsistent properties again have given impetus to consideration of consolidated prealloyed metal powders as a means of circumventing the problem of present material properties and casting and forging practices not being adequate for future demands.

2.2 SCOPE AND PURPOSE OF THE PROGRAM

The program to develop nickel-base superalloys using prealloyed powder metallurgy techniques was conducted under Contract NAS3-15841. The program included fabrication of test specimens and subscale turbine disks from four different prealloyed powders. Based on evaluation of these specimens and disks, two alloys were selected for scale-up evaluation. Using fabricating experience gained in the subscale turbine disk effort, test specimens and full scale turbine disks were formed from the selected alloys. These specimens and disks were then subjected to a rigorous test program to evaluate their physical properties and determine their suitability for use in advanced performance turbine engines. A major objective of the program was to develop processes which would yield consistent alloy properties that would be repeatable in producing jet engine disks from the same powder metallurgy alloys.

2.3 APPROACH TO ACHIEVING PROGRAM OBJECTIVES

The program was divided into two tasks:

- Task I encompassed the qualification and selection of alloys
- Task II included the scale-up study and evaluation

In Task I, four candidate alloys (NASA-TRW-VIA, Unitemp AF2-1DA, MERL 80, and Mar-M-432) were selected for study. Mar-M-432 and NASA-TRW-VIA are high strength cast alloys which showed potential for fabrication into powder metallurgy wrought products. AF2-1DA was the highest strength wrought alloy available at the time the program was conducted. MERL 80 is an experimental, high tantalum content alloy developed by P&WA which showed potential in subscale tests for meeting program goals.

Prealloyed powders were produced from the alloys and analyzed for particle size, chemical purity, and foreign particle inclusions. Quantitative analysis was conducted to determine the final composition of the alloys. To prevent contamination, the powders were handled under a vacuum until after the consolidation process.

Each of the powders was consolidated into billets using HIP techniques. The structure and density of the billets was determined and each alloy was chemically analyzed and the gamma prime or eta solvus temperatures determined. Prior to forging the billets into subscale disks, optimum forging temperatures for each alloy were established empirically by testing subsize billets. The subscale disks were then forged and sonically inspected for soundness and the density of each disk was determined.

Physical properties of each alloy in its final form were determined. Tensile and creep-rupture tests were conducted under a variety of temperature conditions. At each stage of processing, the alloys were metallographically examined by optical techniques to determine structure.

At the end of Task I, two alloys were selected for scale-up study and evaluation. The para-

meters for selecting the alloys for Task II were ultimate tensile strength, yield strength, elongation, creep, rupture life, phase stability, and fabricability.

Task II, Scale-Up Study and Evaluation, was structured similar to Task I. However, in Task II a more extensive property evaluation of the two alloys selected was conducted and full-size rather than subscale turbine disks were forged using techniques developed during Task I. The number of tests conducted on each alloy was increased and LCF characteristics were determined. Microstructural examination was expanded to include both optical and electron micrographs as well as identification of the phases present by X-ray diffraction.

This report presents a description of the fabrication processes and test procedures used throughout the program and documents the results and data obtained.

3.0 TASK I

ALLOY QUALIFICATION AND SELECTION

In Task I, four nickel-base alloys, NASA-TRW-VIA, AF2-1DA, MERL 80, and Mar-M-432 were prepared using powder metallurgy techniques. The powdered metals were compacted and then forged to produce subscale gas turbine engine disks. The physical properties of the disks were then evaluated. Based upon this evaluation two of the alloys were selected for scale-up and more extensive evaluation to be conducted under Task II of the program. Figure 3.0-1, a flow chart, outlines the alloy processing and evaluation sequence followed during Task I.

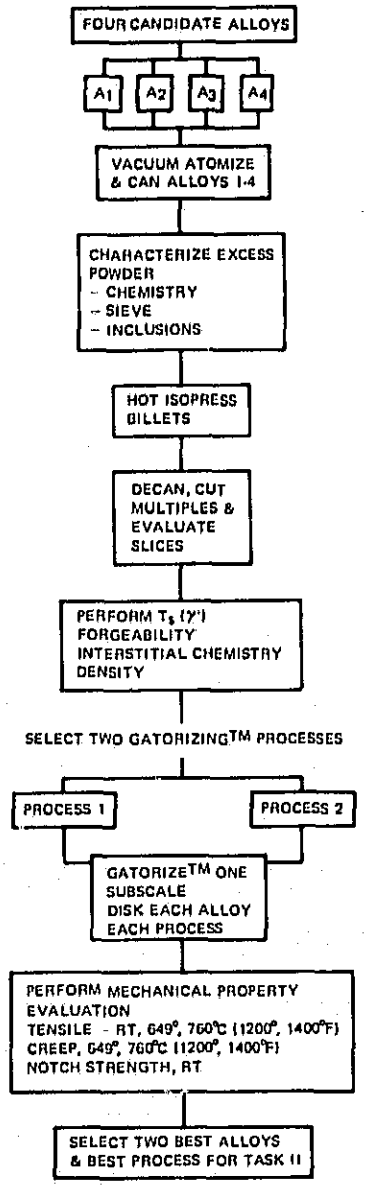

Figure 3.0-1 Task I Alloy and Process Selection

3.1 MATERIAL

Bar stock from virgin master alloy heats of the candidate materials, NASA-TRW-VIA, AF2-1DA, MERL 80 and Mar-M-432 was remelted in vacuum induction furnaces at P&WA to provide optimum alloy purity for conducting this program. This additional refining operation reduced trace element impurities such as sulfur and phosphorus as well as heavy, volatile elements such as lead, bismuth and cadmium. Presence of these elements in the alloys could reduce the ductility of the final product. One 9.09 kg (20 lb) and six 22.75 kg (50 lb) heats of remelt stock of each of the four program alloys were cast into water-cooled, 0.08m (3 inch), copper molds. The top 0.025m (1 in.) of each casting was trimmed to remove gross shrinkage, and the exterior surfaces were ground to remove flash and any thin layers of copper which had been picked up from the molds. Each of the remelt alloys were chemically analyzed, the results of which are presented in Table 3.1-I.

3.1.1 Vacuum Atomization

Homogeneous Metals, Inc., Herkimer, New York was selected to convert the remelt stock to powder because of their capability to produce the required homogeneous powder which would be free from argon-related, thermally-induced porosity (TIP). Homogeneous Metals, Inc. is equipped to process the atomized powder through collection, screening, blending, and canning under all-inert conditions. Use of nitrogen cover gas again precludes the possibility of subsequent thermally-induced porosity formation by avoiding exposure to inert, non-reactive gases such as argon.

The powder was produced by a vacuum/hydrogen process which uses a double chamber vacuum melting and atomizing apparatus. In the lower chamber, the remelt stock is induction melted under vacuum. When the desired degree of superheat, i.e., melt fluidity, is achieved, the melting chamber is back-filled with a positive pressure of a gas which is soluble in the molten alloy. In the case of nickel-base superalloys, the gas used is hydrogen. After pressurizing and saturating the melt with hydrogen, the molten metal is raised to contact a ceramic tube leading to the upper atomizing chamber, which has been previously evacuated to approximately ten torr. A valve, separating the two chambers is opened and the molten metal rushes up the ceramic transfer tube into the atomizing chamber where the rapid expansion of the hydrogen gas causes fractionation into minute droplets. The droplets loose heat by radiation in the vacuum and solidify into prealloyed powder.

Two alloys, NASA-TRW-VIA and MERL 80, included hafnium among their constituent elements. However the master alloys of these materials did not include the hafnium. The hafnium was added separately during the atomization process to reduce the possibility of the hafnium reacting with the ceramic melting crucible and the consequent formation of impurities. The hafnium was added by wrapping it in aluminum foil and suspending it by a 80 Ni-20 Cr wire just above the molten bath. Just prior to atomization the hafnium was submerged in the bath in a manner designed to allow time for adequate homogeneity while minimizing reaction time between the hafnium and the ceramic crucible shell. The aluminum added from the foil was insignificant.

Each alloy was atomized in two runs, melting approximately 82 kg (180 pounds) in each run. The charge for the first run consisted entirely of remelt stock, and the resultant powder was screened under a protective nitrogen atmosphere to separate the -20+60 mesh fraction (-20 indicates that the powder will pass through a mesh screen having 20 openings per linear inch; +60 indicates that the powder will not pass through a mesh screen having 60 openings per linear inch.) and the -60 mesh fraction for subsequent canning prior to consolidation. The -20+60 mesh powder fraction plus the solidified "heel" remaining in the melting crucible were then charged along with the remaining remelt stock in the second atomization run for each alloy. This procedure was employed to ensure adequate yield of -60+400 mesh powder for consolidation.

3.1.2 Chemical Analyses of Powders and Alloys

Samples of each powder lot were subjected to thorough characterization including chemical analysis, cross sectional metallography, particle size distribution, and inclusion inspection of vacuum hot pressed powders.

Metallographic examination of the loose powders was accomplished by mounting a representative sample of loose powders in epoxy resin and mechanically polishing using silicon carbide grinding papers, followed by diamond paste and alumina fine polishing compounds. Polished specimens were etched with Kalling's reagent and examined at 100X, 500X, and 1000X magnification.

Results of this examination showed that the particles exhibited a dendritic solidification pattern typical of a nickel-base superalloy microcasting (Figures 3.1-2 through 3.1-5) and that screening of the powder to remove the +60 mesh fraction essentially eliminated occurrence of hollow powder particles. The microstructures are typical of prealloyed nickel-base superalloy powder and show a uniform, homogeneous as-atomized structure. Carbides are seen to be finely distributed throughout the particles which shows that the desired homogeneity in using prealloyed powders was achieved. Only an occasional instance of secondary particle agglomeration was noted. Particle agglomeration appeared to be of no consequence to subsequent processing.

Particle size distributions were determined for the Mar-M-432 and AF2-1DA powder samples which had been screened by the powder supplier to -60 mesh. It was originally anticipated that there would be only one to five percent of -400 mesh powder based on previous experience with similar alloys of high refractory alloy content. As shown in Figure 3.1-6, the -400 mesh fraction amounted to 12.87 percent for the AF2-1DA and 16.60 percent for Mar-M-432. The supplier was directed to screen out the -325 mesh fraction and determine whether a sufficient yield of powder would be available for the required compaction.

This screening was performed for Mar-M-432 and AF2-1DA, and the resultant yield was sufficient to produce the Task I subscale disk forgings.

Particle size distributions determined for NASA-TRW-VIA and MERL 80 powders also indicated greater than 15 percent of -400 mesh powder (Figure 3.1-7). Homogeneous Metals, Inc. was then directed to rescreen the NASA-TRW-VIA and MERL 80 powders to reach an

upper limit of five percent of -400 mesh particles ("fines"). A sample of these rescreened alloy powders showed that a satisfactory compromise had been reached between reducing the amount of "fines" and maintaining sufficient powder yield to fill the two powder compaction cans.

Particle size distributions were also determined for the four samples of rescreened powders, representing the powder compacted by HIP (Figures 3.1-8 and 3.1-9). The NASA-TRW-VIA and MERL 80 powders showed a reduced amount of -400 mesh powder. The amount of -400 mesh powder present was a determining factor in maintaining the oxygen level of the powder below 100 ppm because small powder particles with their high aggregate surface area may contain a larger quantity of absorbed oxygen than larger particles.

The -20+60 mesh and -325 mesh powder, not canned for hot isostatic compaction, was returned to Pratt & Whitney Aircraft. From this material, an assessment was made of the material utilization from vacuum induction melted remelt stock to atomized powder available for consolidation. This material distribution, by particle size, is given in Table 3.1-II.

A complete chemical analysis of the four as-atomized powder alloys was made. Major elementals were analyzed by atomic absorption, except for refractory metals which were analyzed by X-ray fluorescence. Columbium was cross-checked with wet-chemical techniques. Interstitials (hydrogen, oxygen, and nitrogen) were determined by inert-gas fusion analysis. Table 3.1-III summarizes these results.

In addition, interstitial analyses of -325 mesh samples of each powder alloy were made to determine the effect of increased particle surface area on interstitial content. A comparison of -60 mesh and -325 mesh interstitial contents is presented in Table 3.1-IV. The fine powder (-325 mesh) generally showed a slightly higher amount of nitrogen and hydrogen interstitials and a 50 percent higher occurrence of oxygen when compared to the -60 mesh (nominal) powder. Of particular importance was the apparently high level of oxygen in the as-atomized powder. It ranged from 120 to 170 ppm. This level was considerably higher than typically encountered with gas atomized or vacuum atomized nickel-base alloy powders, which is 30-95 ppm and exceeded the allowable maximum of 100 ppm requirement established for the consolidated billets.

The unusually high oxygen content of the -60 powder (which included approximately 20 percent -325 mesh powder) was probably due to the presence of the -325 mesh "fines". Consequently, it was decided to consolidate the powders and re-evaluate the oxygen content from resulting solid samples in which the inclusion of oxygen absorbed on the surface of the -325 mesh powder would not bias the results.

In order to inspect each powder lot for possible non-metallic inclusions, small amounts of powder were compacted by vacuum hot pressing in 0.025m (1.0 in.) diameter graphite dies. Resultant compacts were approximately 0.019m (0.75 in.) high. These were polished on one end to give an area of 5.064×10^{-4} m^2 (0.785 $in.^2$) for inclusion examination. Metallographic examination of the vacuum hot pressed powders revealed no harmful non-metallic inclusions.

3.1.3 Canning And Shipping

The container for each alloy powder blend was a 0.177m (7 in.) inner diameter, AISI 1010, aluminum-killed, steel pipe with flat plates tungsten inert gas (TIG) welded on each end. An orifice was provided in one of the plates to allow filling the container and evacuating the atmosphere. The four cans were filled, evacuated and sealed. Each of the cans contained one of the program alloy -60+400 mesh powder. Each can was then placed in a helium-filled drum and the drum sealed. This precaution was taken so that, if a leak occurred in a can, the inert helium gas would be drawn into the can.

The drum enclosed cans were shipped to Pratt & Whitney Aircraft so that the cans could be inspected for leaks. Each can was removed from its drum and placed within a P&WA vacuum dry box, which was evacuated through a standard helium leak detector. Had a leak occurred and helium been drawn into the leaking can, the leak detector's vacuum pumps would evacuate it from the can and the mass spectrometer would sense its presence, confirming the leak. All four cans were thus processed, and none gave evidence of leaking.

The cans were then shipped to Battelle Memorial Institute, Columbus Laboratories for hot isostatic pressing.

TABLE 3.1-I

COMPOSITION OF REMELT STOCK USED FOR ATOMIZATION
(Given in Weight Percent)

	NASA-TRW-VIA		AF2-1DA		MERL 80		Mar-M-432	
Element	Remelt Bar	Limits	Remelt Bar	Limits	Remelt Bar	Limits	Remelt Bar	Limits
Chromium	6.1	5.6–6.6	11.9	11.5–12.5	9.2	9.0–10.0	15.3	15.3–15.8
Cobalt	7.8	6.5–8.5	10.0	9.5–10.5	9.7	9.0–10.0	19.9	19.5–20.5
Aluminum	5.6	5.0–5.8	4.9	4.3–5.0	3.7	3.5–4.0	2.8	2.7–3.0
Titanium	0.94	0.75–1.25	3.1	2.5–3.5	0.96	0.75–1.25	4.4	4.2–4.5
Tantalum	8.8	8.5–9.5	1.9	1.0–2.0	9.85	10.5–11.5	2.0	1.8–2.2
Columbium	0.44	0.25–0.75	–	–	–	–	1.8	1.8–2.2
Tungsten	5.8	5.3–6.3	6.0	5.0–6.0	3.1	3.0–3.5	3.1	2.9–3.1
Molybdenum	1.9	1.5–2.5	3.0	2.5–3.5	1.3	1.0–1.5	–	–
Rhenium	0.25	0.1–0.7	–	–	–	–	–	–
Hafnium	*	0.2–0.7	–	–	*	0.9–1.1	–	–
Zirconium	0.06	0.05–0.15	0.11	0.05–0.15	0.36	0.25–0.35	0.04	0.03–0.07
Carbon	0.19	0.08–0.18	0.38	0.3–0.4	0.16	0.10–0.15	0.16	0.12–0.18
Boron	0.016	0.012–0.024	0.012	0.010–0.020	0.017	0.015–0.025	0.013	0.012–0.020
Manganese	–	0.2 max	0.001	0.2 max	<0.001	0.2 max	0.001	0.1 max
Silicon	0.03	0.2 max	0.06	0.2 max	0.03	0.2 max	0.04	0.1 max
Oxygen	–	0.01 max	0.0030	0.01 max	–	0.01 max	–	0.01 max
Nickel	Balance	Balance	Balance	Balance	Balance	Balance	Balance	Balance

*Not added to remelt stock

TABLE 3.1-II

MATERIAL UTILIZATION BY PARTICLE SIZE

Item	Alloy AF2-1DA Kg	AF2-1DA Lb	Mar-M-432 Kg	Mar-M-432 Lb	NASA-TRW-VIA Kg	NASA-TRW-VIA Lb	MERL 80 Kg	MERL 80 Lb
Remelt Stock	144.24	318.0	139.7	308.0	140.39	309.5	137.58	303.31
-20 + 60 Mesh Powder	21.23	46.81	21.04	46.38	35.01	77.19	20.50	45.19
-60 Mesh Sample (for characterization)	1.96	4.31	5.33	11.75	1.42	3.13	1.67	3.69
-60 + 325 Mesh (canned for HIP)	62.99	138.87	62.37	137.5	64.98	143.25	64.72	142.69
-325 Mesh Powder	8.79	19.38	16.41	36.19	3.63	8.0	1.41	31.19
+20 Mesh and Scrap	49.27	108.63	48.17	106.19	35.29	77.81	36.54	80.56

TABLE 3.1-III

CHEMICAL ANALYSES OF AS-ATOMIZED -60 MESH POWDERS
(Given in Percent)

Element	AF2-1DA	Mar-M-432	NASA-TRW-VIA	MERL 80
Chromium	10.0	15.4	6.0	9.0
Cobalt	12.2	20.2	7.4	9.6
Aluminum	4.9	2.6	5.3	3.6
Titanium	2.8	4.2	0.92	0.95
Tantalum	1.5	1.9	9.2	11.2
Columbium	–	2.2	0.60	–
Tungsten	5.6	3.1	5.5	3.0
Molybdenum	3.1	–	1.9	1.2
Rhenium	–	–	0.25	–
Hafnium	–	–	0.47	0.84
Zirconium	0.11	0.06	0.09	0.28
Carbon	0.35	0.18	0.15	0.11
Boron	0.014	0.013	0.015	0.021
Manganese	0.002	0.006	0.002	0.002
Iron	0.06	0.06	0.04	0.05
Silicon	0.06	0.06	0.04	0.05
Sulfur	0.0045	0.0052	0.002	0.002
Phosphorus	0.0240	0.0250	0.0072	0.0081
Lead	<0.0002	<0.0002	<0.0002	<0.0002
Bismuth	<0.00005	<0.00005	<0.00005	<0.00005
Nitrogen	0.0016	0.0025	0.0014	0.0014
Oxygen	0.0120	0.0120	0.0150	0.0150
Hydrogen	–	–	0.0013	0.0011
Nickel	Balance	Balance	Balance	Balance

TABLE 3.1-IV

COMPARISON OF INTERSTITIAL CONTENT FOR -60 AND -325 MESH POWDER
(Content in ppm)

	AF2-1DA		Mar-M-432		NASA-TRW-VIA		MERL 80	
Element	-60	-325	-60	-325	-60	-325	-60	-325
Nitrogen	16	14	25	32	14	17	14	21
Oxygen	120	150	120	170	150	170	150	150
Hydrogen	–	11	–	16	13	17	11	14

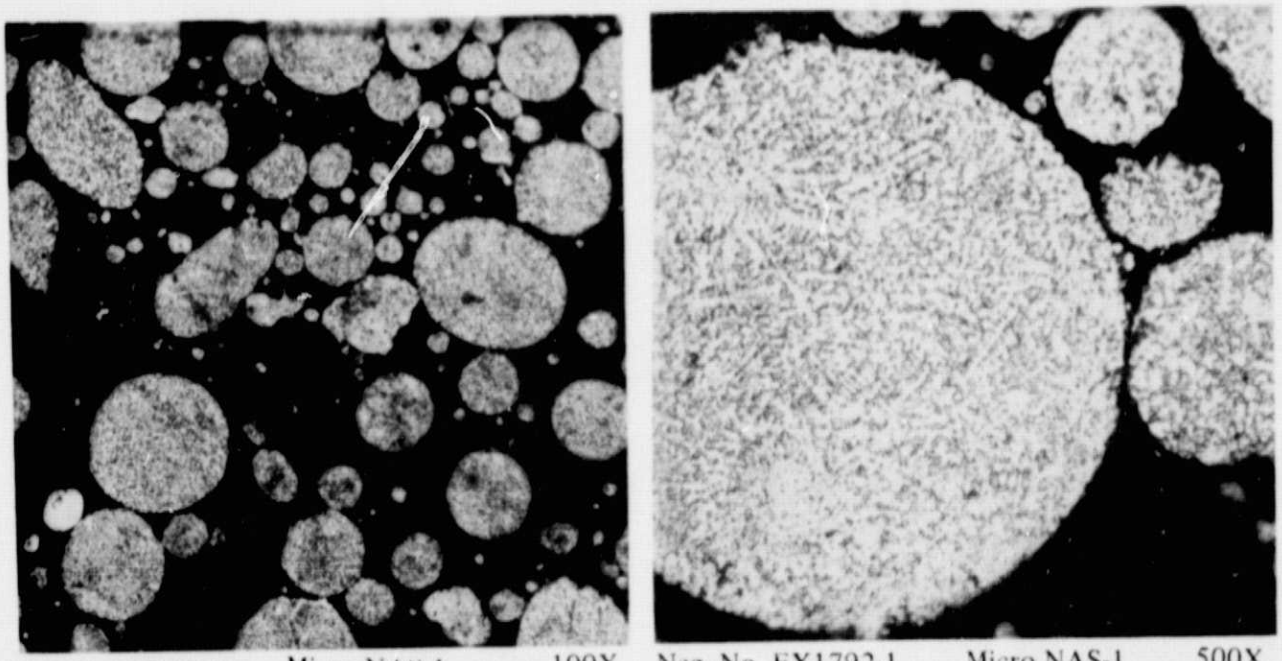

Neg. No. EX1792-7 Micro NAS-1 100X Neg. No. EX1792-1 Micro NAS-1 500X

Figure 3.1-2 Typical Microstructure of As-Atomized Mar-M-432 Alloy Powder
Etchant: Kalling's Reagent

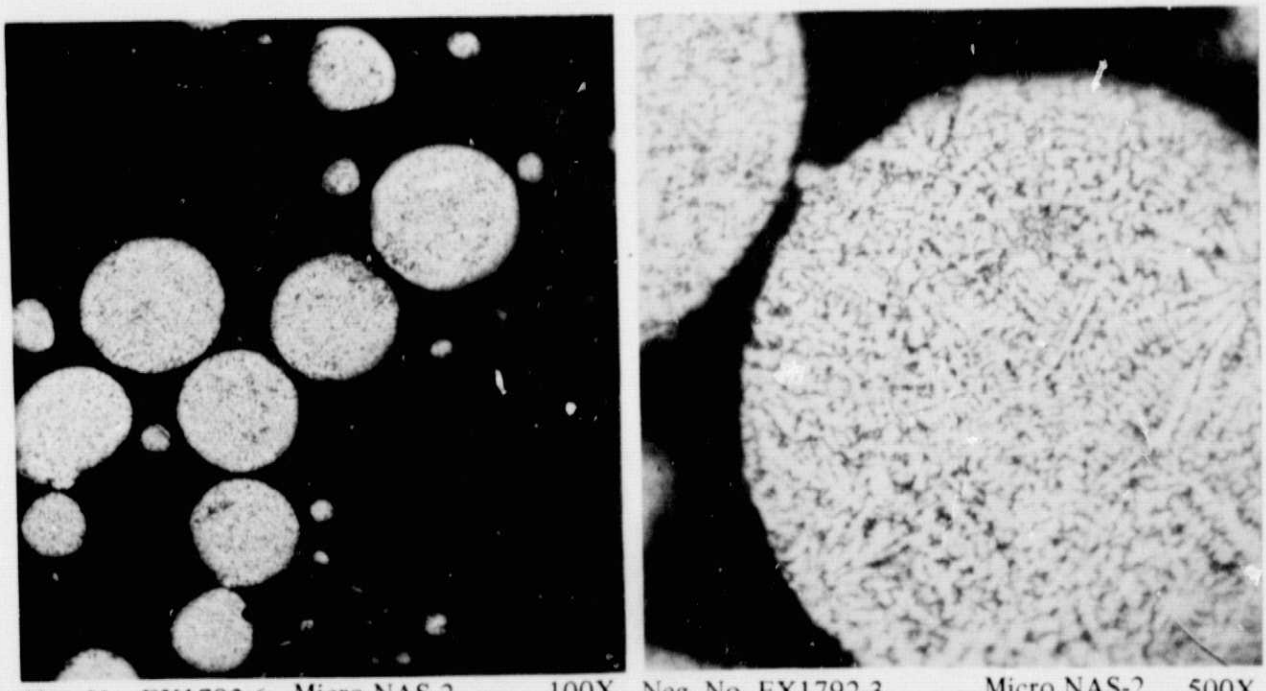

Neg. No. EX1792-6 Micro NAS-2 100X Neg. No. EX1792-3 Micro NAS-2 500X

Figure 3.1-3 Typical Microstructure of As-Atomized AF2-1DA Alloy Powder
Etchant: Kalling's Reagent

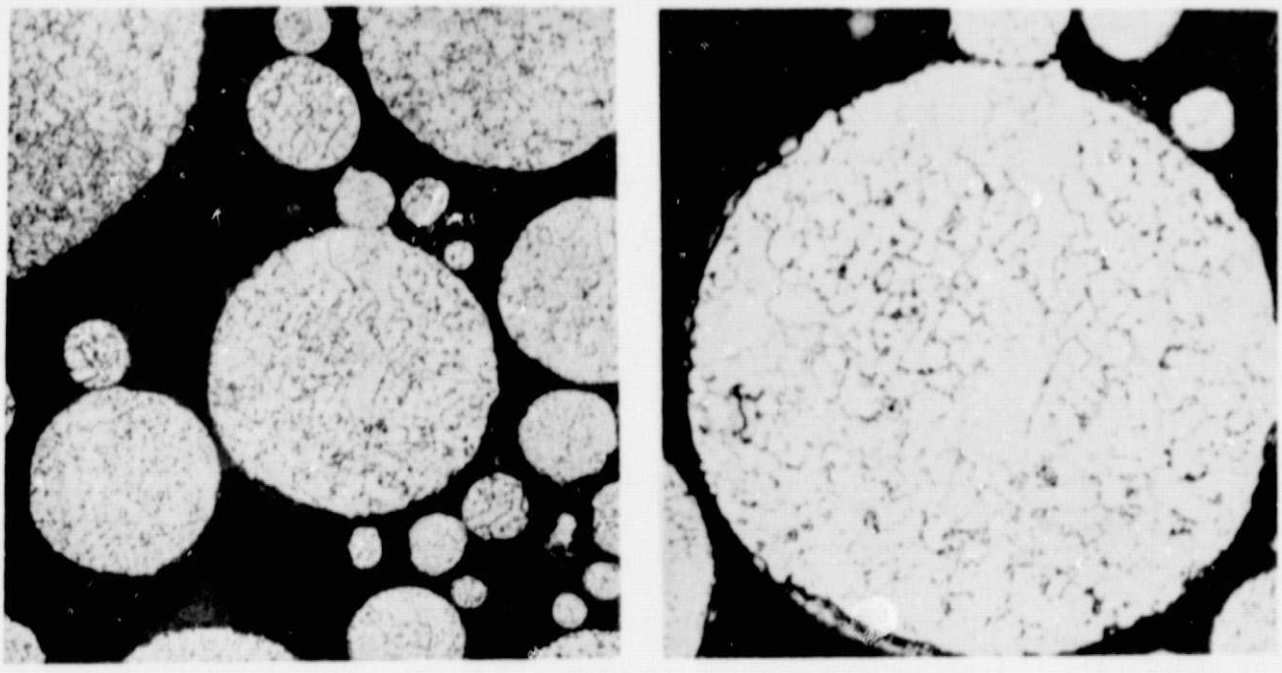

Micro: NASA 9 Mag: 500X Micro: NASA 9 Mag: 1000X

Figure 3.1-4 Typical Microstructure of As-Atomized NASA-TRW-VIA Alloy Powder, Etchant: Kalling's Regent

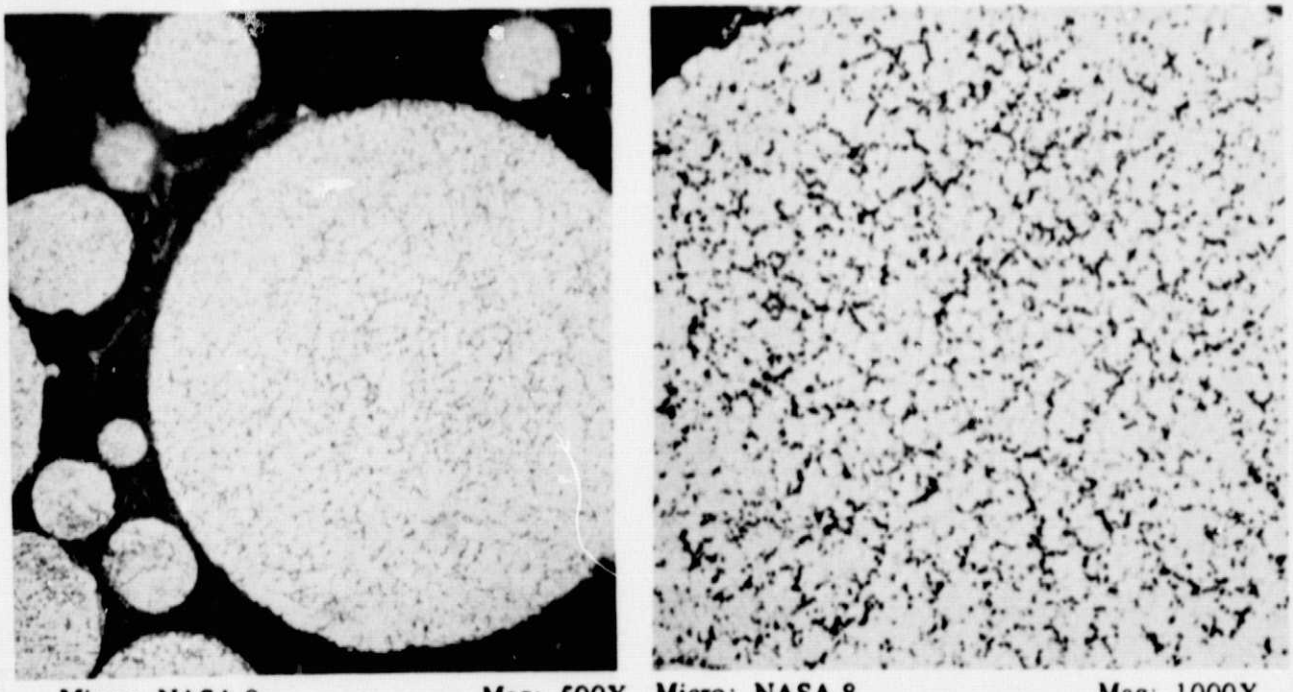

Micro: NASA 8 Mag: 500X Micro: NASA 8 Mag: 1000X

Figure 3.1-5 Typical Microstructure of As-Atomized MERL-80 Alloy Powder, Etchant: Kalling's Reagent

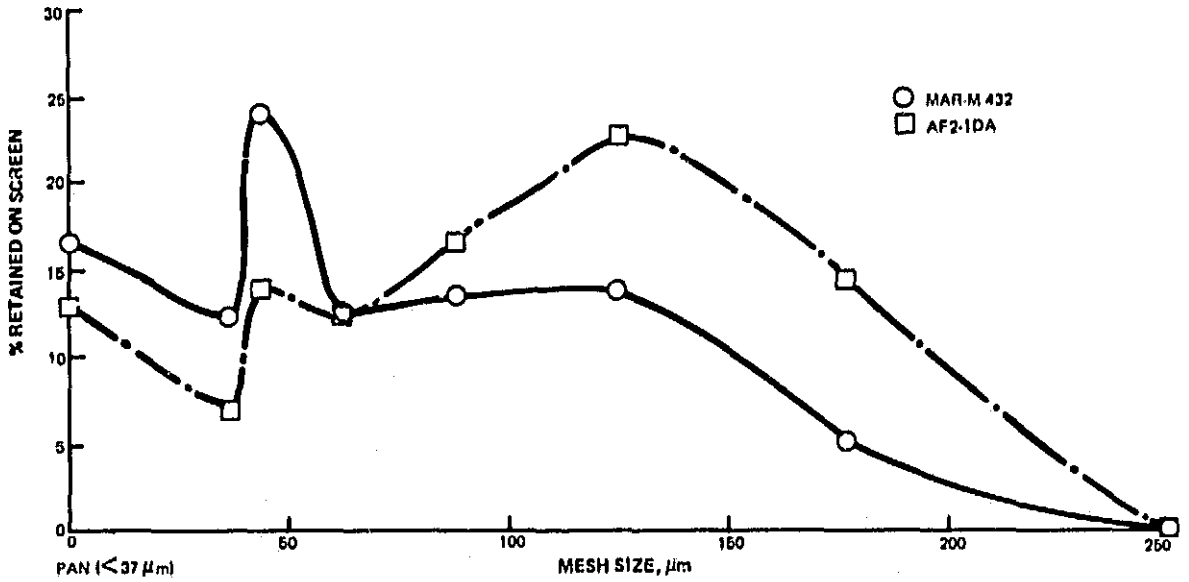

Figure 3.1-6 Particle Size Distribution Curves for Mar-M432 and AF2-1DA -60 Mesh Powder Samples

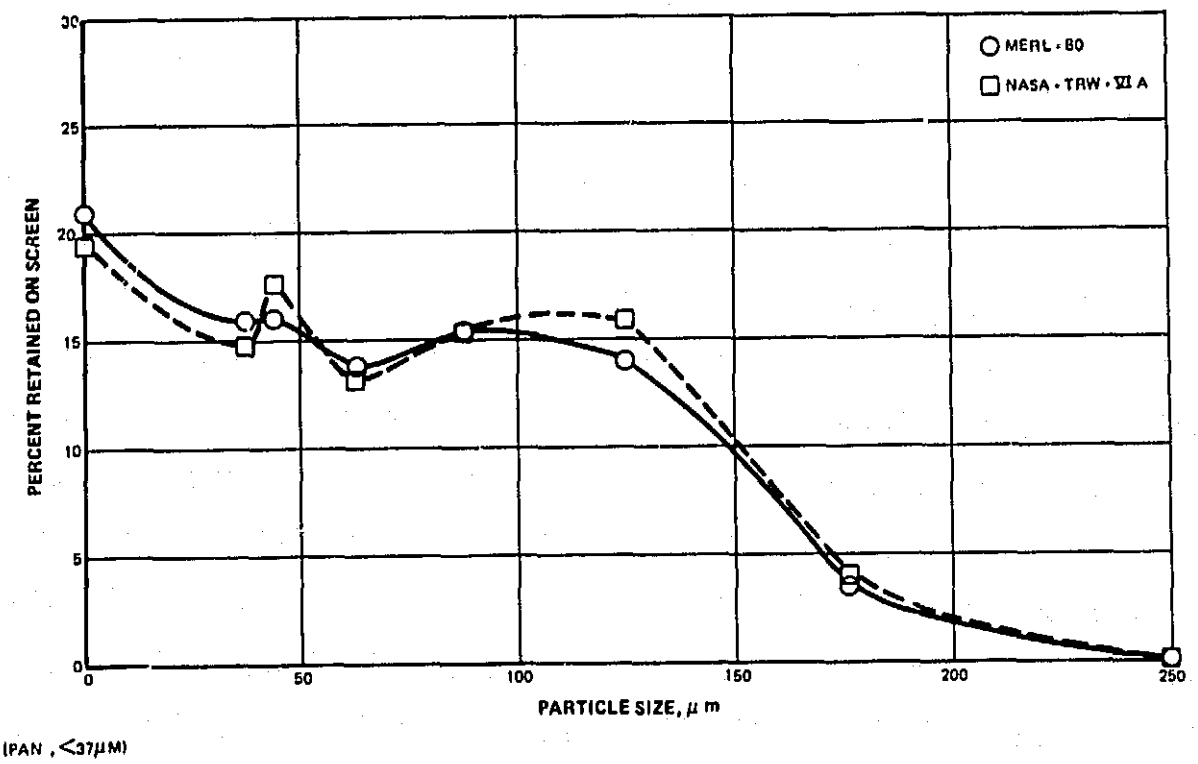

Figure 3.1-7 Particle Size Distribution Curves for NASA-TRW-VIA and MERL-80 -60 Mesh Powder Samples

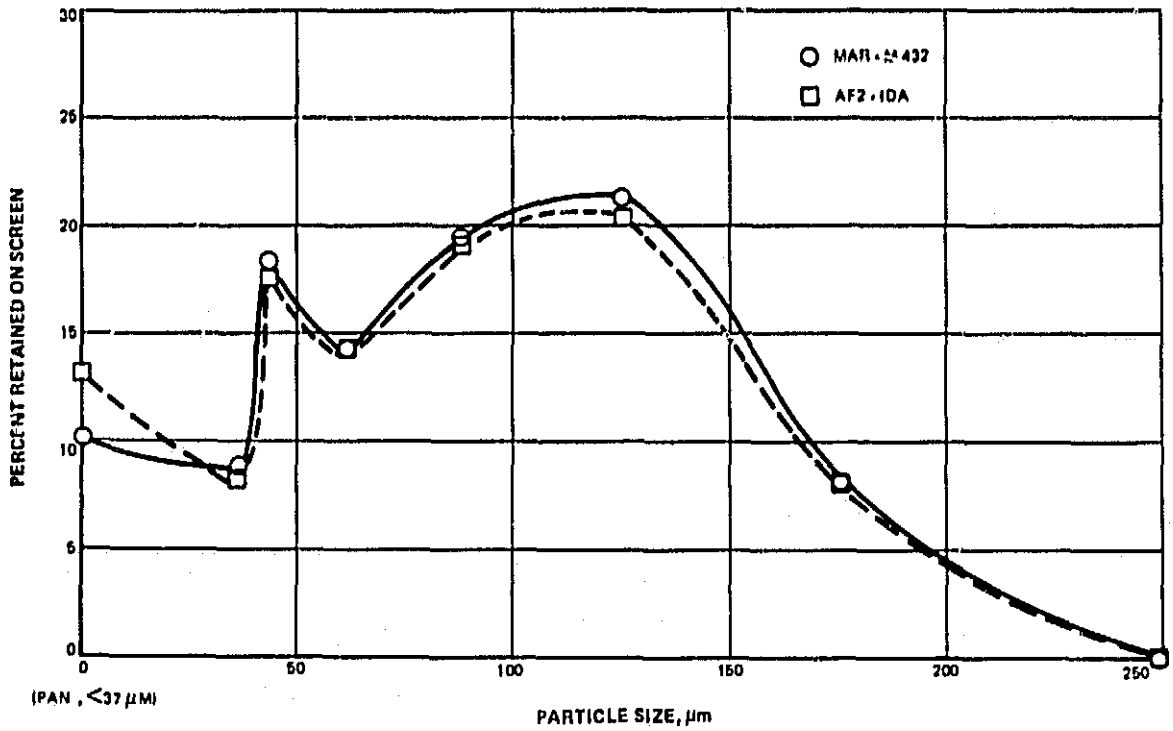

Figure 3.1-8 Particle Size Distribution Curves for Rescreened Mar-M432 and AF2-1DA Powder Samples

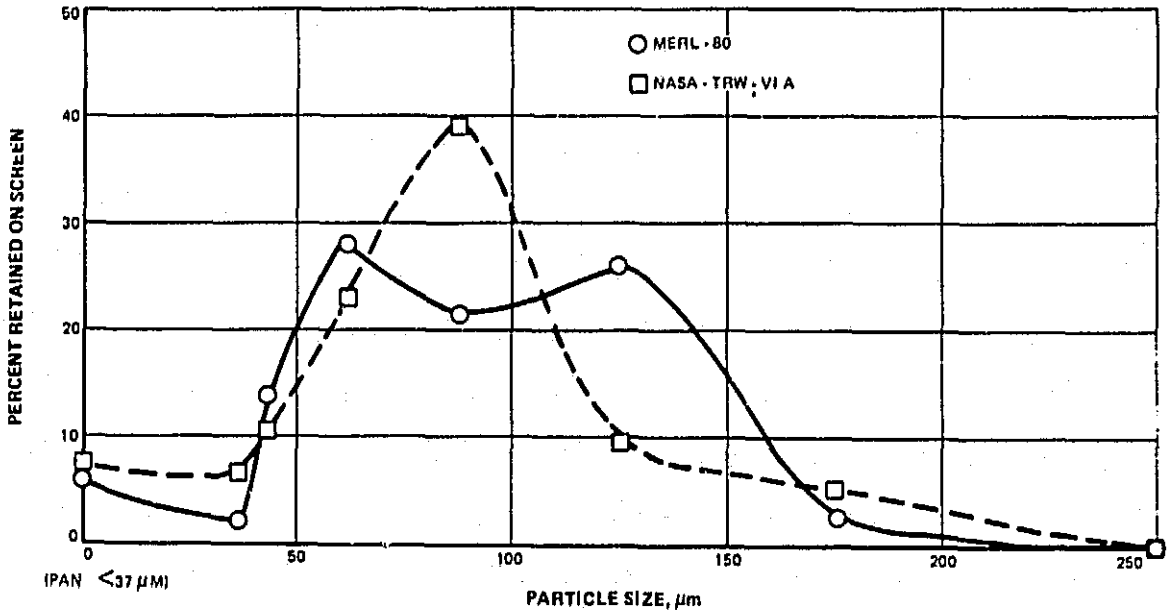

Figure 3.1-9 Particle Size Distribution Curves for Rescreened NASA-TRW-VIA and MERL-80 Powder Samples

3.2 CONSOLIDATION AND FORMING

3.2.1 Hot Isostatic Pressing

At Battelle Memorial Institute the four cans were loaded into an autoclave with a 0.457m (18 inches) diameter by a 1.27m (50 inches) hot zone. The autoclave was purged with helium (the pressurizing gas), evacuated and purged with helium once again during initial heat-up. The temperature and pressure cycle is outlined in Table 3.2-V while thermocouple locations are given in Table 3.2-VI.

When the cans were removed from the autoclave, two of the cans had decreased in size indicating that consolidation had occurred. A third showed only a slight tapering toward one end, and the fourth had bulged to a larger diameter and length than that prior to loading in the autoclave.

It was judged that the fourth can which contained MERL 80 powder had developed a leak during handling and/or the hot isopressing cycle. The bulge was due to pressurization of the inside of the can, followed by inability to rapidly equalize pressure as the autoclave was being vented to atmospheric pressure. Visual inspection did not indicate the source of the leak. The can was returned, along with the other three, to P&WA where fluorescent penetrant inspection also failed to disclose any cracked weld or other fissure in the can.

The tapered can, which contained Mar-M-432 powder, was sectioned on the end which had not decreased in diameter. Approximately a 0.003m (0.12 in.) gap was found between the can wall and the partially sintered powder.

A sample of Mar-M-432 powder was taken for interstitial analysis, to determine whether the powder had become contaminated during processing. Results of that analysis showed 176 ppm of oxygen and 125 ppm of nitrogen, which was in excess of the acceptable 100 ppm limit.

Additional remelt stock of the two unconsolidated alloys, Mar-M-432 and MERL 80, was prepared by vacuum induction melting. The Mar-M-432 was supplied by Howmet Corporation, Alloy Division, Dover, New Jersey, and the MERL 80 was melted at Pratt & Whitney Aircraft. Chemical analysis of these powder lots was made as described in Section 3.1 of this report. The results of the analysis are shown in Table 3.2-VII.

The two lots of remelt stock were delivered to Homogeneous Metals, Inc. for atomization. The atomized powder was screened to -60 +325 mesh, and sealed in evacuated mild steel seamless tubing containers. For the re-make of these two compaction cans, 0.0096m (0.375-inch) thick end plates were used to permit more thorough weld bead penetration. Homogeneous Metals, Inc. modified their proprietary closure device to make it compatible with these end plates, and all welded joints were sealed with multiple pass welds. These welds were subsequently ground smooth and dye-penetrant inspected and the cans were thoroughly helium leak checked prior to filling with powder.

Particle size distribution for these two powder lots (Table 3.2-VIII) indicated effective screening to -60 +325 mesh, with approximately ten percent of the powder being less than 325 mesh (44 μm) diameter.

Metallographic examination of the consolidated contents of the two remaining cans, AF2-1DA and NASA-TRW-VIA, was accomplished. The NASA-TRW-VIA was fully dense, i.e., no porosity was noted.

The AF2-1DA, which initially appeared fully dense, exhibited localized, microporosity as shown in Figure 3.2-10. This porosity was apparently due to inability of the material to become fully dense at 1149°C, 103.5 MN/m^2 (2100°F, 15,000 psi) in two hours. An attempt was made to re-compact the two AF2-1DA forging billets when the remade cans of Mar-M-432 and MERL 80 were hot isostatically pressed at Battelle Memorial Institute. Because temperatures as high as 1190°C (2175°F) had not been in excess of the incipient melting point of AF2-1DA, it was judged that a re-compaction at 1176°C, 103.5 MN/m^2 (2150°F, 15,000 psi) conditions for two to three hours would cause the two billets to become fully dense.

The re-pressed AF2-1DA billets, as well as the re-made cans of Mar-M-432 and MERL 80, were hot isostatic pressed at 1176°C, 103.5 MN/m^2 (2150°F, 15,000 psi) for 2.25 hours and delivered to P&WA. Metallographic examination of the re-pressed AF2-1DA billets indicated that much of the local microporosity had been closed, and that the billets were suitable for use. Two forging billets, 0.152m (6 in.) diameter by 0.152m (6 in.) high were machined from each compact. Figure 3.2-11 shows an example of such a billet. Microstructures of the as-consolidated billets are shown in Figure 3.2-12.

Chemical analysis was completed on the four as-consolidated compacts. As summarized in Table 3.2-IX, all reported values fall within previously designated limits with the exception of oxygen in NASA-TRW-VIA, and chromium and columbium in the Mar-M-432. The high oxygen in the NASA-TRW-VIA is attributed to the hafnium and rhenium in the alloy reacting with the ceramic oxide melting and atomization crucibles. The chromium and columbium contents are within limits of analytic error relative to the remelt stock. Values for these elements in the remelt stock were at the lower limit for chromium and upper limit for columbium, respectively.

Density of each of the compacted billets was determined pycnometrically and is listed in Table 3.2-X. These values indicate full density of the billets and are, within limits of accuracy of the pycnometric technique, equivalent to the nominal density for the four alloys.

3.2.2 Forging

3.2.2.1 Forgeability Trials

Pratt & Whitney Aircraft determined that the most uniform thermomechanical processing could be obtained, and the best mechanical properties achieved, by fully homogenizing the forging billets by a four hour exposure at, or slightly above, the gamma prime solvus temperature prior to forging.

Sections of the as-compacted alloys were subjected to four hour exposure at elevated temperature to determine the gamma prime and eta (Ni_3Ta found in MERL 80) solvus temperatures. Solvus temperature for both Mar-M-432 and AF2-1DA was found to be 1177°C (2150°F). Both gamma prime and eta phase were in solution in the MERL 80 alloy after four hours at 1246°C (2275°F). For the NASA-TRW-VIA, 1260°C (2300°F) was not sufficient to cause 100 percent gamma prime solutioning. At 1288°C (2350°F) evidence of incipient melting was noted. Rather than risk incipient melting at 1274°C (2325°F), allowing for a ±14°C (±25°F) variation of temperature, during solution treating of the forging billets, 1260°C (2300°F) was selected as the solution treating temperature for NASA-TRW-VIA.

The two forging billets from each alloy, plus several 0.019 m (0.75-inch) by 0.025 m (one inch) subscale forgeability coupons of each alloy were solution treated for four hours at the gamma prime solvus temperatures of:

- 1177°C (2150°F) for Mar-M-432 and AF2-1DA
- 1246°C (2275°F) for MERL 80
- 1260°C (2300°F) for NASA-TRW-VIA

To select the appropriate GATORIZING™ process forging temperature for the 0.1/min and 0.5 min^{-1} strain rates, small cylindrical forgeability coupons were upset 50 percent on flat open dies using P&WA's Florida Research and Development Center (FRDC) "mini-gator" press. The GATORIZING™ forging process, developed by Pratt & Whitney Aircraft uses an isothermal, heated-die technique to forge a highly-plastic billet which produces complex shapes at low forging stresses. The press is a 300 ton capacity tensile machine equipped with strain rate pacing control, TZM molybdenum alloy dies and an inert-atmosphere forging chamber. The billet and dies are maintained at an isothermal condition with a four element strip heater.

Forgeability coupons of each alloy were upset at a series of temperatures, using 0.5 min^{-1} strain rate, with the lowest temperature which did not result in cracking selected as the forging temperature. A final coupon was then GATORIZED™ at that temperature at 0.1 min^{-1} strain rate. A record was made of load as a function of deformation, and these loads were converted to unit pressures, by dividing by the cross sectional area. The unit pressure at the completion of the cycle, together with GATORIZING™ process parameters for each alloy are summarized in Table 3.2-XI.

Table 3.2-XI shows that forging stress increases with a decrease in forging temperature, with Mar-M-432 generally showing the highest stresses.

Metallographic examination of the GATORIZED™ coupons was conducted to verify absence of cracking. In the Mar-M-432, at 1093°C (2000°F), it was noted that internal cracking occurred despite absence of cracking at the periphery. For the two lower temperatures, 1066 and 1080°C (1950 and 1975°F), the peripheral cracking appeared to be associated only with the portion of the specimen in contact with the lower die, while the interior of the piece was sound. Because the lower die was approximately 33°C (60°F) hotter than the upper die, it was determined that a uniform temperature of 1093° (2000°F) would result in a "hot-short" condition for the material. Therefore, the lower temperature of 1074°C (1965°F) was selected for GATORIZING™ of Mar-M-432.

No cracking was noted in the MERL 80 forgeability coupons at 0.5 min^{-1} strain rate at temperatures as low as 1066°C (1950°F); however, the rapidly increasing unit pressure indicated potential die wear problems at GATORIZING™ temperatures below 1066°C (1950°F). For this reason, no further specimens were processed at lower temperatures.

Due to insufficient material for fabricating more than three coupons from NASA-TRW-VIA, no piece was forged at 1163°C (2125°F), 0.5 min^{-1} strain rate. Based on the extremely low unit pressure of 52.06 MN/m^2 (7550 psi) at 1163°C (2125°F), 0.1 min^{-1} strain rate, it was determined that this temperature would suffice at 0.5 min^{-1} strain rate to yield a sound pancake forging.

3.2.2.2 Sub-Scale Disks

Ultrasonic inspection of the forging billets revealed no rateable defects. The background noise level of the two AF2-1DA billets was higher than that of the others, which was judged to be a result of the microporosity throughout the parts. This porosity was generally smaller than 25 μm (0.001 in) in diameter, while the smallest pore which current ultrasonic methods may detect is approximately 150 μm (0.006-inch). Some inspection of the NASA-TRW-VIA billets detected six indications of non-metallic type inclusions which, at maximum signal amplification, gave a signal peak height about one half that of a standard 0.4 mm (1/64-inch) flat bottomed hole (FBH). This standard FBH is the minimum size rateable defect employed in current quality control practice on production powder metallurgy turbine disks at Pratt & Whitney Aircraft.

Eight flat pancake forgings were GATORIZED™ at Ladish Co., Cudahy, Wisconsin. Before the thermomechanical processing, each billet was sonically inspected and given a visual and dye-penetrant inspection by Ladish Co. Ultrasonic inspection showed one NASA-TRW-VIA billet, S/N 1, to have a suspected indication of nonmetallic inclusions. It was located halfway between the flat faces and 0.013 m (0.5-inch) in from the edge. This billet was selected for forging at 0.1 min^{-1} strain rate. The AF2-1DA billet, S/N 3, exhibited a thin surface crack along one side. The billet was ground back 0.019 m (0.75-in.) to eliminate the possibility of crack propagation during thermomechanical processing.

The basic thermomechanical processing sequence at Ladish Co. consisted of a 2.5 hour heat-up to the forging temperature, a 0.5 hour homogenization soak at the forging

temperature, followed by isothermal forging on heated TZM molybdenum dies to 0.035 m (1.5 in) thickness. Transfer time from the pre-heating furnace to the dies was approximately ten seconds. After being positioned in the dies, the billet was allowed to return to thermal equilibrium at the forging temperature.

Forging time varied from 3.03 minutes for those billets processed at 0.5 min^{-1} to 14.95 minutes for those processed at 0.1 min^{-1} strain rate. Upon completion of the forging cycle, the flat disk was ejected from the die, transferred to an exit load lock, removed from the furnace, and allowed to air cool. Time from ejection to removal from the vacuum chamber was approximately one minute. Pertinent forging data for the pancake forgings are summarized in Table 3.2-XII.

The appearance of the eight forgings was satisfactory. Rim cracking was noted in MERL 80, Mar-M-432, and AF2-1DA at both 0.1 and 0.5 min^{-1} strain rates. Cracks were uniformly distributed around the periphery and ranged in depth from 0.006 to 0.019 m (0.25 to 0.75 in). The cracks did not affect the ability to obtain the required number of mechanical property specimens. The NASA-TRW-VIA forgings exhibited little or no cracking and had a smoother surface with less galling tendency than did the other three alloys. Typical appearance of the forgings is shown in Figure 3.2-13.

The post-forging processing sequence used by Ladish Co. is that used in the production of powder metallurgy disks for P&WA aircraft gas turbine engines: grind OD cracks to avoid their propagation during heat treatment, grind top and bottom faces flat and parallel for ultrasonic inspection, remove center core around locating pin indentations, inspect by dye penetrant, precipitation heat treat, inspect by ultrasonic methods, and machine mechanical property specimens.

Precipitation heat treatment of the forgings made at Ladish Co. was conducted under the conditions shown in Table 3.2-XIII. Following precipitation heat treatment, and subsequent ultrasonic inspection, mechanical property test specimens were machined from the eight forgings to be used for measuring tensile and creep-rupture properties.

Forging stresses were calculated as a function of percent reduction of height for the flat pancake forgings. As shown in the curves of Figures 3.2-14 and 3.2-15, the stress generally decreased with increasing reduction of height and was higher for those forgings made at 0.5 min^{-1} strain rate than for those made at 0.1 min^{-1} strain rate. Those forgings made at the slower strain rate typically exhibited an increase in forging stress above approximately a 50 percent reduction. This was attributed to increased die friction as increasing amounts of billet area came into contact with the die.

Metallographic evaluation was made of the fully processed disk forgings to document the microstructure prior to mechanical property evaluation. As shown in Figures 3.2-16, 3.2-17, 3.2-18, and 3.2-19, the structure is typified by very fine grain size of approximately 15-25 μm and flattened powder particle shapes, outlined in the AF2-1DA disks by MC type carbides.

TABLE 3.2-V

HOT ISOSTATIC PRESSING CYCLE CONDITIONS

Time, Hr-Min		Temperature, °C						Pressure
Total	Cycle	T/C-1	T/C-2	T/C-5	T/C-6	T/C-7	T/C-8	MN/m^2
Start	–	–	22	–	–	–	–	0–11.2
1-34	–	240	238	233	238	233	182	20.65
4-10	–	502	502	502	504	502	433	39.95
5-50	–	837	841	832	851	847	793	59.25
6-55	–	929	933	929	941	941	907	70.25
7-42	–	1004	1010	1002	1010	1010	994	79.20
8-45	–	1122	1122	1117	1122	1122	1112	93.60
9-03	–	1149	1149	1143	1152	1149	1138	96.40
9-30	Start	1152	1149	1149	1154	1154	1146	102.8
10-00	0-30	1149	1149	1149	1154	1155	1149	103.3
10-30	1-00	1149	1149	1149	1149	1152	1146	103.3
11-30	1-30	1146	1146	1144	1149	1149	1149	103.3
11-30	2-00	1149	1149	1149	1154	1152	1149	103.3

Time, Hr-Min		Temperature, °F						Pressure
Total	Cycle	T/C-1	T/C-2	T/C-5	T/C-6	T/C-7	T/C-8	PSI
Start	–	–	72	–	–	–	–	0-1626
1-34	–	464	460	451	460	451	360	3,000
4-10	–	936	936	936	939	936	811	5,800
5-50	–	1539	1546	1530	1564	1557	1459	8,604
6-55	–	1704	1711	1704	1726	1726	1664	10,200
7-42	–	1839	1850	1836	1850	1850	1821	11,500
8-45	–	2052	2052	2043	2052	2052	2052	13,590
9-03	–	2100	2100	2089	2106	2100	2080	14,000
9-30	Start	2106	2100	2100	2109	2109	2095	14,930
10-00	0-30	2100	2100	2100	2109	2111	2100	15,000
10-30	1-00	2100	2100	2100	2100	2106	2095	15,000
11-00	1-30	2095	2095	2091	2100	2100	2100	15,000
11-30	2-00	2100	2100	2100	2109	2106	2100	15,000

TABLE 3.2-VI

LOCATIONS OF THERMOCOUPLES DURING HOT ISOSTATIC PRESSING RUN

T/C Number	Location
1	Side, 1.28m (50.5 inch) from bottom heater
2	Side, 0.94m (37 inch) from bottom heater
5	Side, 1.105m (43.5 inch) from bottom heater
6	Side, 0.775m (30.5 inch) from bottom heater
7	Side, 0.445m (17.5 inch) from bottom heater
8 (imbedded in Al_2O_3)	Side, 0.114m (4.5 inch) from bottom heater

TABLE 3.2-VII

RESULTS OF CHEMICAL ANALYSIS OF MAR-M-432 AND MERL 80 POWDERS FROM REPLACEMENT HEATS
(Given in Weight Percent)

Element	Mar-M-432	MERL 80
Cobalt	20.0	9.7
Chromium	14.7	9.2
Molybdenum	0.0	1.0
Titanium	4.3	1.0
Aluminum	2.7	3.9
Tungsten	3.1	2.9
Tantalum	2.0	11.0
Columbium	2.3	0.0
Hafnium	0.0	1.02
Zirconium	0.06	0.30
Carbon	0.16	0.12
Boron	0.014	0.020
Iron	0.12	0.03
Manganese	0.003	0.002
Silicon	0.06	0.04
Nitrogen	0.0024	0.0016
Oxygen	0.0086	0.0060
Hydrogen	0.0008	0.0007
Lead	<0.0002	<0.0002
Bismuth	<0.00005	<0.00005
Nickel	Balance	Balance

TABLE 3.2-VIII

PARTICLE SIZE DISTRIBUTION FOR MAR-M-432 AND MERL 80 POWDERS FROM REPLACEMENT HEATS

Particle Size		Weight Percent Retained on Screen	
Mesh	μm	Mar-M-432	MERL 80
60	250	–	–
80	177	26.14	13.80
120	125	23.43	23.34
170	88	16.49	19.52
230	62	11.82	15.30
325	44	12.91	17.84
400	37	5.81	7.71
<400	<37	3.40	2.49

TABLE 3.2-IX

CHEMICAL ANALYSIS OF CONSOLIDATED POWDER BILLETS
(Given in Weight Percent)

Element	AF2-1DA	Mar-M-432	NASA-TRW-VIA	MERL 80
Chromium	11.7	15.1	5.8	9.2
Cobalt	10.0	20.1	7.4	9.6
Aluminum	4.7	2.8	5.5	3.8
Titanium	2.9	4.2	1.0	0.9
Tantalum	1.3	2.1	9.2	11.0
Columbium	0.0	2.3	0.51	0.0
Tungsten	5.4	3.0	5.9	3.3
Molybdenum	2.8	0.0	2.0	1.0
Rhenium	0.0	0.0	0.33	0.0
Hafnium	0.0	0.0	0.47	0.97
Zirconium	0.10	0.07	0.08	0.30
Carbon	0.33	0.17	0.15	0.13
Boron	0.015	0.016	0.014	0.018
Manganese	0.002	0.003	0.002	0.002
Iron	0.16	0.17	0.14	0.04
Silicon	0.05	0.07	0.06	0.05
Sulfur	0.004	0.004	<0.002	0.002
Lead	<0.0002	<0.0002	<0.0002	<0.0002
Bismuth	<0.0005	<0.00003	<0.00005	<0.00003
Nitrogen	0.0037	0.0039	0.0025	0.0015
Oxygen	0.0070	0.0080	0.0130	0.0060
Nickel	Balance	Balance	Balance	Balance

TABLE 3.2-X

DENSITY OF AS-COMPACTED BILLETS

Alloy	Density g/cm^3	Density lbm/in^3
NASA-TRW-VIA	8.82	0.321
AF2-1DA	8.19	0.298
Mar-M-432	8.34	0.303
MERL 80	8.94	0.325

TABLE 3.2-XI

SUBSCALE GATORIZING™ PARAMETERS AND RESULTS

Alloy	Temperature °C	Temperature °F	Strain Rate min^{-1}	Unit Pressure MN/m^2	Unit Pressure psi	Comments
AF2-1DA	1,093	2,000	0.5	130	18,900	Moderate Cracking
	1,121	2,050	0.5	100	14,500	No Cracking
	1,121	2,050	0.1	66.5	9,650	No Cracking
Mar M-432	1,093	2,000	0.5	183	25,600	No Cracking
	1,066	1,950	0.5	200	29,100	Slight Cracking
	1,080	1,975	0.5	213	30,900	Very Tiny Cracks
	1,093	2,000	0.1	101	14,600	No Cracks
NASA-TRW-VIA	1,107	2,025	0.5	134	19,500	Moderate Cracking
	1,135	2,075	0.5	144	20,900	Moderate Cracking
	1,163	2,125	0.1	52.1	7,550	No Cracking
MERL 80	1,107	2,025	0.5	117	16,900	No Cracking
	1,080	1,975	0.5	136	19,800	No Cracking
	1,066	1,950	0.5	160	23,250	No Cracking
	1,066	1,950	0.1	88.3	12,800	No Cracking

TABLE 3.2-XII

ISOTHERMAL FORGING DATA

Alloy	Serial Number	Forged Diameter (m)	Forged Diameter (inches)	Forging Force (MN)	Forging Force (Tons)	Forging Time, Min.	Nominal Strain Rate, Min^{-1}
MERL 80	6	0.31	12.2	13,200	1486	14.25	0.1
MERL 80	8	0.30	11.9	13,650	1534	3.10	0.5
Mar-M-432	5	0.31	12.3	11,800	1329	14.95	0.1
Mar-M-432	7	0.30	12.0	14,000	1570	3.10	0.5
AF2-1DA	3	0.26	10.3*	7,500	840	14.60	0.1
AF2-1DA	4	0.31	12.1	11,800	1329	3.15	0.5
NASA-TRW-VIA	1	0.32	12.7	8,600	966	14.60	0.1
NASA-TRW-VIA	2	0.31	12.3	11,500	1293	3.05	0.5

*Smaller than others because of material removed in grinding out crack.

TABLE 3.2-XIII

PRECIPITATION HEAT TREATMENT FOR FORGINGS

Alloy	Heat Treatment
NASA-TRW-VIA	870°C (1600°F), 16 hours, Air Cool
AF2-1DA	760°C (1400°F), 16 hours, Air Cool
Mar-M-432	760°C (1400°F), 12 hours, Air Cool
MERL 80	815°C (1500°F), 16 hours, Air Cool

Micro: NASA 12 Mag: 100X

Figure 3.2-10 Appearance of Microporosity in As-Consolidated AF2-1DA, Etchant: Kalling's Reagent

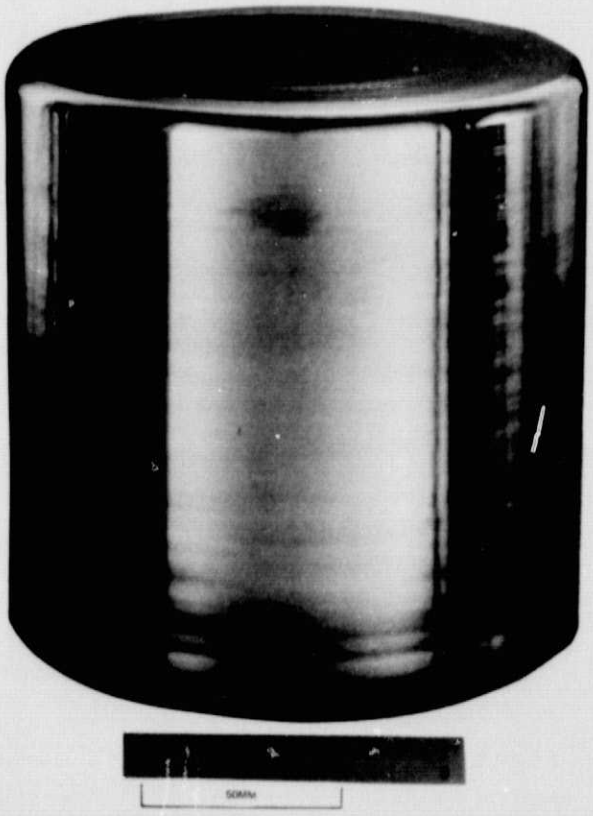

Figure 3.2-11 As-Consolidated Forging Billet

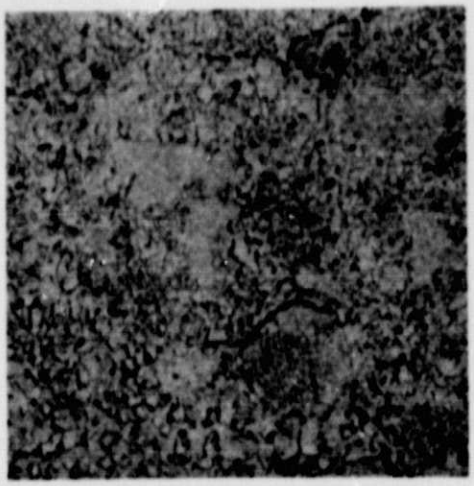

NASA-TRW-VI-A Mag:500X

AF2-IDA Mag: 500X

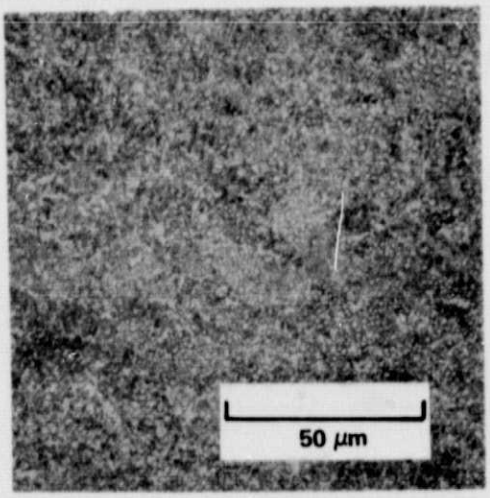

MERL-80 Mag: 500X

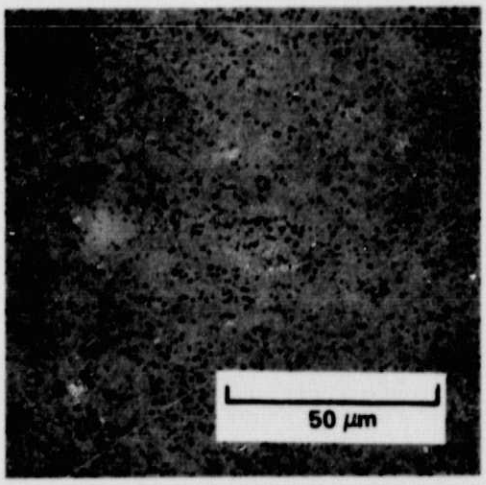

Mar-M432 Mag: 500X

Figure 3.2-12 As-Consolidated Microstructure of Billets

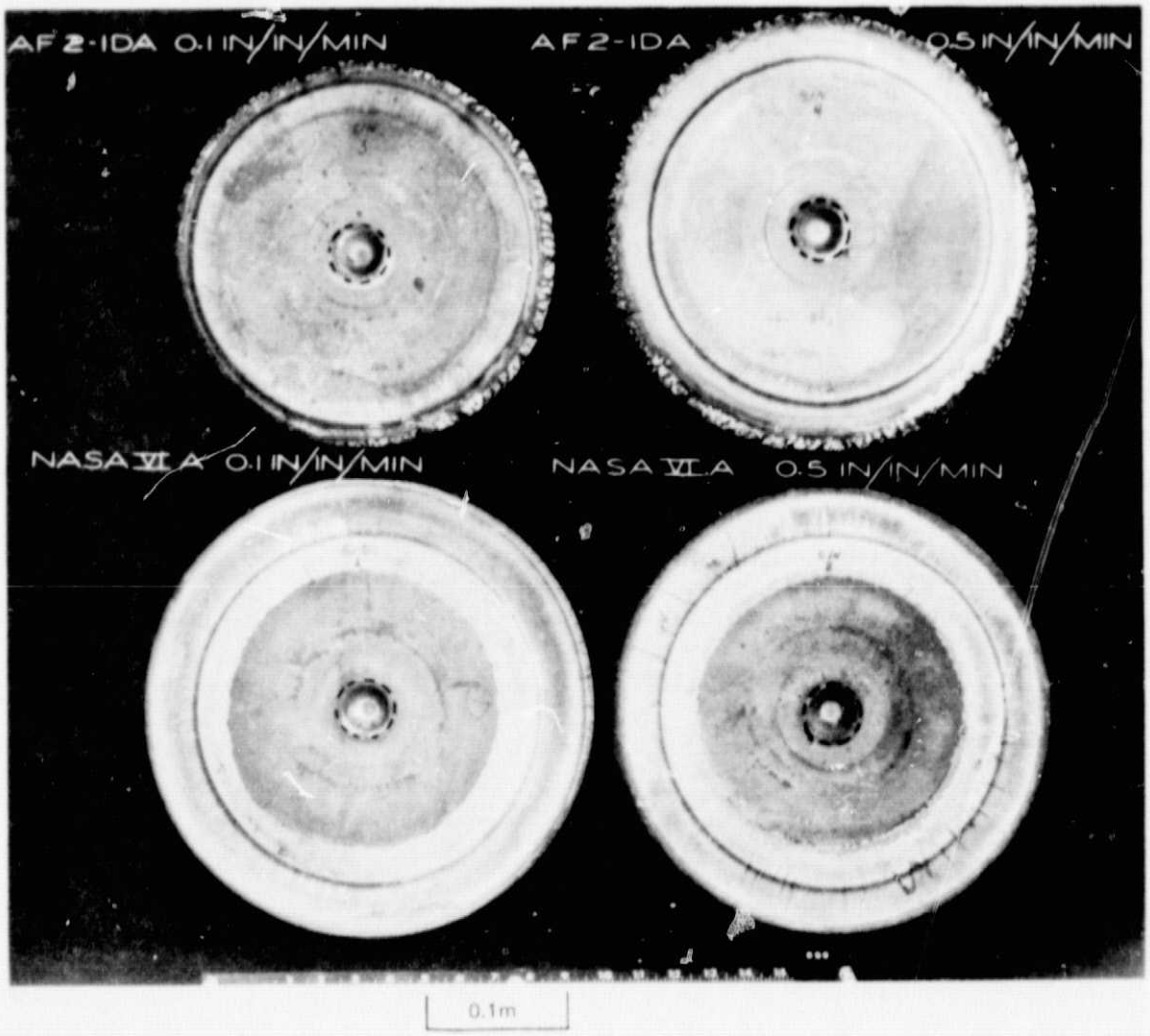

Figure 3.2-13 A Appearance of AF2-1DA and NASA-TRW-VIA Pancakes As-Forged. Dotted Line Indicates Location of Center Core

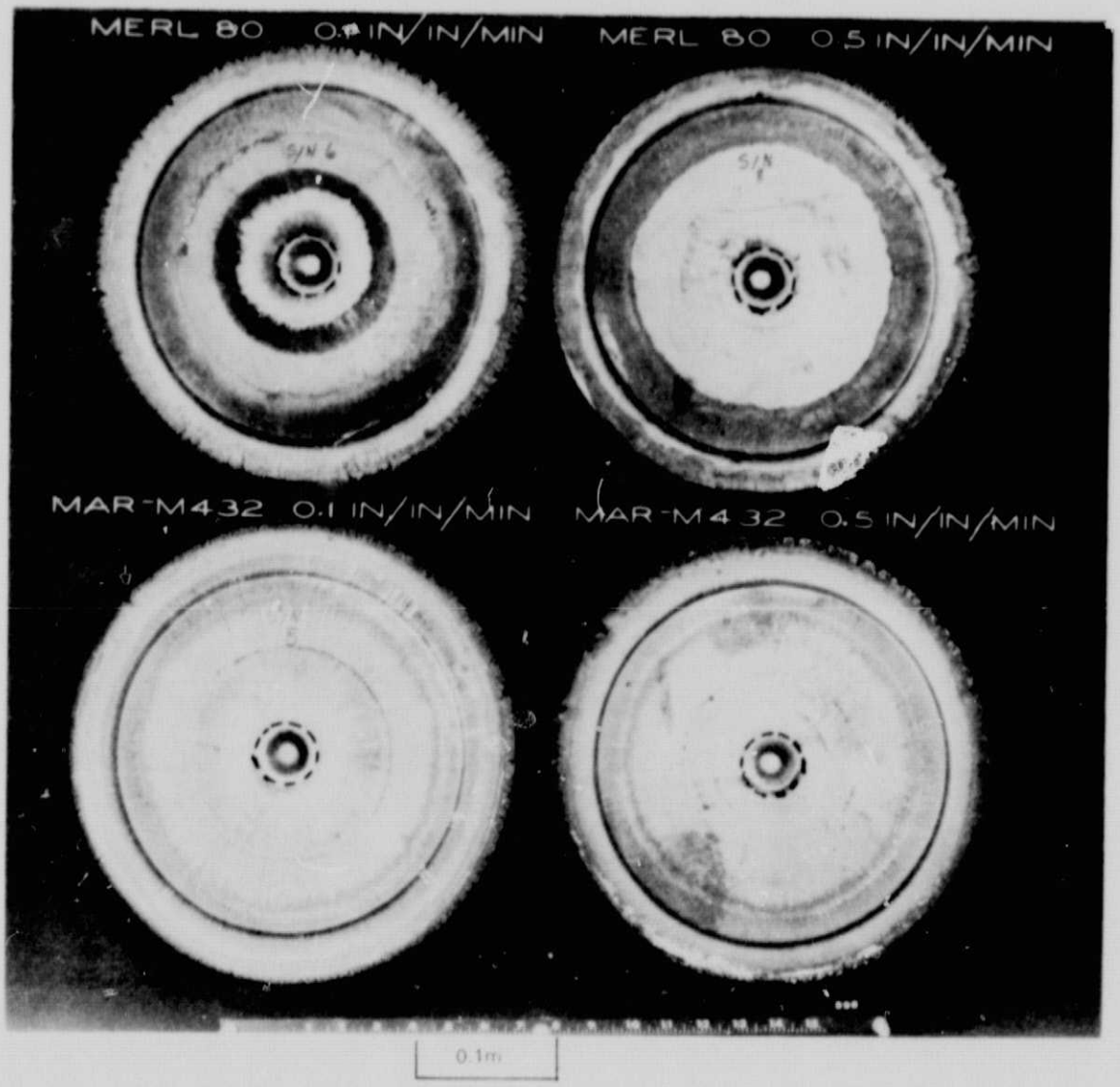

Figure 3.2-13 B Appearance of MERL-80 and Mar-M432 Pancakes As-Forged. Dotted Line Indicates Location of Center Core

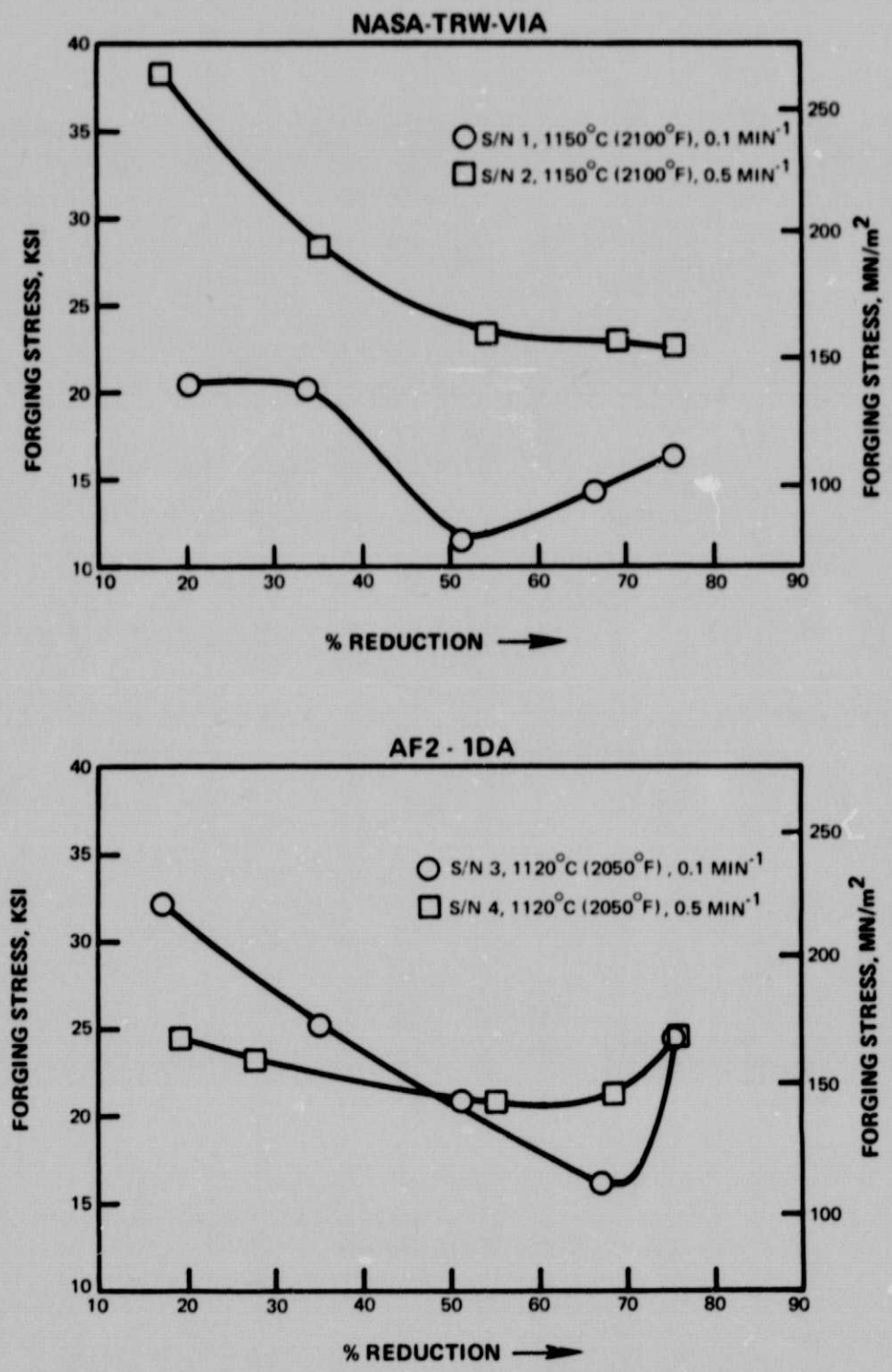

Figure 3.2-14 Forging Stress Versus Reduction in Height for NASA-TRW-VIA and AF2-1DA Forgings

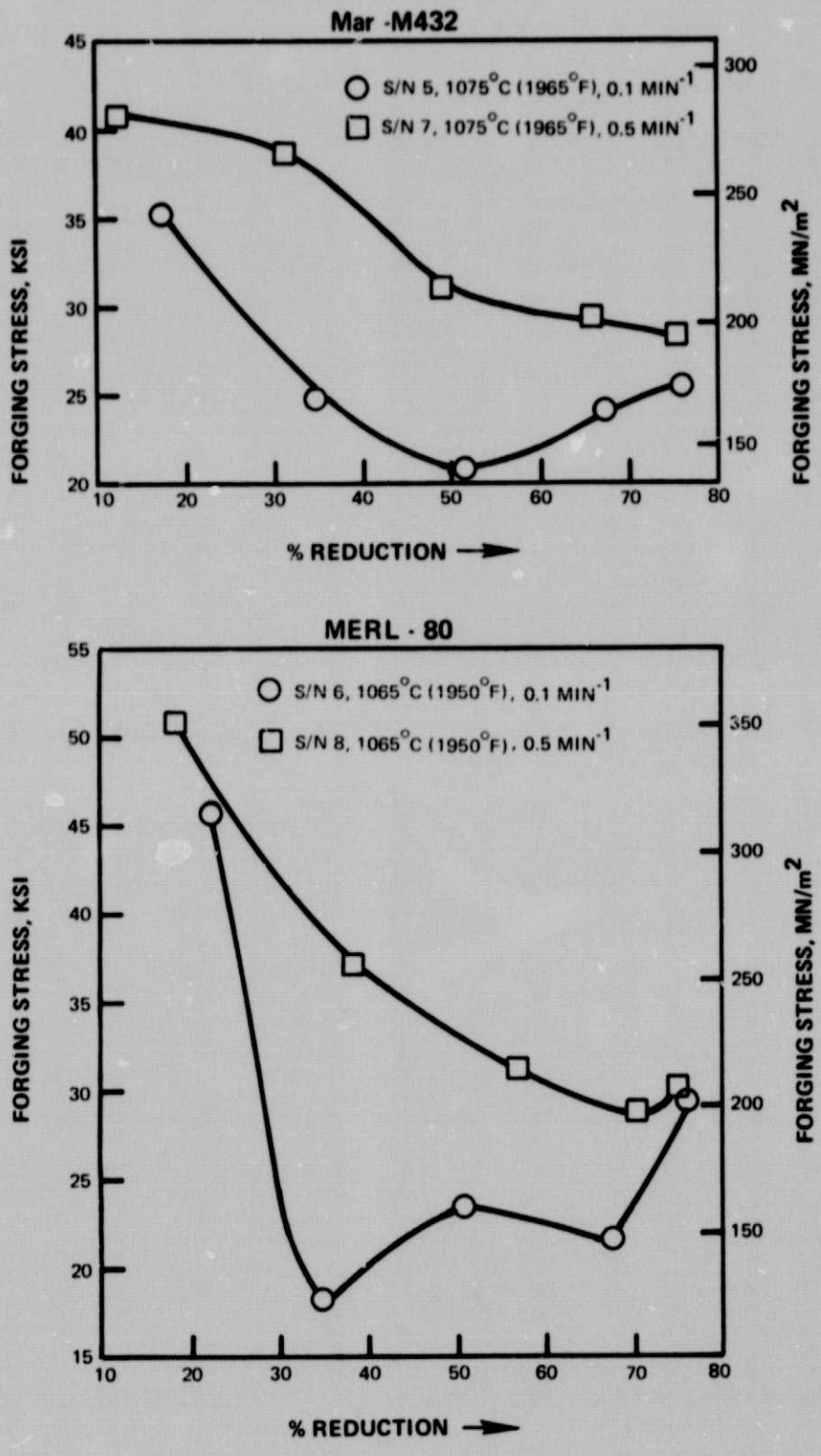

Figure 3.2-15 Forging Stress Versus Reduction in Height for Mar-M-432 and MERL 80 Forgings

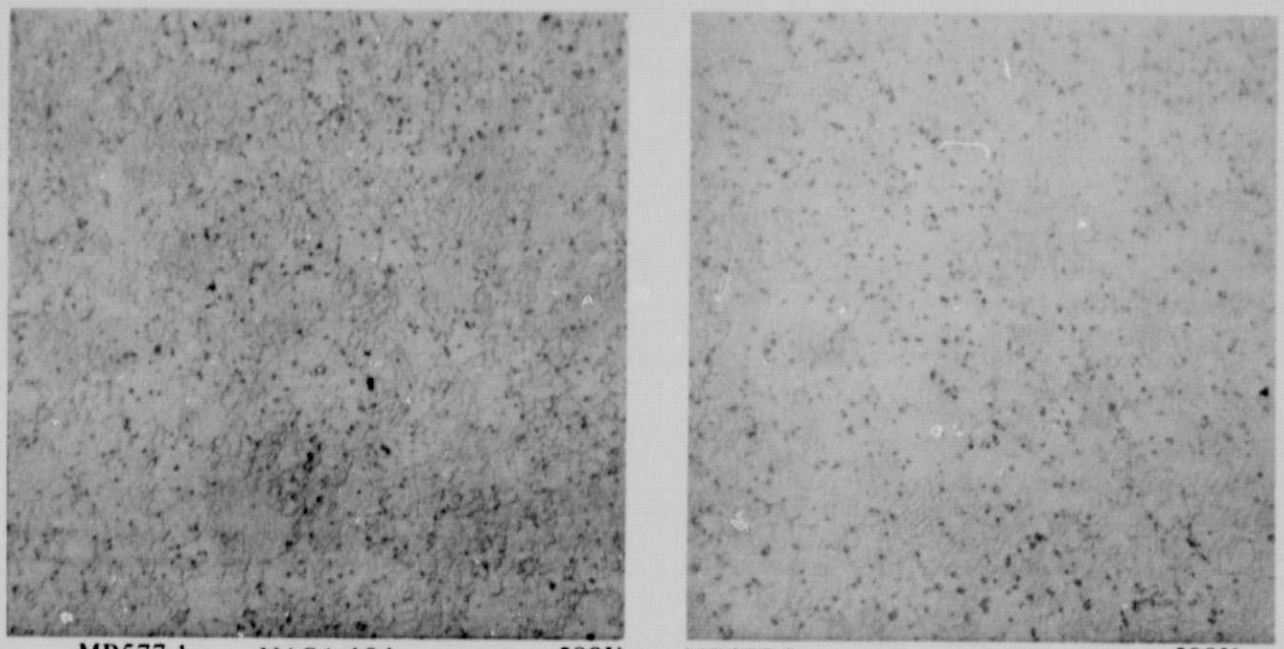

Figure 3.2-16 Microstructure of Fully Processed NASA-TRW-VIA Disks Forged at 0.1 min^{-1} (Left) and 0.5 min^{-1} (Right)

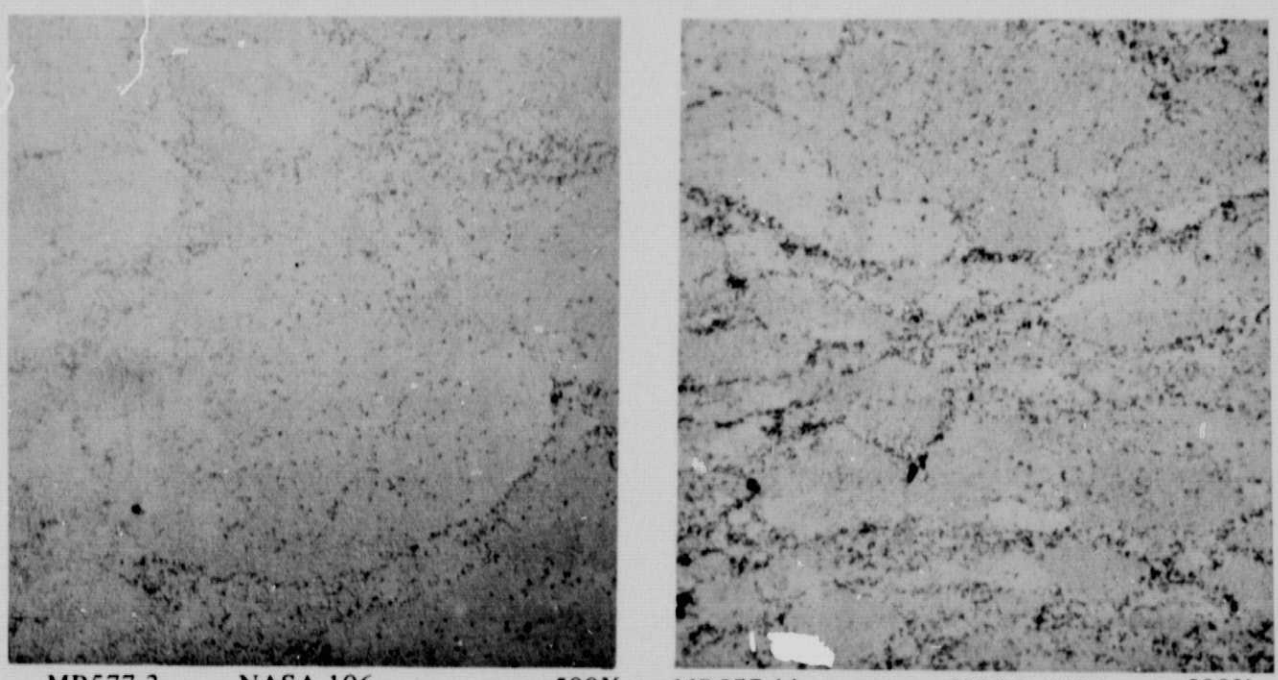

Figure 3.2-17 Microstructure of Fully Processed AF2-1DA Disks Forged at 0.1 min^{-1} (Left) and 0.5 min^{-1} (Right)

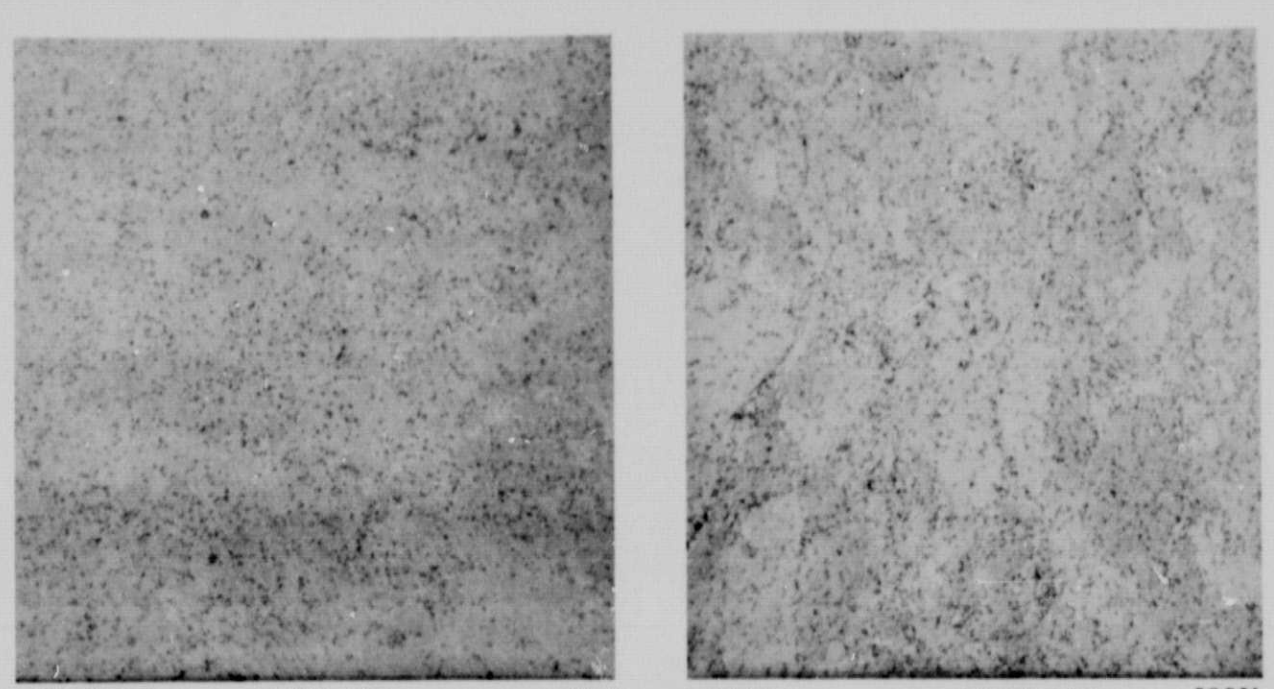

MB577-4 NASA 108 500X MB577-7 NASA 110 500X

Figure 3.2-18 Microstructure of Fully Processed Mar-M-432 Disks Forged at 0.1 min^{-1} (Left) and 0.5 min^{-1} (Right)

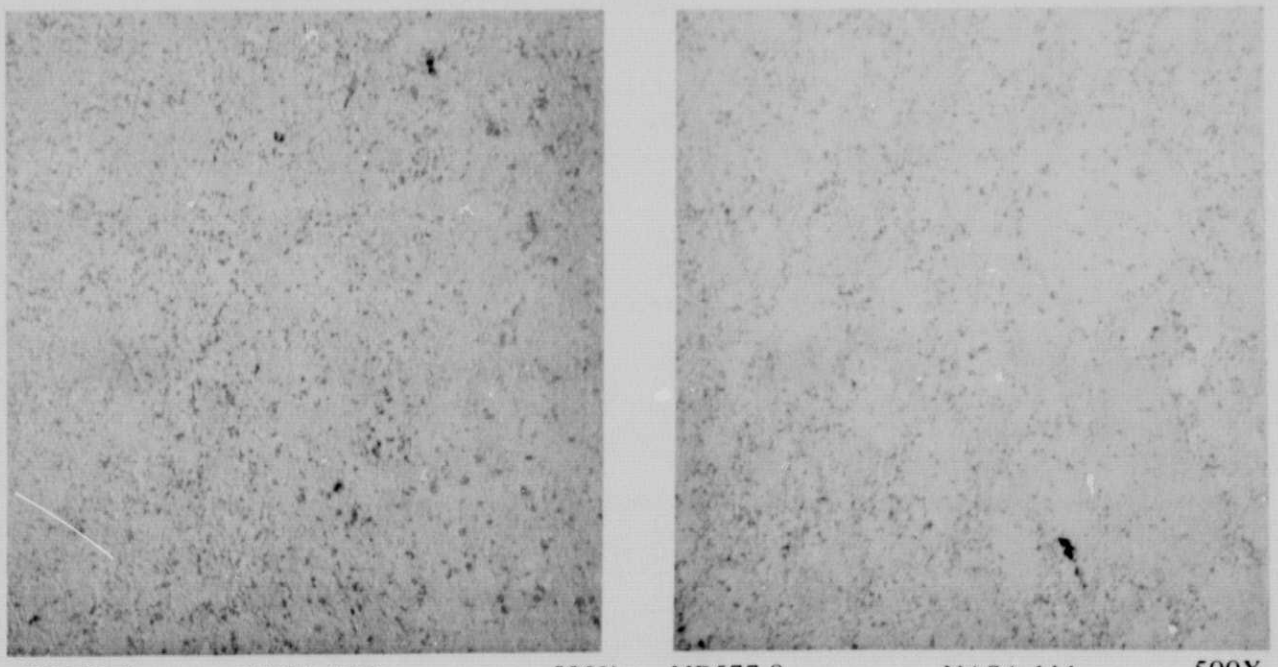

MB577-5 NASA 109 500X MB577-8 NASA 111 500X

Figure 3.2-19 Microstructure of Fully Processed MERL 80 Disks Forged at 0.1 min^{-1} (Left) and 0.5 min^{-1} (Right)

3.3 MECHANICAL TESTING

3.3.1 Specimens and Test Procedures

Tensile testing of two specimens of each of the four selected alloys, NASA-TRW-VIA, AF2-1DA, Mar-M-432, and MERL 80, was conducted at Ladish Co. at room temperature, 540°C (1000°F), and 650°C (1200°F). Creep-rupture testing at 650°C/1035 MN/(m)^2 (1200°F/150 ksi) was also conducted at Ladish Co.

3.3.2 Tensile and Creep-Rupture Tests

The data from the tensile and creep-rupture tests are presented in Tables 3.3-XIV through 3.3-XVII. In general, strengths increased with increasing forging strain rate, and Mar-M-432 showed the best balance of strength and ductility. As with the room temperature results, strength increased with increasing forging strain rate. Both Mar-M-432 and MERL 80 showed superior strength and ductility relative to the other two alloys. Results of the 650°C (1200°F) tensile tests show that MAR-M-432 maintains the strength and ductility advantages shown at room temperature and 540°C (1000°F).

These data indicate that the goal of 0.2 percent creep in 100 hours was not met. This was judged to be due to the fine grain size (15-25μm) which might be expected to yield rupture lives shorter than would the same material in a coarse-grained condition.

The density of each forging was determined at three locations and resulting data are summarized in Table 3.3-XVIII.

The data from Table 3.3-XVIII were subsequently used to adjust the tensile and creep-rupture strengths measured on the forgings to a baseline density of 8.3 g/cm^3 (0.3 lb/in^3). The density-corrected strengths are presented in Tables 3.3-XIX through 3.3-XXII.

When corrected to a density of 8.3 g/cm^3 (0.3 lb/in^3) the alloys with densities greater than 8.3 g/cm^3 (0.3 lb/in^3) (NASA-TRW-VIA and MERL 80) have inferior properties relative to the lighter alloys (AF2-1DA and Mar-M-432) than before the density correction.

As seen for the room temperature and 540°C (1000°F) data, correction to a baseline density of 8.3 g/cm^3 (0.3 lb/inch^3) increases the apparent strength advantage of Mar-M-432 and AF2-1DA over NASA-TRW-VIA and MERL 80.

In summary, on a density-corrected basis, the tensile strength of Mar-M-432 exceeded that of the other alloys at all test temperatures, while creep strengths of AF2-1DA and Mar-M-432 were approximately equal, and superior to the creep strengths of the other two alloys.

Microstructure of failed creep specimens after testing at 650°C (1200°F) and 1035 MN/m^2 (150 ksi) is documented in Figures 3.3-20 and 3.3-21. It is apparent that the fracture path is generally intergranular, typical of fine-grained, high strength alloys. Fracture along prior particle boundaries occurred only where the boundary ran perpendicular to the applied stress axis and was in line with the advancing crack path.

There was little incidence of secondary cracking, away from the primary fracture. However, the most pronounced example of this was noted in the AF2-1DA specimens. The very fine grain size, which may be a contributing factor to the short rupture lives and time to 0.5 percent creep, was also noticed. In general, the AF2-1DA, with the coarsest grain size, yielded the longest rupture life.

Tensile tests at 650°C (1200°F) were conducted on specimens machined from forgings after 1000 hours exposure at 790°C (1450°F). Results of these tests are summarized in Table 3.3-XXIII.

When compared to similar tests conducted on fully-processed (but not thermally exposed) forgings, it is noted that for NASA-TRW-VIA, the 0.2 percent yield strength increased while ultimate strength and ductility decreased with exposure. For both AF2-1DA and Mar-M-432, exposure had little effect on yield strength and decreased ultimate strength 60-80 MN/m^2 (8.7 - 11.6 ksi). In AF2-1DA ductility decreased slightly, from six percent elongation to five percent, but was little affected in Mar-M-432. For MERL 80, the ultimate strength decreased about 150 MN/m^2 (21.7 ksi) after thermal exposure, with little change in ductility noted. Overaging was judged to be the cause of decrease in strength. Although the ductilities of NASA-TRW-VIA and AF2-1DA showed decreases, the cause of the decrease could not be determined. Metallographic examination of these forgings after thermal exposure revealed no indication of microstructural instability. (Figures 3.3-22 and 3.3-23).

The data obtained in the Task I mechanical property evaluation indicate that the program strength goals were not met. Insufficient thermomechanical work was accomplished to achieve the required strength levels.

Although increasing the forging strain rate from 0.1 to 0.5 min^{-1} improved the properties of the forgings, 0.5 min^{-1} was not a sufficiently high rate to achieve the desired strength. Therefore, subsequent trials included forging at higher strain rates.

A series of small subscale forgings was made to define a thermomechanical processing (TMP) sequence more suitable to achieve program strength goals. These small pieces were thermally treated, prior to forging, in a manner designed to coarsen grain size for subsequent stress-rupture improvement and to coarsen gamma prime to promote forgeability. The conditions examined are summarized in Table 3.3-XXIV.

The revised TMP sequences resulted in higher flow stresses than experienced in the initial Task I subscale specimens. However, the hardness of the forged pieces was greater than previous subscale work. Typical hardness values with the revised TMP sequences were Rc 49-53 compared to Rc 38.5-48 for the TMP schedules used to fabricate the original forgings. Evidence of edge cracking indicated that forging was at too low a temperature.

A second series of subscale work was initiated using 1040°C (1900°F) to increase forgeability, but with an increase in strain rate to 5.0 min^{-1} to build up the necessary dislocation substructure.

Using consolidated powder taken from the ends of as-consolidated billets, subscale forging multiples of approximately 0.05 m (2 inch) diameter by 0.045 m (1.75 in.) high were machined for additional thermomechanical processing studies. The machined billets were pre-exposed according to the heat treatments in Table 3.3-XXV to coarsen the grain size for improved creep properties and to slightly coarsen gamma prime for improved forgeability.

The heat treated billets, one of NASA-TRW-VIA, two each of AF2-1DA and Mar-M-432, and three of MERL 80, were then canned in carbon steel containers. Sidewalls were approximately 0.006 m (0.250-inch) thick, with top and bottom plates approximately 0.003 m (0.130-inch) thick.

The billets were forged at the Wyman-Gordon Company, Millbury Plant, Millbury, Massachusetts, on a 1500 ton hydraulic forge press. The press was equipped with IN-100 dies, which were heated with electrical resistance heaters encircling the upper and lower flat dies. To reduce heat loss through radiation, the forging multiples were wrapped in glass fiber cloth. To prevent die chill they were encased in thin stainless steel top and bottom plates. The billets were pre-heated for four hours at a temperature of 1040°C (1900°F). The pre-heated multiples were forged on dies heated to 930°C (1700°F) at press speed corresponding to an initial strain rate of 5.0 min^{-1}. Forging of approximately 75 percent reduction to 0.013 m (0.50-inch) was done in a single pass, and the forged pancakes were quenched in oil off the press.

These subscale forgings were then decanned at Wyman-Gordon Company and given a direct aging treatment. The AF2-1DA was aged at 760°C (1400°F) for 16 hours (Air Cool); the Mar-M-432 was aged at 760°C (1400°F) for 12 hours (Air Cool); and the MERL 80 was aged at 815°C (1500°F) for 16 hours (Air Cool). Appearance of all forgings, except that made from NASA-TRW-VIA which was edge cracked, was excellent. The cracking was apparently related to the severity of the forging on the smaller NASA-TRW-VIA billet. Because of limited material availability, the billet was approximately two-thirds the size of those of the other alloys.

Mechanical property testing was performed on specimens machined from subscale forgings made at Wyman-Gordon Company. Because the NASA-TRW-VIA forging was badly cracked, no specimens were taken from that alloy. Tensile data generated at room temperature and at 650°C (1200°F) are summarized in Table 3.3-XXVI.

An increase in strength relative to the Task I GATORIZED™ forging was noted, particularly for Mar-M-432 which showed a 200 MN/m^2 (29 ksi) increase in ultimate strength at room temperature.

Results of creep-rupture tests conducted at 650°C/1035 MN/m^2 (1200°F/150 ksi) are summarized in Table 3.3-XXVII.

While improvements in tensile strengths occurred as a result of the lower temperature, higher strain rate forging conditions, a similar improvement in creep-rupture behavior was not developed.

Metallographic examination of specimens after creep test revealed an ultrafine grain size which contributes to short-time tensile strength, but adversely affects long-time properties, such as creep.

The strength levels achieved to date, using single-pass heated die forging, were compared to those achieved in other reported data (References 1 and 2) using multiple-pass rolling or swaging methods. Definite strength advantages were evident in multiple pass thermomechanical working. Therefore, one set of additional subscale forgings was made at Wyman-Gordon where a total reduction of 75 percent in height was made.

One compact each of the four contract alloys was prepared by hot isostatic pressing at 1175°C (2150°F) and 103.5 MN/m^2 (15,000 psi) for two hours. Size of the resultant compacts was 0.046 m (1.8 inch) diameter by 0.084 m (3.3 inch) long. The compacts, jacketed in stainless steel were thermally treated to coarsen grain size, for improved creep strength, and to improve forgeability. Thermal treatment consisted of a partial solution treatment two hours at or near the gamma prime solvus for each alloy, followed by a furnace cool to 1120°C (2050°F), holding at that temperature for two hours and then air cooling to room temperature. The partial solution treating temperature for each alloy was:

1260°C (2300°F) for NASA-TRW-VIA

1175°C (2150°F) for AF2-1DA and Mar-M-432

1230°C (2250°F) for MERL 80

Forging of the four compacts was performed at Wyman-Gordon Company. A total reduction in height of 75 percent was achieved in nine forging passes. Each individual reduction was approximately 15 percent, with intermediate reheats between reductions. This approach was selected to approximate the methods of processing which have yielded highest mechanical properties to date in nickel-base superalloys, namely rolling and swaging.

The initial reduction on each alloy was made at 1035°C (1900°F), as were the fourth and ninth (last) reductions. The other six forging operations were made following thirty minute soaks at 1090°C (2000°F). The purpose of these higher temperature re-heats was to promote partial recovery, while eliminating recrystallization to a fine grain size which would result in poor creep properties. Following the final forging operation, each forging was oil quenched off the forging press and direct-aged at 760°C (1400°F) for 16 hours followed by an air cool to room temperature.

The use of higher temperature reheats in an attempt to promote recovery without achieving full recrystallization did not achieve expected increases in tensile and creep-rupture properties. Metallographic examination of forged and heat treated compacts indicated extensive (but not complete) recrystallization from the starting grain size of ASTM 7-9 to a final grain size of ASTM 11-12. This fine grain size, however, was not present in the NASA-TRW-VIA to the same extent as in the other alloys, and presumably explains the extended creep life in this alloy.

The amount of recrystallization which occurred may be attributed to two factors:

- too lengthy a reheat (15 minutes) at 1090°C (2000°F) between reductions
- the compacts were not allowed to cool from 1090°C to 1035°C (2000°F to 1900°F) prior to forging the intermediate reductions.

Two tensile and one creep-rupture specimen were machined from each forging. One tensile test was conducted on specimens from each forging at room temperature and at 650°C (1200°F). Creep-rupture tests were run at 650°C/1035 MN/m^2 (1200°F/150 ksi). Results of these tests are shown in Tables 3.3-XXVIII and 3.3-XXIX.

TABLE 3.3-XIV

ROOM TEMPERATURE TENSILE STRENGTH OF FORGINGS

Alloy	S/N	Strain Rate Min^{-1}	0.2% YS (MN/m^2)	0.2% YS (ksi)	UTS (MN/m^2)	UTS (ksi)	El. (%)	R.A. (%)
NASA-TRW-VIA	1	0.1	950	137.7	1385	201.1	8	11
			945	137.1	1415	205.1	9	11
NASA-TRW-VIA	2	0.5	1030	149.1	1440	208.9	8	10
			1020	147.6	1525	221.7	12	13
AF2-1DA	3	0.1	1040	150.9	1355	196.5	8	10
			1040	150.9	1460	212.1	12	11
AF2-1DA	4	0.5	1100	159.2	1535	222.7	14	14
			1100	159.4	1495	216.2	11	12
Mar-M-432	5	0.1	1215	176.1	1680	242.8	10	11
			1215	175.9	1660	240.6	10	11
Mar-M-432	7	0.5	1280	185.7	1750	253.2	12	11
			1260	182.1	1745	252.8	14	16
MERL 80	6	0.1	1230	177.9	1660	240.3	9	11
			1225	177.3	1705	247.2	11	12
MERL 80	8	0.5	1265	183.3	1670	243.2	9	9
			1280	185.4	1650	238.7	8	10

TABLE 3.3-XV

540°C (1000°F) TENSILE STRENGTH OF FORGINGS

Alloy	S/N	Strain Rate Min^{-1}	0.2% YS (MN/m^2)	0.2% YS (ksi)	UTS (MN/m^2)	UTS (ksi)	El. (%)	R.A. (%)
NASA-TRW-VIA	1	0.1	985	142.5	1390	201.3	14	15
			955	138.4	1335	193.1	12	13
NASA-TRW-VIA	2	0.5	1050	151.9	1425	206.5	13	13
			1060	153.7	1370	198.1	*	11
AF2-1DA	3	0.1	995	144.2	1210	175.7	6	7
			995	144.2	1230	178.5	6	9
AF2-1DA	4	0.5	1045	151.7	1350	195.3	8	12
			1045	151.8	1350	195.7	9	12
Mar-M-432	5	0.1	1125	163.1	1510	229.0	15	20
			1140	165.7	1500	227.2	13	17
Mar-M-432	7	0.5	1175	170.6	1595	231.1	13	18
			1175	170.8	1600	231.8	12	16
MERL 80	6	0.1	1170	169.3	1570	227.5	16	22
			1175	170.8	1565	226.5	14	17
MERL 80	8	0.5	1215	176.2	1605	232.2	12	13
			1205	174.6	1590	231.0	14	17

*Elongation measurement not possible.

TABLE 3.3-XVI

650°C (1200°F) TENSILE STRENGTH OF FORGINGS

Alloy	S/N	Strain Rate Min^{-1}	0.2% YS (MN/m^2)	0.2% YS (ksi)	UTS (MN/m^2)	UTS (ksi)	El. (%)	R.A. (%)
NASA-TRW-VIA	1	0.1	990	143.3	1280	185.3	9	11
			980	142.0	1290	186.9	10	13
NASA-TRW-VIA	2	0.5	1060	153.0	1310	189.2	9	13
			1055	152.7	1315	191.3	10	13
AF2-1DA	3	0.1	1030	149.6	1325	192.0	11	13
			1020	147.2	1290	186.8	8	12
AF2-1DA	4	0.5	1050	152.3	1380	198.1	9	12
			1045	151.7	1340	194.5	9	12
Mar-M-432	5	0.1	1130	163.7	1460	211.7	15	20
			1130	163.7	1460	211.7	17	21
Mar-M-432	7	0.5	1180	170.2	1480	214.5	14	18
			1180	170.6	1470	213.7	10	16
MERL 80	6	0.1	1170	169.7	1400	203.3	6	9
			1180	170.3	1445	209.7	4	13
MERL 80	8	0.5	1220	177.1	1455	212.5	6	8
			1190	173.0	1450	210.1	16	16

TABLE 3.3-XVII

650°C/1035 MN/m^2 (1200°F/150 ksi) CREEP-RUPTURE OF FORGINGS

Alloy	S/N	Strain Rate Min^{-1}	Time to, hours 0.5%	2.0%	Rupture	El.* (%)
NASA-TRW-VIA	1	0.1	0.5	9.5	10.6	6.0
			0.5	–	10.2	5.0
NASA-TRW-VIA	2	0.5	4.2	30.0	51.4	5.0
			2.0	22.0	24.7	4.0
AF2-1DA	3	0.1	1.0	7.0	13.6	5.0
			2.0	11.0	24.4	4.0
AF2-1DA	4	0.5	1.7	15.7	35.1	4.0
			2.0	12.0	37.0	5.0
Mar-M-432	5	0.1	2.0	8.0	22.7	5.3
			1.5	14.0	52.2	7.0
Mar-M-432	7	0.5	1.0	5.2	18.8	10.0
			1.0	5.5	21.4	9.0
MERL 80	6	0.1	2.0	9.0	19.6	2.6
			3.0	14.0	14.4	2.0
MERL 80	8	0.5	1.5	7.2	14.7	6.0
			1.5	–	4.3	1.4

*Measured at room temperature after rupture.

TABLE 3.3-XVIII

DENSITY OF FORGINGS

Alloy	S/N	Density, g/cm^3 Location 1 2 3	Density, lb/in^3 Location 1 2 3
NASA-TRW-VIA	1	8.91, 8.84, 8.91	0.323, 0.321, 0.323
NASA-TRW-VIA	2	8.88, 8.95, 8.91	0.322, 0.325, 0.323
AF2-1DA	3	8.23, 8.30, 8.24	0.299, 0.301, 0.299
AF2-1DA	4	8.33, 8.37, 8.34	0.302, 0.304, 0.303
Mar-M-432	5	8.36, 8.48, 8.47	0.303, 0.308, 0.307
Mar-M-432	7	8.50, 8.43, 8.42	0.309, 0.306, 0.306
MERL 80	6	8.99, 8.94, 9.03	0.326, 0.325, 0.328
MERL 80	8	8.96, 8.95, 8.95	0.325, 0.325, 0.325

TABLE 3.3-XIX

ROOM TEMPERATURE TENSILE STRENGTH OF FORGINGS CORRECTED TO DENSITY OF 8.3 g/cm^3 (0.3 lb/in^3)

Alloy	S/N	Strain Rate (Min^{-1})	0.2% YS (MN/m^2)	0.2% YS (ksi)	UTS (MN/m^2)	UTS (ksi)	El. (%)	R.A. (%)
NASA-TRW-VIA	1	0.1	880	127.9	1280	186.8	8	11
			880	127.4	1315	190.5	9	11
NASA-TRW-VIA	2	0.5	955	138.5	1340	194.0	8	10
			950	137.0	1420	205.5	12	13
AF2-1DA	3	0.1	1035	150.0	1350	195.5	8	10
			1035	150.0	1455	211.0	12	11
AF2-1DA	4	0.5	1095	158.5	1530	221.7	14	14
			1095	158.5	1490	215.5	11	12
Mar-M-432	5	0.1	1190	172.5	1640	237.5	10	11
			1190	172.0	1625	235.5	10	11
Mar-M-432	7	0.5	1255	181.5	1710	247.5	12	11
			1235	178.3	1705	247.0	14	16
MERL 80	6	0.1	1135	164.0	1530	213.0	9	11
			1130	163.6	1575	228.0	11	12
MERL 80	8	0.5	1165	169.0	1540	224.0	9	9
			1180	170.8	1520	220.0	8	10

TABLE 3.3-XX

540°C (1000°F) TENSILE STRENGTH OF FORGINGS CORRECTED TO DENSITY OF 8.3 g/cm^3 (0.3 lb/in^3)

Alloy	S/N	Strain Rate Min^{-1}	0.2% YS (MN/m^2)	0.2% YS (ksi)	UTS (MN/m^2)	UTS (ksi)	El. (%)	R.A. (%)
NASA-TRW-VIA	1	0.1	915	132.3	1290	187.0	14	15
			885	128.5	1240	179.3	12	13
NASA-TRW-VIA	2	0.5	975	141.0	1325	192.0	13	13
			985	142.7	1270	184.0	*	11
AF2-1DA	3	0.1	990	143.5	1205	174.5	6	7
			990	143.5	1225	177.5	6	9
AF2-1DA	4	0.5	1040	151.0	1345	194.5	8	12
			1040	151.0	1345	194.5	9	12
Mar-M-432	5	0.1	1100	159.5	1475	224.0	15	20
			1115	162.0	1465	222.0	13	17
Mar-M-432	7	0.5	1150	166.9	1560	226.0	13	18
			1150	166.9	1565	226.4	12	16
MERL 80	6	0.1	1080	156.1	1450	209.5	16	22
			1082	157.4	1440	208.5	14	17
MERL 80	8	0.5	1120	162.5	1480	214.1	12	13
			1110	161.0	1465	213.0	14	17

*Elongation measurement not possible.

TABLE 3.3-XXI

650°C (1200°F) TENSILE STRENGTH OF FORGINGS CORRECTED TO DENSITY OF 8.3 g/cm^3 (0.3 lb/in^3)

Alloy	S/N	Strain Rate Min^{-1}	0.2% YS (MN/m^2)	0.2% YS (ksi)	UTS (MN/m^2)	UTS (ksi)	El. (%)	R.A. (%)
NASA-TRW-VIA	1	0.1	920	133.2	1190	172.2	9	11
			910	131.9	1200	173.5	10	13
NASA-TRW-VIA	2	0.5	985	142.1	1220	176.0	9	13
			980	141.9	1220	177.8	10	13
AF2-1DA	3	0.1	1025	148.5	1320	191.0	11	13
			1015	146.5	1285	185.5	8	12
AF2-1DA	4	0.5	1045	151.6	1375	197.1	9	12
			1040	150.8	1335	193.5	9	12
Mar-M-432	5	0.1	1105	160.0	1430	206.6	15	20
			1105	160.0	1430	206.6	17	21
Mar-M-432	7	0.5	1155	166.5	1445	210.0	14	18
			1155	167.0	1440	208.8	10	16
MERL 80	6	0.1	1080	156.2	1290	187.3	6	9
			1090	157.0	1330	193.0	4	13
MERL 80	8	0.5	1125	168.3	1340	195.5	6	8
			1095	159.5	1335	194.0	16	16

TABLE 3.3-XXII

650°C/1035 MN/m^2 (1200°F/150 ksi) CREEP-RUPTURE OF FORGINGS CORRECTED TO DENSITY OF 8.3 g/cm^3 (0.3 lb/in^3)

Alloy	S/N	Strain Rate Min^{-1}	Time to, hours: 0.5%	2.0%	Rupture	El.* (%)
NASA-TRW-VIA	1	0.1	0.5	8.8	9.8	6.0
			0.5	–	9.5	5.0
NASA-TRW-VIA	2	0.5	3.9	27.9	47.7	5.0
			1.9	20.4	22.9	4.0
AF2-1DA	3	0.1	1.0	6.9	13.5	5.0
			2.0	10.9	24.0	4.0
AF2-1DA	4	0.5	1.7	15.6	35.0	4.0
			2.0	11.9	37.0	5.0
Mar-M-432	5	0.1	2.0	7.8	22.2	5.3
			1.5	13.7	51.1	7.0
Mar-M-432	7	0.5	1.0	5.1	18.4	10.0
			1.0	5.4	20.9	9.0
MERL 80	6	0.1	1.8	8.3	18.1	2.6
			2.8	12.9	13.3	2.0
MERL 80	8	0.5	1.4	6.6	13.6	6.0
			1.4	–	4.0	1.4

*Measured at room temperature after rupture.

TABLE 3.3-XXIII

650°C (1200°F) TENSILE RESULTS OF FORGINGS AFTER 1000 HOUR EXPOSURE AT 790°C (1450°F)

Alloy	Forging S/N	0.2% YS		UTS		% El.	% R.A.
		MN/m^2	ksi	MN/m^2	ksi		
NASA-TRW-VIA	1	1035	150.0	1204	174.6	5.4	5.3
		1016	147.3	1120	162.2	5.6	6.1
	2	1110	161.1	1112	173.1	3.5	3.1
		1092	158.1	1192	172.9	2.3	5.0
AF2-1DA	3	986	142.9	1161	168.2	4.7	4.3
		1002	145.1	1161	168.2	5.4	5.0
	4	1093	158.6	1260	182.8	4.5	7.1
		1093	158.6	1259	182.6	5.8	4.2
Mar-M-432	5	1153	167.1	1322	191.8	13.0	11.4
		1153	167.1	1315	190.7	14.1	14.2
	7	1169	169.3	1362	197.1	12.1	14.2
		1197	173.3	1384	200.7	14.0	16.2
MERL 80	6	1165	168.9	1290	187.0	8.3	8.3
		1135	164.6	1287	186.6	7.7	5.0
	8	1170	169.6	1300	188.3	8.2	8.1
		1169	169.3	1231	178.6	6.0	5.3

TABLE 3.3-XXIV

REVISED THERMOMECHANICAL PROCESSING CONDITIONS EVALUATED

Alloy	Prior Thermal Exposure	TMP Sequence	
		Temperature	Strain Rate
NASA-TRW-VIA	1120°C (2050°F)/2 hours/AC	1010°C (1850°F)	1.25 min^{-1}
AF2-1DA	1175°C (2150°F)/2 hours/FC → 1120°C (2050°F)/2 hours/AC	1010°C (1850°F)	1.25 min^{-1}
AF2-1DA	1120°C (2050°F)/2 hours/AC	1010°C (1850°F)	1.25 min^{-1}
Mar-M-432	1175°C (2150°F)/2 hours/FC → 1120°C (2050°F)/2 hours/AC	1010°C (1850°F)	1.25 min^{-1}
Mar-M-432	1120°C (2050°F)/2 hours/AC	980°C (1800°F)	1.25 min^{-1}
MERL 80	1245°C (2275°F)/2 hours/FC → 1120°C (2050°F)/2 hours/AC	980°C (1800°F)	1.25 min^{-1}
MERL 80	1120°C (2050°F)/2 hours/AC	980°C (1800°F)	1.25 min^{-1}

TABLE 3.3-XXV

SUBSCALE FORGING MULTIPLE THERMAL PRE-TREATMENTS

Alloy	Heat Treatment
NASA-TRW-VIA	1260°C (2300°F)/2 hours/FC → 1120°C (2050°F/2 hours/AC
AF2-1DA	1175°C (2150°F)/2 hours/FC → 1120°C (2050°F)/2 hours/AC
Mar-M-432	1175°C (2150°F)/2 hours/FC → 1120°C (2050°F)/2 hours/AC
MERL 80	1230°C (2250°F)/2 hours/FC → 1120°C (2050°F)/2 hours/AC

TABLE 3.3-XXVI

TENSILE STRENGTHS OF SUBSCALE PANCAKES FORGED AT WYMAN-GORDON

Alloy	Temperature	0.2% YS MN/m^2	0.2% YS ksi	UTS MN/m^2	UTS ksi	% El.	% R.A.
AF2-1DA	RT	1510	218.7	1634	236.8	5.2	4.3
	650°C(1200°F)	1360	197.1	1452	210.3	5.2	7.8
Mar-M-432	RT	1622	235.3	1950	282.7	11.2	12.3
	650°C(1200°F)	1430	207.7	1550	224.7	9.3	8.1
MERL 80	RT	1493	216.2	1840	266.4	9.2	7.0
	RT	1528	221.5	1824	264.2	6.2	6.0
	650°C(1200°F)	1375	199.3	1492	216.1	6.8	6.5
	650°C(1200°F)	1418	205.7	1525	221.4	6.0	6.2

TABLE 3.3-XXVII

650°C/1035 MN/m^2 (1200°F/150 ksi) CREEP STRENGTHS OF SUBSCALE PANCAKES FORGED AT WYMAN-GORDON COMPANY

Alloy	Time to, Hours 0.2% Creep	Rupture
AF2-1DA	N.A.*	79.0
Mar-M-432	1.6(0.25%)	8.7
MERL 80	0.7	16.3
MERL 80	0.8	13

*N.A. = Not Available

TABLE 3.3-XXVIII

TENSILE RESULTS FOR FORGINGS MADE AT WYMAN-GORDON

Alloy	Temperature	0.2% YS MN/m^2	0.2% YS ksi	UTS MN/m^2	UTS ksi	% El.	% R.A.
NASA VIA	RT	1299	188.3	1660	240.8	8.6	7.2
	650°C(1200°F)	1270	184.1	1416	205.7	5.5	3.2
AF2-1DA	RT	1438	208.1	1840	266.8	13.4	14.3
	650°C(1200°F)	1283	186.1	1470	213.3	13.0	17.5
Mar-M-432	RT	1252	181.5	1727	250.2	18.1	18.4
	650°C(1200°F)	1170	169.9	1362	197.8	13.1	16.8
MERL 80	RT	1298	188.0	1822	264.2	15.4	14.5
	650°C(1200°F)	1258	182.2	1425	206.7	9.8	11.1

TABLE 3.3-XXIX

CREEP-RUPTURE DATA FOR FORGINGS MADE AT WYMAN-GORDON

Alloy	Temperature	Stress	Time to, hrs. 0.2%	Rupture	% El.	% R.A.
NASA VIA	650°C(1200°F)	1035 MN/m^2 (150 ksi)	16.9	402.4	N/A**	N/A**
AF2-1DA	650°C(1200°F)	1035 MN/m^2 (150 ksi)	0.4	8.3	8.49	12.0
Mar-M-432	650°C(1200°F)	1035 MN/m^2 (150 ksi)	0.8	21.2	5.11	10.9
MERL 80	650°C(1200°F)	1035 MN/m^2 (150 ksi)	1.5	2.9*	N/A*	N/A*

* Thread Failure
** N/A = Not Available

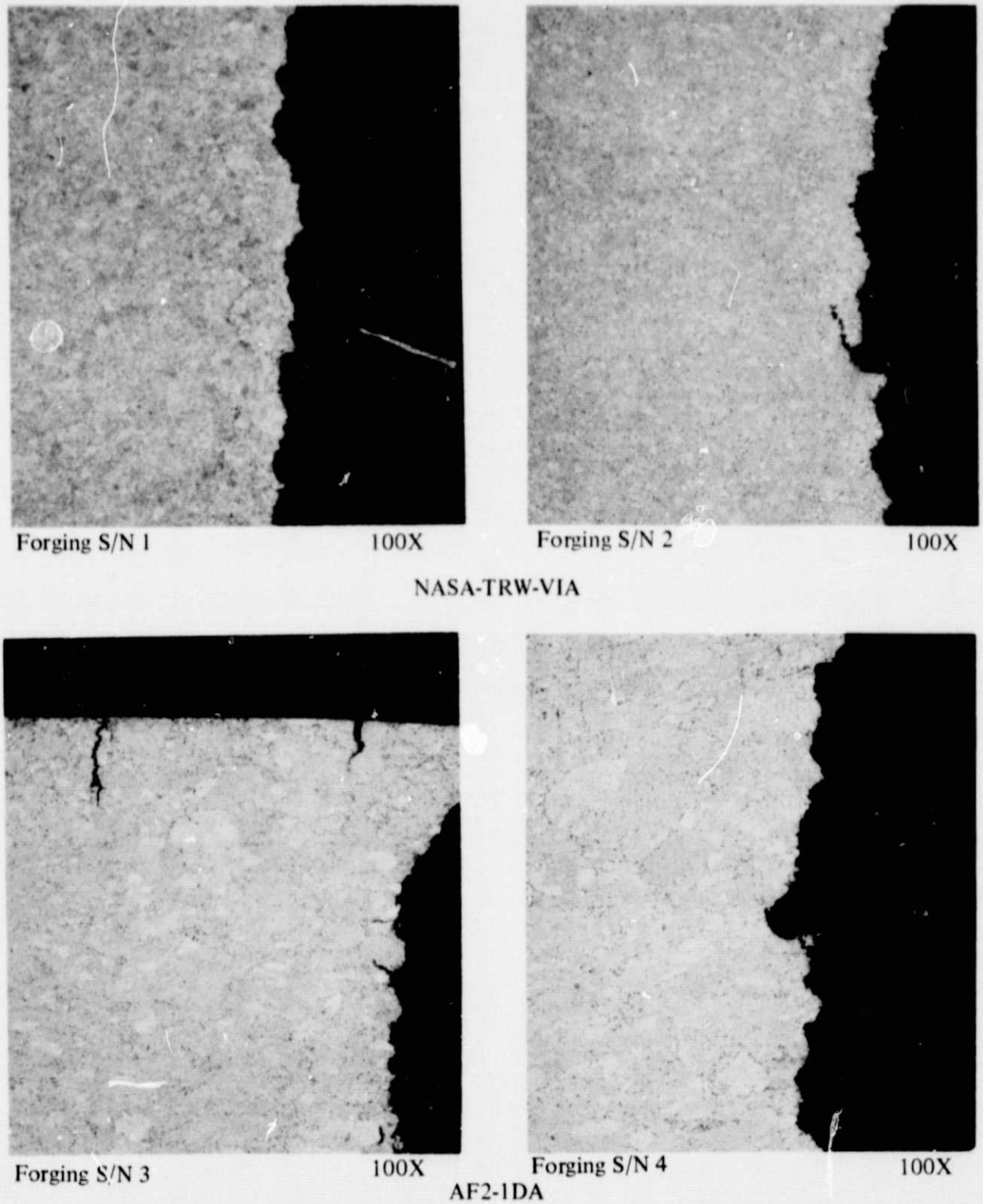

Figure 3.3-20 Microstructures of Forgings After 650°C/1035 MN/m^2 (1200°F/150 ksi) Creep Test

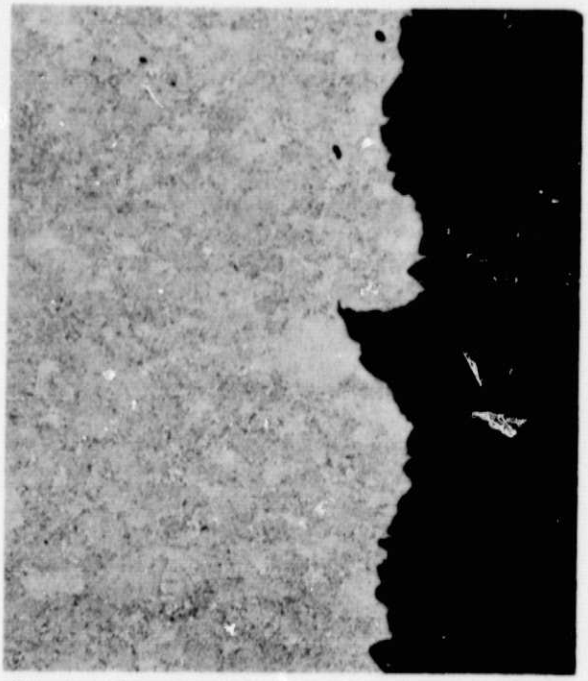

Forging S/N 5 100X

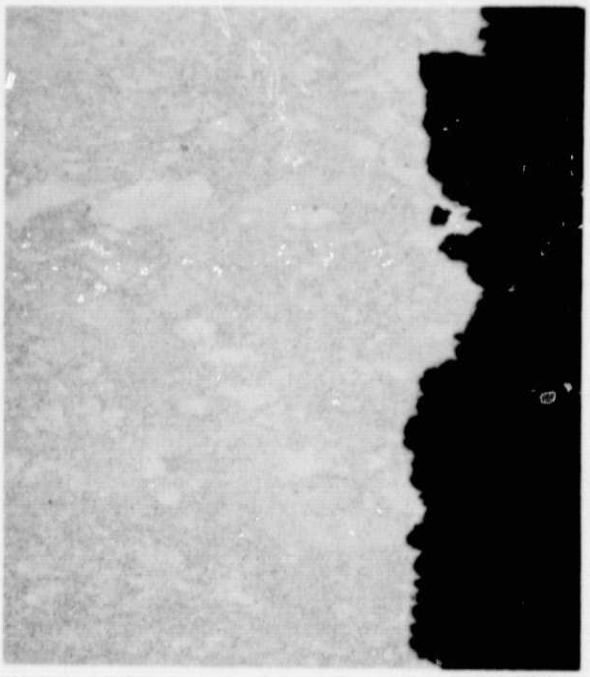

Forging S/N 7 100X

Mar-M432

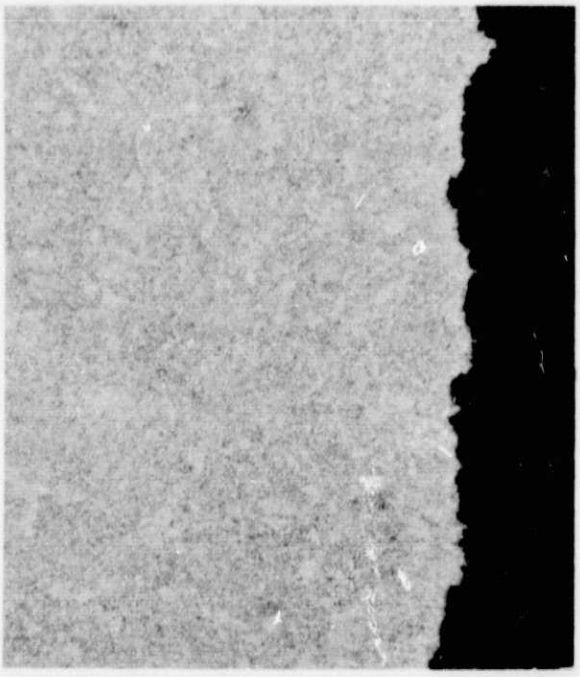

Forging S/N 6 100X

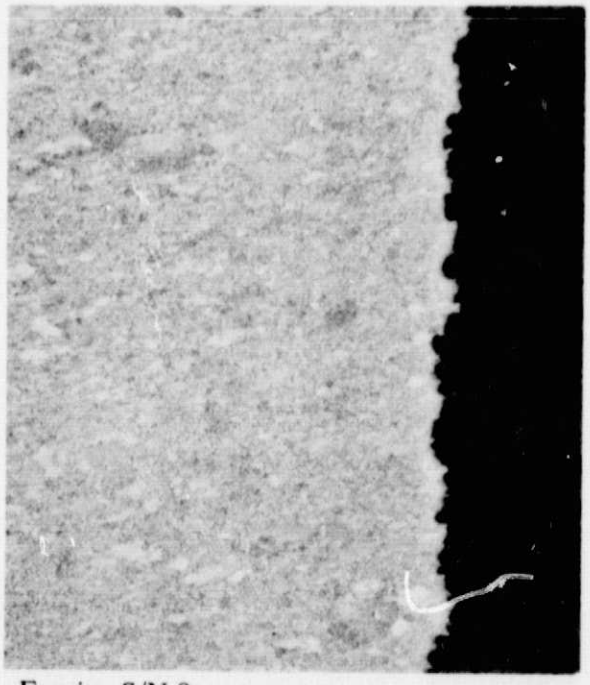

Forging S/N 8 100X

MERL-80

Figure 3.3-21 Microstructures of Forgings After 650°C/1035 MN/m^2 (1200°F/150 ksi) Creep Test

Forging S/N 1 500X

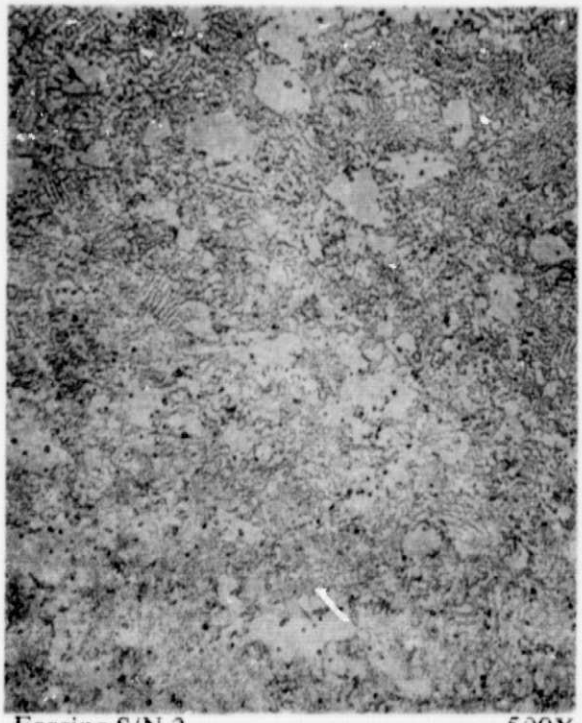

Forging S/N 2 500X

NASA-TRW-VIA

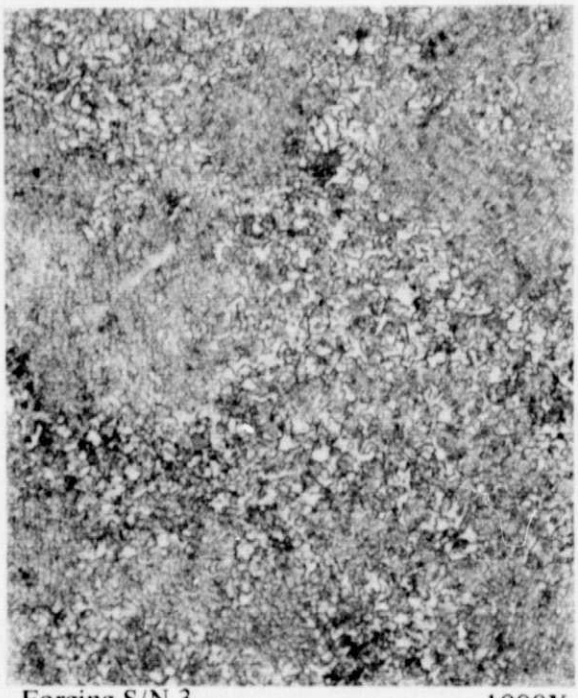

Forging S/N 3 1000X

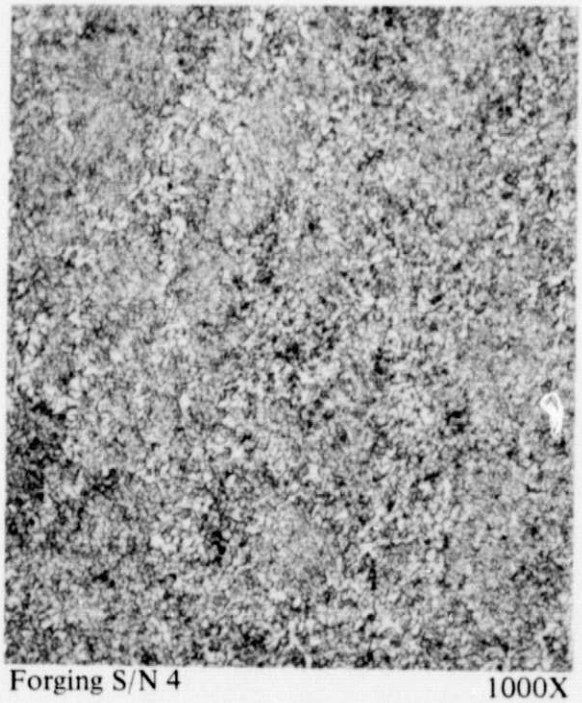

Forging S/N 4 1000X

AF2-1DA

Figure 3.3-22 Microstructures of Forgings After 1000 Hours Exposure at 790°C (1450°F)

Forging S/N 5 500X

Forging S/N 7 500X

Mar-M432

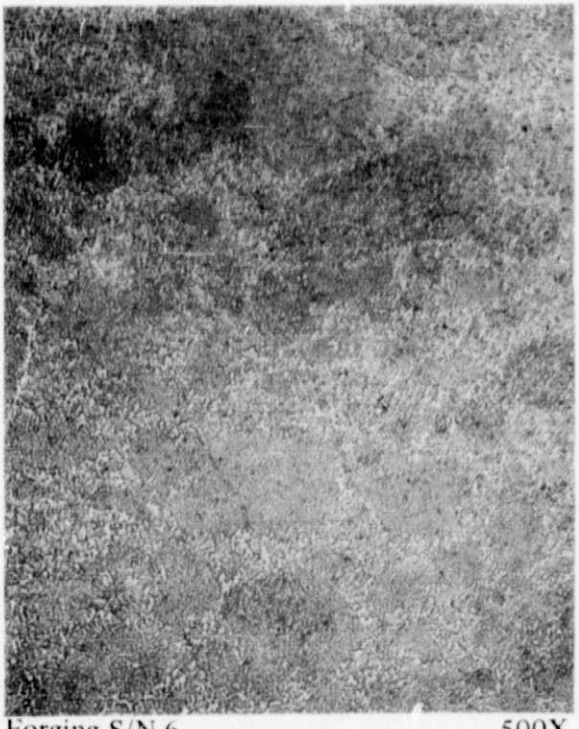

Forging S/N 6 500X

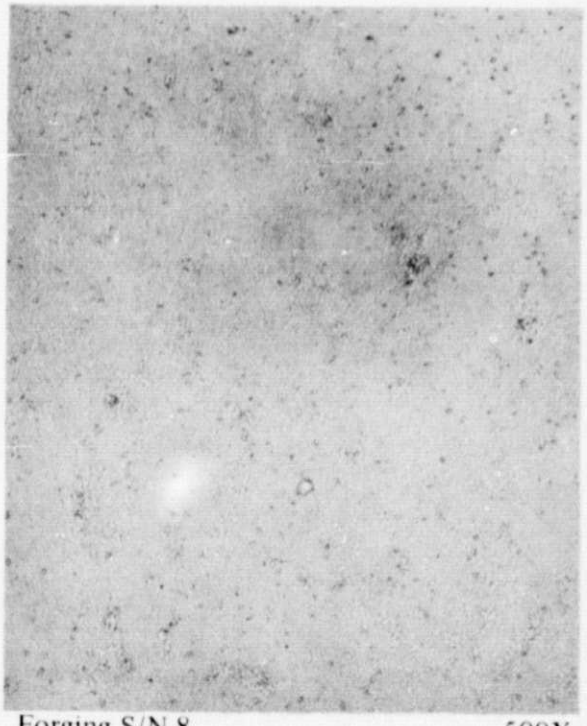

Forging S/N 8 500X

MERL-80

Figure 3.3-23 Microstructures of Forgings After 1000 Hours Exposure at 790°C (1450°F).

4.0 TASK II SCALE-UP STUDY AND EVALUATION

Based on the results of Task I, Mar-M-432 and AF2-1DA were selected for further evaluation in Task II. Under this task more extensive physical property tests were conducted and full-scale turbine disks were fabricated. Figure 4.0-I outlines the scale-up study and evaluation sequence followed in Task II.

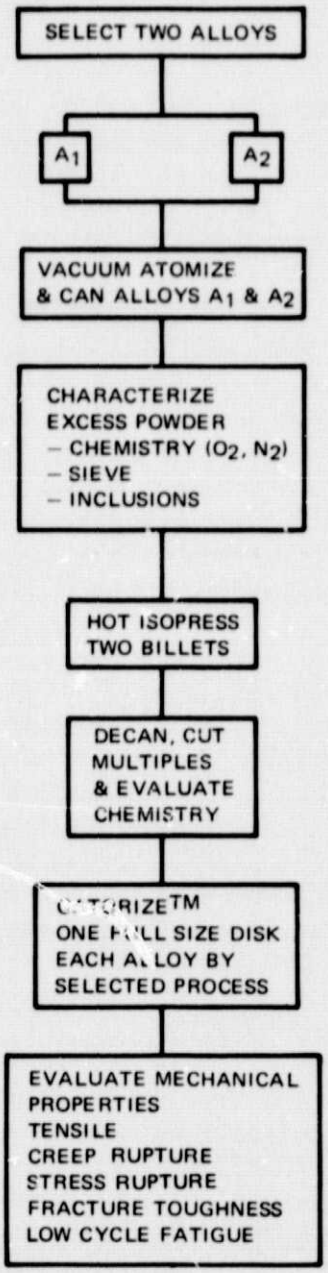

Figure 4.0-1 Task II Alloy and Process Scale-Up Study and Evaluation Sequence

4.1 SUBSCALE STUDIES ON SELECTED ALLOYS

4.1.1 Attempt to Improve Material Properties

The evaluation conducted under Task I indicated that, on a density-corrected basis, Mar-M-432 and AF2-1DA were the two most promising alloys for alloy/process scale-up in Task II. However, the desired combination of improved tensile strengths and longer creep-rupture lives had not been achieved through a single thermomechanical process for either alloy.

In an attempt to achieve improved creep characteristics without sacrificing tensile strength, different forging schedules were developed and two subscale HIP compacts were prepared for each alloy. These compacts were 0.06 m (2.5 inches) in diameter by 0.14 m (5.37 inches) high. Hot isostatic pressing was accomplished at Industrial Materials Technology, Woburn, Massachusetts at 1175°C (2150°F) and 103.5 MN/m^2 (15,000 psi) for two hours.

Prior to forging at Wyman-Gordon Co. each billet was wrapped in fiberglass cloth, which insulated the billets against die chill and also served as a lubrication. Each billet was contained within thin sheets of Inconel, which aided in heat retention and provided a grip for transferring the billets from the preheating furnace to the forge press. Billet preheating was done at 1040°C (1900°F). Two forging schedules were devised; one was directed toward developing maximum tensile properties (Schedule A) and the second toward optimizing creep-rupture behavior (Schedule B). Conventional forging techniques using heated dies were used. The sequence of operations for these two forging schedules is summarized in Table 4.1-I.

Load versus reduction-in-height data was recorded throughout forging the subscale billets. By dividing billet volume by height, the area after each step in the forging schedule was calculated. An average forging stress was then determined, dividing final forging load by area. These data are plotted as a function of reduction-in-height for the two alloys in Figures 4.1-2 and 4.1-3. For each alloy, forging Schedule B, with intermediate recovery anneals at 1090°C (2000°F) resulted in higher final forging stresses. Increased interfacial friction was judged to be a possible contributing factor to these stresses but the more probable cause was the planned retention of a more coarse grain size to result in improved creep-rupture behavior.

4.1.2 Resulting Improved Material Properties

Mechanical property evaluation of the four subscale billets, two of each alloy, forged at Wyman-Gordon Company included tensile testing at room temperature and 650°C (1200°F) and creep-rupture testing at 650°C/1035 MN/m^2 (1200°F/150 ksi). Results of these tests, summarized in Tables 4.1-II through 4.1-IV, confirm tensile results obtained on Task I subscale forgings and indicate improvements in creep-rupture behavior of the alloys.

The AF2-1DA three-step direct-aged pancake forging exhibited cracks and although sound specimens were produced for conducting tensile testing, a sound creep-rupture test

specimen, of the required size, could not be produced. Consequently, as indicated in Table 4.1-IV, creep rupture strength tests were not conducted on the AF2-1DA three-step forging. However based on the Mar-M-432 test data, it was judged that the results of the omitted test would have shown that the creep-rupture life of the direct-aged forging would have been less than nine-step, partial solution plus age forging.

Upon completion of the mechanical property evaluation of the forgings, an assessment was made regarding the feasibility of scale-up of either the Schedule A or Schedule B processing technique to an economical, production forging sequence for full size disks up to 0.432m (17 inches) in diameter. It was concluded that in using either forging procedure reproducibility would be difficult to control and the process would be more expensive than the GATORIZING™ approach taken in Task I. Therefore, it was decided to use the GATORIZING™ forging process to produce the full size disks for evaluation in Task II.

TABLE 4.1-I

SUBSCALE FORGING SCHEDULES FOR PROCESS OPTIMIZATION

Schedule A	Schedule B
1) Preheat billet to 1040°C (1900°F) hold for 30 minutes	1) Preheat billet to 1040°C (1900°F), hold for 30 minutes
2) Forge 30 percent reduction in height on 925°C (1700°F) dies	2) Forge 15 percent reduction in height on 925°C (1700°F) dies
3) Return to 1040°C (1900°F) furnace, restore temperature, hold for 15 minutes	3) Place forging in 1090°C (2000°F) furnace, allow to come to temperature, hold 15 minutes
4) Repeat second and third actions above, forging to a final thickness of 0.030-0.033m (1.2-1.3 inches), oil quench from final forging reduction	4) Return forging to 1040°C (1900°F) furnace, allow to come to temperature, hold 15 minutes
5) Heat treat at 760°C (1400°F) for 16 hours, air cool to room temperature	5) Repeat second, third, and fourth actions above until final forging height of 0.030-0.033m (1.2-1.3 inches) is reached; oil quench from final forging reduction
	6) Heat treat 870°C (1600°F) for 16 hours, furnace heat to 1090°C (2000°F) for 1 hour, oil quench, plus 760°C (1400°F) for 16 hours, air cool to room temperature

TABLE 4.1-II

ROOM TEMPERATURE TENSILE STRENGTH OF SUBSCALE FORGINGS

Alloy	Thermomechanical Processing*	0.2% YS MN/m^2	0.2% YS ksi	UTS MN/m^2	UTS ksi	%El.	%R.A.
AF2-1DA	3 Step Forge; D.A.	1523	220.7	1619	234.6	3.0	3.2
	9 Step Forge; P.S.A.	1315	190.6	1701	246.6	14.0	13.2
	9 Step Forge; P.S.A.	1275	184.8	1784	258.5	9.6	7.6
Mar-M-432	3 Step Forge; D.A.	1624	235.3	1853	268.5	7.2	6.3
	3 Step Forge; D.A.	1599	231.7	1824	264.3	6.7	8.1
	3 Step Forge; D.A.	1555	225.3	1883	272.9	10.0	10.4
	9 Step Forge; P.S.A.	1466	212.4	1855	268.9	15.8	16.4
	9 Step Forge; P.S.A.	1431	207.4	1833	265.7	14.5	16.2

*P.S.A. = Partial solution + age; D.A. = Direct age

TABLE 4.1-III

650°C (1200°F) TENSILE STRENGTH OF SUBSCALE FORGINGS

Alloy	Thermomechanical Processing*	0.2% YS MN/m^2	0.2% YS ksi	UTS MN/m^2	UTS ksi	%El.	%R.A.
AF2-1DA	3 Step Forge; D.A.	1345	195.0	1484	215.0	1.7	1.0
	3 Step Forge; D.A.	1331	192.9	1435	208.0	2.2	2.1
	9 Step Forge; P.S.A.	1212	175.7	1434	207.8	9.5	9.2
	9 Step Forge; P.S.A.	1207	174.9	1425	206.6	7.7	6.2
Mar-M-432	3 Step Forge; D.A.	1345	195.0	1566	227.0	7.1	9.1
	3 Step Forge; D.A.	1330	192.7	1511	219.0	6.6	6.2
	9 Step Forge; P.S.A.	1316	190.8	1517	219.8	7.0	6.3
	9 Step Forge; P S.A.	1267	183.6	1525	221.0	12.0	18.0

*D.A. = Direct age; P.S.A. = Partial solution + age

TABLE 4.1-IV

650°C/1035 MN/m^2 (1200°F/150 ksi) CREEP-RUPTURE STRENGTH

Alloy	Thermomechanical Processing*	Time to Hours 0.1%	0.2%	Rupture	%El.	%R.A.
AF2-1DA	9 Step Forge; P.S.A.	1.15	3.5	34.1	1.94	10.4
	9 Step Forge; P.S.A.	1.20	4.2	24.6	1.20	7.76
Mar-M-432	3 Step Forge; D.A.	0.1	0.25	4.8	3.37	7.68
	3 Step Forge; D.A.	0.1	0.20	4.3	6.97	10.20
	9 Step Forge; P.S.A.	0.2	0.5	9.2	3.74	13.0
	9 Step Forge; P.S.A.	0.1	0.4	11.2	5.49	8.65

*P.S.A. = partial solution + age; D.A. = direct age

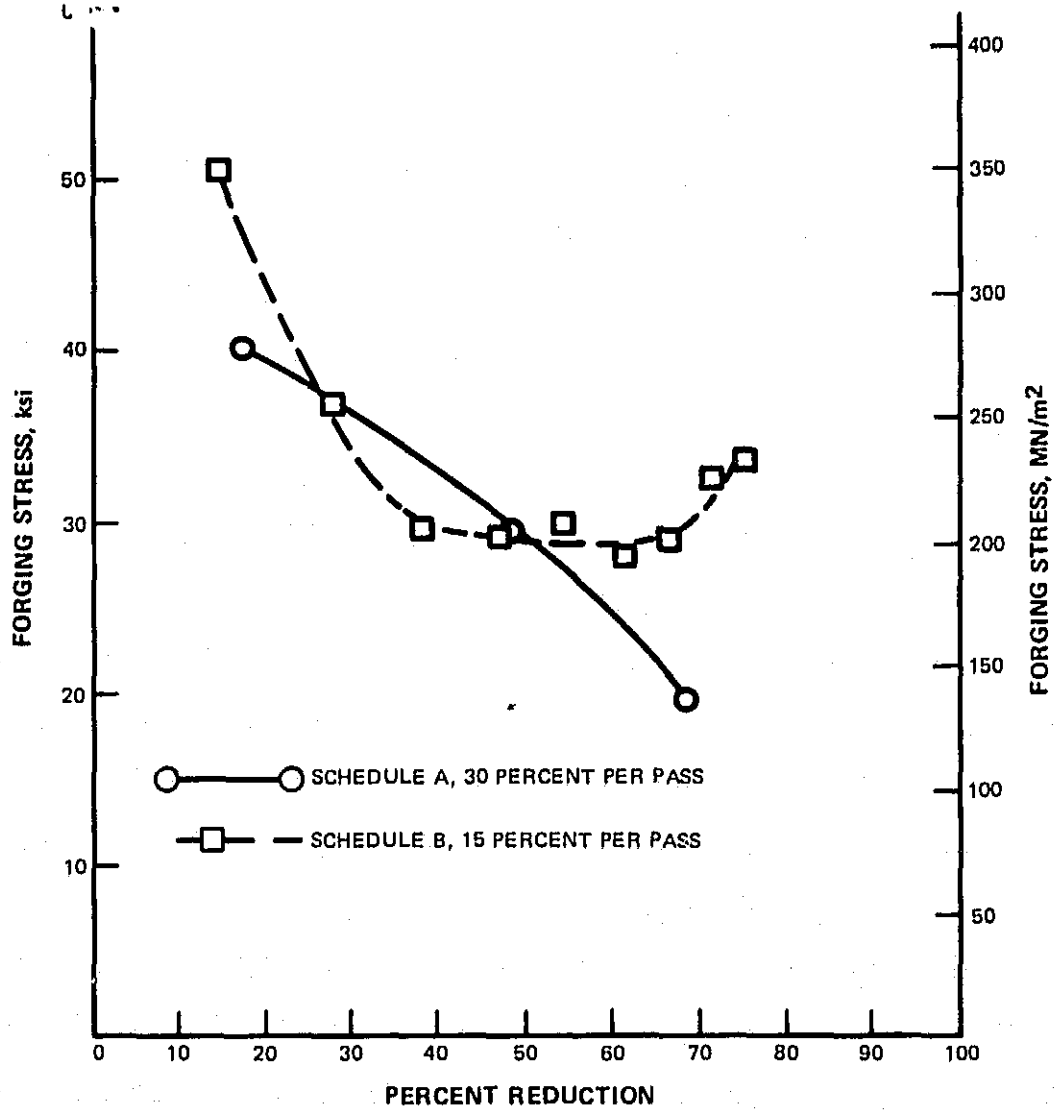

Figure 4.1-2 Forging Stress Versus Percent Reduction for Subscale Mar-M432 Forgings

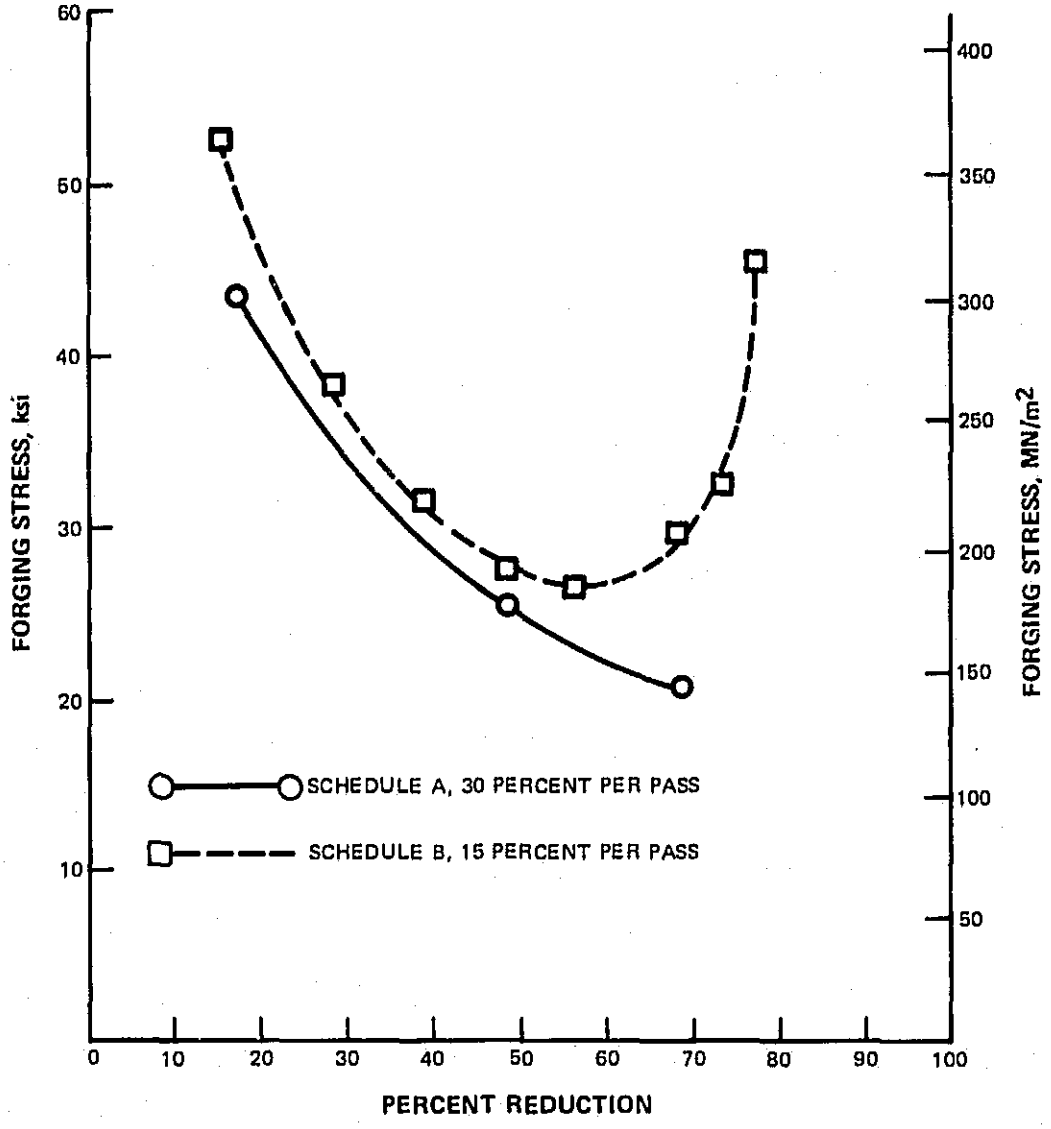

Figure 4.1-3 Forging Stress Versus Percent Reduction for Subscale AF2-1DA Forgings

4.2 MATERIAL PROCESSING OF TASK II DISK FORGINGS

4.2.1 Disk Fabrication and Microstructural Evaluation

A sufficient amount of vacuum induction melted bar was ordered from Alloy Division, Howmet Corporation, Dover, New Jersey for atomization of the powders of AF2-1DA and Mar-M-432. The remelt stock, supplied in a 0.07m (2.75 inches) diameter bar, was shipped directly to Homogeneous Metals, Inc., Herkimer, New York where it was vacuum atomized to -60 mesh powder using the procedures discussed in Section 3.0 of this report.

Two stainless steel containers, 0.267m (10.5 inches) in diameter by 0.357m (14 inches), were filled with -60 mesh powder under all-inert handling conditions, evacuated, and sealed. The balance of the powder from each alloy was shipped to Pratt & Whitney Aircraft for powder characterization studies.

Results of particle size distribution and chemical analysis of the powders are summarized in Tables 4.2-V, 4.2-VI, and 4.2-VII.

The billets for full-scale disk forging were consolidated at Battelle Memorial Institute at 1175°C (2150°F) and 105 MN/m^2 (15,000 psi) for two hours. Figure 4.2-4 shows the billets after consolidation while Figures 4.2-5 and 4.2-6 show the as-consolidated microstructure.

The Mar-M-432 structure contained a distribution of coarse gamma prime at the prior powder particle boundaries. Fewer of what appeared to be MC-type carbides were seen at the boundaries. Although the amount of carbides seen in the AF2-1DA structure was more than the amount in the Mar-M-432 (as would be expected for its nominal 0.35 percent carbon level), the build-up of carbides at prior particle boundaries was not excessive. It was anticipated that the minimal prior particle boundary carbides plus the gamma prime concentration in Mar-M-432 would assist in forgeability.

Density measurements were made and chemical analysis was determined on the as-consolidated billets at P&WA. Duplicate density measurements showed good agreement for the Mar-M-432, but some unexplained scatter was noted for the AF2-1DA. Density measurements of the two alloys are listed in Table 4.2-VIII. Chemical analysis of the billets are presented in Table 4.2-IX.

After reviewing alloy properties achieved in conducting Task I as well as projected productivity and property repeatability using high strain rate TMP approaches, it was decided to forge the two Task II billets using hot die, low strain rate (0.1 min^{-1}) GATORIZING™ forging techniques. Forging temperatures were established by P&WA at 1090°C (2000°F) for Mar-M-432 and 1135°C (2075°F) for AF2-1DA. These temperatures were approximately 14°C (25°F) above the Task I forging levels made at Ladish Company, and were increased to reduce forging stress and increase forging die life.

Two forging billets, 0.23m (9 inches) in diameter by 0.23m (9 inches) high were machined from the as-consolidated compacts, and conical shaped locating centers were machined in each end to allow accurate positioning in the dies. Forging was done on the P&WA, East

Hartford, 3000 ton hydraulic press, using TZM molybdenum alloy dies currently used for forging production engine disks. Figure 4.2-7 is a cross sectional schematic of the disk configuration.

Because the size of the billets was incompatible with the automatic handling device, the billets were manually loaded onto cold dies. The billet-die stack combination was induction heated to the desired forging temperature and allowed to reach thermal equilibrium before forging. The entire die stack-heater assembly, together with a manipulator assembly for billet loading and disk removal, was enclosed in a vacuum system to protect the molybdenum alloy dies from oxidation. Forging temperature was monitored by eight thermocouples located at various positions in the die stack, and was controlled at 1040°C (2000°F) for the Mar-M-432 and 1135°C (2075°F) for the AF2-1DA disk. Forging strain rate was automatically controlled at 0.1 min^{-1} throughout the entire operation by means of a strain rate controller. Upon completion of the disk forging cycle, each disk was removed from dies and removed from the furnace using an automatic part manipulator and a series of load locks. The forgings were then allowed to air cool to room temperature.

Initial examination of the forgings, Figures 4.2-8 and 4.2-9, indicated that the Mar-M-432 disk had experienced extensive radial cracking at the rim, with some additional rupturing of the spacer protrusions. The AF2-1DA disk was completely sound. Because the two alloys had exhibited approximately equal forgeability during Task I subscale forging trials, it was apparent that some unknown factors had adversely affected the forgeability of the Mar-M-432 disk.

Initial measurements of the two forgings indicated slight differences in size, as noted in Table 4.2-X. This was attributed to the fact that the billets, approximately 10450 cm^3 (572 in^3) volume, overflowed the 7420 cm^3 (450 in^3) volume of the die cavity and the dies did not reach the fully-closed position during forging. Consequently a slight difference in the dimensional height of the billets would result in slight differences in the forging material distribution. The reason for the excess billet volume was to ensure sufficient availability of forged material so that the required test specimens could be fabricated.

Metallographic evaluation of small sections cut from the rim of each disk was conducted. As seen in Figure 4.2-10, the AF2-1DA structure was sound and apparently typical of hot isostatically pressed and forged AF2-1DA. The Mar-M-432 (Figure 4.2-11) exhibited gross porosity and as well as tearing along powder particle boundaries. This was more prevalent at the surface, but persisted to a depth of 0.006m (0.25-inch) below the surface at some locations. Tearing of this type, plus the porosity associated with powder particle boundaries, has been detected previously in hot isostatically pressed powder metallurgy compacts which sustain minor can leaks during HIP. A small volume of gas which leaks into the container can prevent metallurgical bonding between particles, although not preventing 100 percent mechanical consolidation. Consequently it is not possible to completely confirm by metallographic evaluation of the as-consolidated billet whether or not such a leak had occurred.

Ultrasonic inspection of the forgings was accomplished at P&WA by laboratory, longitudinal mode C-scan techniques, involving automatic radial indexing of the transducer, while rotating the disk about its center line. Because no standards existed for either Mar-M-432 or

AF2-1DA forgings, the qualitative evaluations made used production experience gained from inspecting disks fabricated from powder metallurgy IN-100.

The AF2-1DA disk, which was visually and microstructurally sound, gave excellent sonic response in the as-forged condition. Approximately one quadrant of the disk had a somewhat higher background noise level than the remainder. Careful attention was paid to the microstructure throughout this area when removing mechanical property test specimens. In addition to the region of increased background noise, four regions of suspected sonic defects were also detected. Three were in the general area of the high noise region, while one was approximately 180° removed from the others.

The Mar-M-432 disk showed a very high noise level throughout the disk and an especially high noise level in the center. Certain areas which had surface distress had a loss in back-face signal resolution. A total of seven indications were noted, scattered circumferentially around the disk. Most of these indications were located in the thick flange area, with some near the top surface and others near the axial mid-plane.

Both disks were heat treated in the Pratt & Whitney Aircraft production heat treat shop. Solution treatment of 1125°C (2050°F) for four hours followed by an oil quench was chosen to balance high tensile strengths with an adequate rupture behavior. A single-step precipitation heat treatment of 760°C (1400°F) for 16 hours with an air cool was selected to effectively develop a fine gamma prime structure while keeping overall heat treatment costs (for future production considerations) at a reasonable level.

During heat treatment of the two full size disk forgings, the Mar-M-432 disk cracked into four pieces. Metallographic examination of the disk was performed at several representative locations and the entire structure was found to be highly porous (Figure 4.2-12.) This phenomenon, as noted previously, is very indicative of a hot isostatically pressed compact which developed a can leak during the early stages in the compaction cycle. The extensive porosity of the material precluded any mechanical property evaluation of this disk forging and no further evaluation of the Mar-M-432 disk was made.

The AF2-1DA disk exhibited a typical microstructure consisting of coarse, over-aged gamma prime mixed with a dispersion of fine, aging gamma prime and fine, well interspersed carbides (Figure 4.2-13).

In order to evaluate the microstructural stability of the AF2-1DA disk after prolonged periods of exposure to elevated temperatures, radial sections of the disk were subjected to 1500 hour exposures at 650 and 705°C (1200 and 1300°F). These temperatures reflect anticipated disk rim operating temperatures and a 55°C (100°F) temperature overshoot capability for advanced gas turbine engines. The effect of these periods of high temperature exposure on both microstructure and tensile properties (smooth and notched) was evaluated.

Microstructural characterization of the AF2-1DA billet and disk forging consisted of metallographic documentation throughout each step of the thermomechanical processing, as well as phase identification by X-ray diffraction. Metallographic techniques involved

conventional optical microscopy examination at magnifications to 1000X, and replica and thin-foil transmission electron microscopy at higher magnifications. Subsequent discussion in this report will treat characterization of the AF2-1DA structure at each step in processing.

Optical microscopy of the as-consolidated billet revealed a structure consisting of relatively fine grained (ASTM 8 or approximately 15-20 μm diameter) material, where there was a detectable, but not pronounced outlining of prior powder particle boundaries with discrete globular particles, presumably MC-type carbides (Figure 4.2-6). Although the carbon content of AF2-1DA (0.35 weight percent, nominal) is approximately five to nine times higher than that of currently used powder metallurgy, nickel-base superalloys (IN-100 at 0.07 percent, René 95 at 0.06 percent, and Astroloy at 0.04 percent), no heavy carbide agglomeration was noted. The distribution of fine carbides in the as-consolidated billet was uniform and well dispersed.

Replica electron microscopy of the as-consolidated billet (Figure 4.2-14) indicated that three distinct sizes of gamma prime exist, in addition to the carbides and borides which are frequently associated with the largest gamma prime. Consolidation was accomplished at 1175°C (2150°F), which is within 5.5°C (10°F) of the gamma prime solvus for the alloy. Consequently large, irregularly shaped gamma prime particles outline grain boundaries where, due to localized microsegregation effects, these particles presumably had a slightly higher solution temperature than the matrix gamma prime within the grain. These former particles coarsened during HIP, while the latter appear to have gone into solution, and re-precipitated rather uniformly as more regular (sometimes cuboidal) particles. A third, much finer sized particle is also seen in Figure 4.2-14.

Transmission electron micrographs made of the as-consolidated billet confirm the generally regular, cuboidal shape of the intermediate sized gamma prime and show a very low density of dislocations (Figure 4.2-15). This would be expected in a material heated to near the gamma prime solvus and then slowly cooled.

Separate electrolytic extractions were conducted for separating gamma prime and minor phases, such as carbides and borides, from the matrix. Phase identification was made using standard X-ray diffractometer techniques. A quantitative determination of the amount of phases separated indicated a weight percent of gamma prime (approximately equal to volume fraction) of 43.1 percent, while 3.4 percent of the sample consisted of carbide and boride phases. In addition to the gamma prime, carbides of the type MC and $M_{23}C_6$ were observed, as well as M_3B_2-type borides. The relative X-ray diffraction line intensities of the latter two phases were characterized as weak and very weak, respectively. A summary of the diffraction pattern measured for the extracted phases of as-consolidated AF2-1DA is presented in Table 4.2-XI.

Similar microstructural characterization of the disk was conducted after forging and heat treatment. Three sections representing different disk section thicknesses, and consequently different cooling rates from the solution treatment temperature of 1120°C (2050°F), were chosen for characterization. The sections were the disk rim, web, and bore locations.

The microstructure as observed optically is shown in Figure 4.2-16. Little difference was seen among the three areas examined, and the same basic microstructural features were noted as in the as-consolidated billet. However, when observed using shadowed carbon replicas in the electron microscope, distinctive differences in gamma prime size and morphology were seen (Figures 4.2-17 through 4.2-19). At the rim, Figure 4.2-17, three distinct sizes of gamma prime particles are resolvable, as well as fine, globular carbides. Coarse, irregular patches of gamma prime are seen outlining grain boundaries, with smaller, blocky gamma prime and very fine aging gamma prime dispersed throughout the matrix. In the web and bore, however, much more of the coarse, irregular gamma prime was observed, with a coarser aging gamma prime and almost no intermediate sized blocky particles. These two areas also showed a rather uniform distribution of globular carbides.

A comparison of average gamma prime particle sizes between the as-consolidated billet and the three representative disk areas is summarized in Table 4.2-XII.

It is apparent that the cooling rate influences the size of the fine, aging gamma prime. The web of the disk, which contains the spacer projections, cools more slowly, and the fine precipitate occurring there is the coarsest (0.13 μm average diameter). The bore and rim although approximately the same thickness exhibit different cooling rates. The rim cools more rapidly because it is exposed on three sides, and, as a result, has a slightly finer aging gamma prime than does the bore (0.04 versus 0.06 μm).

Transmission electron micrographs were used to characterize the substructure of the disk rim, web, and bore after forging and heat treatment. A uniform dislocation density was noted for the three areas (Figures 4.2-20 through 4.2-22) with the greatest concentrations occurring at gamma/gamma prime interfaces. Some stacking faults were observed, Figures 4.2-20 and 4.2-21, as well as instances of clearly separated partial dislocations moving through large gamma prime particles (Figure 4.2-20). Evidence of sub-grain boundaries was observed in all areas. A sub-grain size of approximately 3.24 μm was measured. This is equivalent to 1.5 times the average size of the coarsest gamma prime particles, and suggests that the size and spacing of these precipitates affect grain or sub-grain size. The equivalent ASTM grain size is 13.5.

X-ray diffraction analysis of phases present in the disk after forging and heat treatment gave the same results as those for the as-consolidated billet, with one exception. In the bore location, a very weak X-ray diffraction line intensity for M_6C carbide was noted.

Phases which were present and their relative extracted percentages are summarized in Table 4.2-XIII. The effect of the heat treatment was to increase the total volume fraction of precipitated gamma prime from 43 percent in the as-consolidated condition to approximately 50 percent after full processing.

Very little change was noted in the line spacings of the carbide and boride phases after heat treatment. The MC phase showed a slight contraction of the lattice parameter relative to the as-consolidated billet. Likewise, little change was seen in the lattice parameter for the gamma prime.

To complete the microstructural characterization, optical and replica electron micrographs of the structure were made after sections of the disk had been exposed to temperatures of either 650 or 705°C (1200 or 1300°F) for 1500 hours. X-ray diffraction analyses were made to determine whether relative phase stability was effected by prolonged exposure at high operating service temperatures.

Neither the optical micrographs (Figure 4.2-23) nor the replica electron micrographs (Figures 4.2-24 and 4.2-25) revealed the presence of any acicular morphology precipitates which might occur with precipitation of topologically close-packed phases such as sigma. The electron micrographs of the structure of aged material taken from near the bore, show the low concentration intermediate-sized blocky gamma prime which occurred in unexposed disk material.

The X-ray diffraction results indicate the presence of similar minor phases (gamma prime, MC, $M_{23}C_6$, and M_3B_2) as in the fully processed disk forging. This confirms the phase stability, noted microscopically, for the exposure conditions studied. Slightly more carbide phase was extracted after the 705°C (1300°F) exposure than for the 650°C (1200°F) exposed material (3.7 versus 3.2 percent).

TABLE 4.2-VIII

DENSITY OF AS-CONSOLIDATED, TASK II BILLETS

Alloy	Density g/cm^3	Density lb/in^3
AF2-1DA	8.52, 8.29	0.3078, 0.2995
Mar-M-432	8.21, 8.22	0.2966, 0.2969

TABLE 4.2-IX

CHEMICAL ANALYSIS OF AS-CONSOLIDATED, TASK II BILLETS
(Percent by Weight)

Element	AF2-1DA	Mar-M-432
Cobalt	9.7	20.1
Titanium	2.9	4.5
Tantalum	1.5	2.0
Tungsten	5.5	3.4
Molybdenum	3.0	–
Columbium	–	2.1
Boron	0.13	0.016
Zirconium	0.11	0.06
Iron	0.07	0.10
Silicon	0.06	0.06
Manganese	0.001	0.001
Sulfur	<0.002	0.003
Phosphorous	0.0079	0.0017
Aluminum	4.5	3.0
Chromium	11.92	15.10
Nitrogen	0.001	0.005
Oxygen	0.004	0.007
Carbon	0.38	0.19
Hydrogen	0.0018	0.0004
Argon	0.0003	0.0002
Nickel	Balance	Balance

TABLE 4.2-X

DIMENSIONS OF TASK II FORGINGS

Disk	Diameter	Rim Thickness	Spacer Thickness
Mar-M-432	0.44m (17.25 in.)	0.051m (2.0 in.)	0.14 (5.38 in.)
AF2-1DA	0.45m (17.63 in.)	0.051m (2.0 in.)	0.13m (5.13 in.)

TABLE 4.2-V

PARTICLE SIZE DISTRIBUTION OF -60 MESH TASK II POWDERS

Screen Size		Percent Retained on Screen	
Mesh	Microns	AF2-1DA	Mar-M-432
60	250	0.03	0.00
80	177	8.08	1.97
120	125	19.72	8.16
170	88	16.96	10.36
230	63	13.67	11.35
325	44	16.11	18.73
400	37	10.42	19.18
<400	<37	15.01	30.25

TABLE 4.2-VI

CHEMICAL ANALYSIS OF TASK II AF2-1DA POWDER

Composition, weight percent

Carbon	0.37	Boron	0.014
Nitrogen	0.0012	Manganese	0.001
Oxygen	0.0060	Zirconium	0.08
Chromium	11.8	Iron	0.07
Cobalt	9.9	Silicon	0.06
Titanium	3.0	Sulfur	<0.002
Tantalum	1.5	Phosphorus	0.001
Tungsten	5.5	Hydrogen	0.0013
Molybdenum	3.1	Argon	0.00012
Aluminum	5.0	Nickel	Balance

TABLE 4.2-VII

CHEMICAL ANALYSIS OF TASK II MAR-M-432 POWDER

Carbon	0.18	Boron	0.015
Nitrogen	0.0040	Manganese	0.001
Oxygen	0.0090	Zirconium	0.07
Chromium	14.8	Iron	0.09
Cobalt	19.8	Silicon	0.06
Titanium	4.4	Sulfur	<0.002
Tantalum	2.0	Phosphorous	0.0043
Columbium	2.1	Hydrogen	0.0006
Tungsten	3.3	Argon	0.0001
Aluminum	2.9	Nickel	Balance

TABLE 4.2-XI

X-RAY DIFFRACTION PATTERN OF PHASES EXTRACTED FROM AS-CONSOLIDATED AF2-1DA BILLET

(In 10^{-10}m)

γ'	MC	$M_{23}C_6$	M_3B_2
			3.11 (3)
			2.574 (6)
	2.501 (100)		
		2.398 (7)	
	2.173 (78)		
			2.122 (5)
		2.062 (12)	
2.060 (100)*			
			1.991 (7)
		1.893 (3)	
		1.819 (3)	1.819 (3)
1.789 (40)			
	1.541 (43)		
	1.313 (29)		
1.267 (18)			
	1.258 (12)		
	1.089 (5)		
1.081 (13)			
1.035 (4)			
	0.999 (9)		
	0.975 (12)		

*Relative line intensities are shown in parenthesis, with separate scans having been made for gamma-prime and the carbide/boride phases.

TABLE 4.2-XII

AVERAGE GAMMA PRIME PARTICLE SIZES FOR AF2-1DA BILLET AND DISK

Specimen Location	Gamma Prime Type		
	Coarse, Irregular	Blocky	Fine, Aging
Billet	2.0 μm	0.53 μm	0.13 μm
Disk Rim	2.0	0.80	0.04
Disk Web	2.3	0.80	0.13
Disk Bore	2.9	0.80	0.06

TABLE 4.2-XIII

RESULTS OF X-RAY DIFFRACTION PHASE IDENTIFICATION ON FULLY PROCESSED AF2-1DA DISK

Area	Phases Present	Percent by Weight
Rim	Gamma-Prime	53.6
	MC, $M_{23}C_6$, M_3B_2	3.2*
Web	Gamma-Prime	49.9
	MC, $M_{23}C_6$, M_3B_2	3.0*
Bore	Gamma-Prime	49.7
	MC, $M_{23}C_6$, M_3B_2, M_6C	3.2*

*Sum of all carbide and boride phases

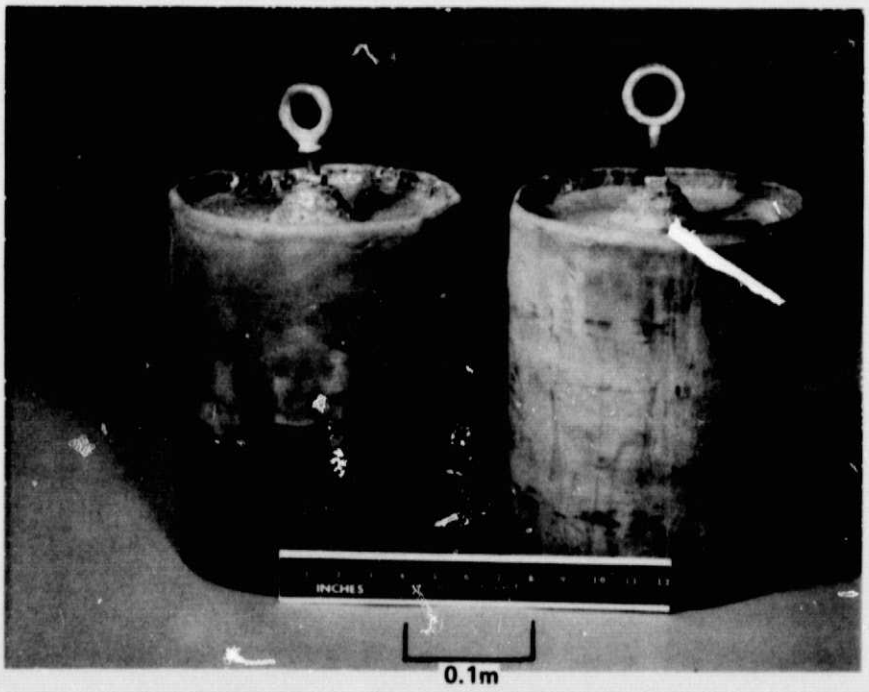

Figure 4.2-4 Appearance of Full-Scale Forging Billets After HIP Consolidation

MA917-2 250X

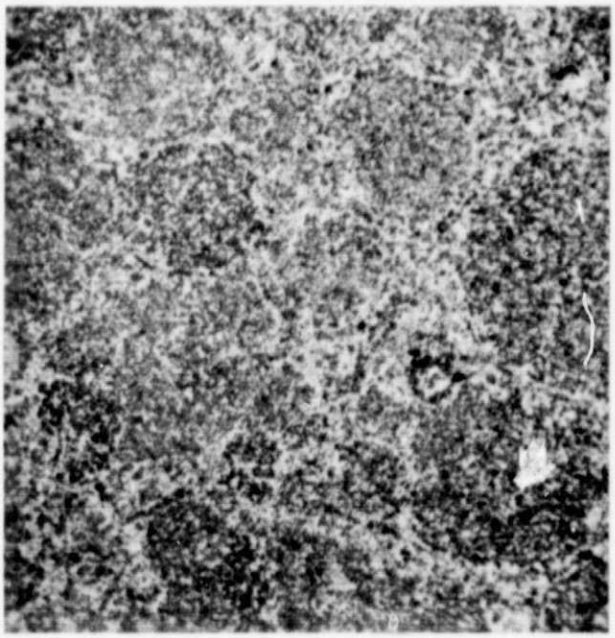

MA917-4 500X

Figure 4.2-5 As-Consolidated Microstructures of Mar-M-432 Billet
Etchant: Kalling's Reagent

MA917-1 250X

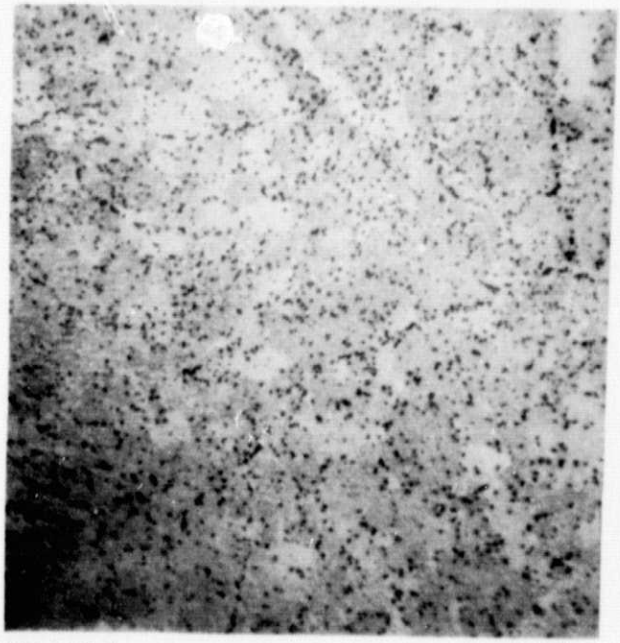

MA917-3 500X

Figure 4.2-6 As-Consolidated Microstructures of AF2-1DA Billet
Etchant: Kalling's Reagent

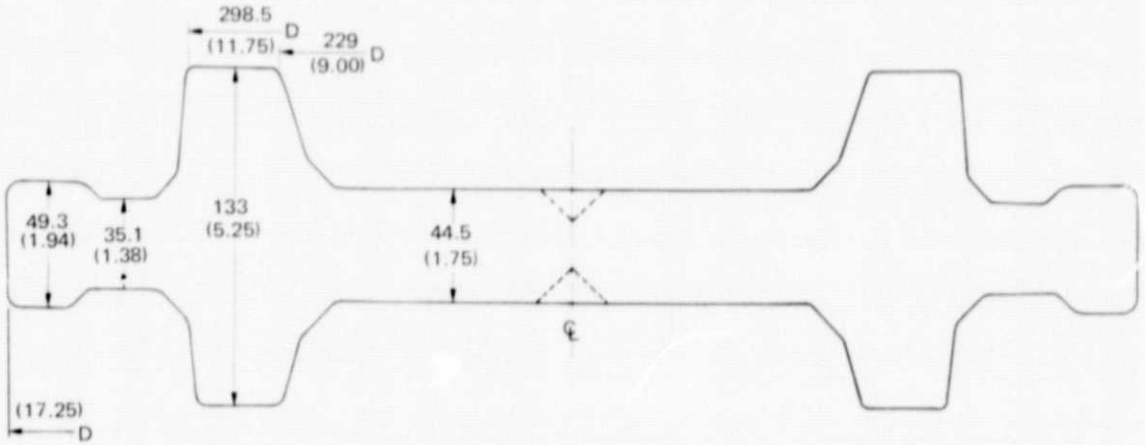

Figure 4.2-7 Cross Sectional Schematic of Full Scale Disks, Dimensions in m m (inches)

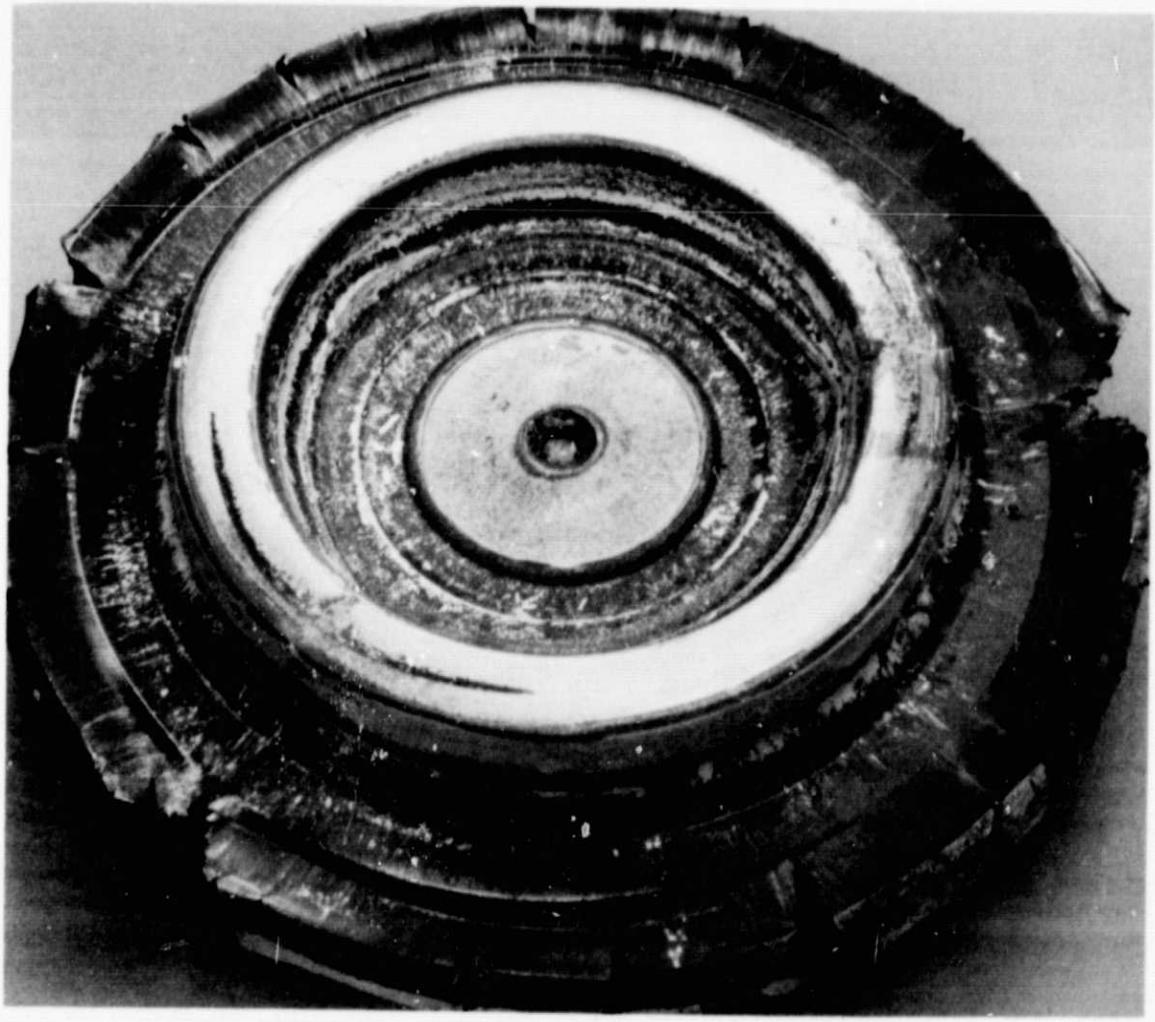

Figure 4.2-8 As-Forged Mar-M-432 Full Scale Forging

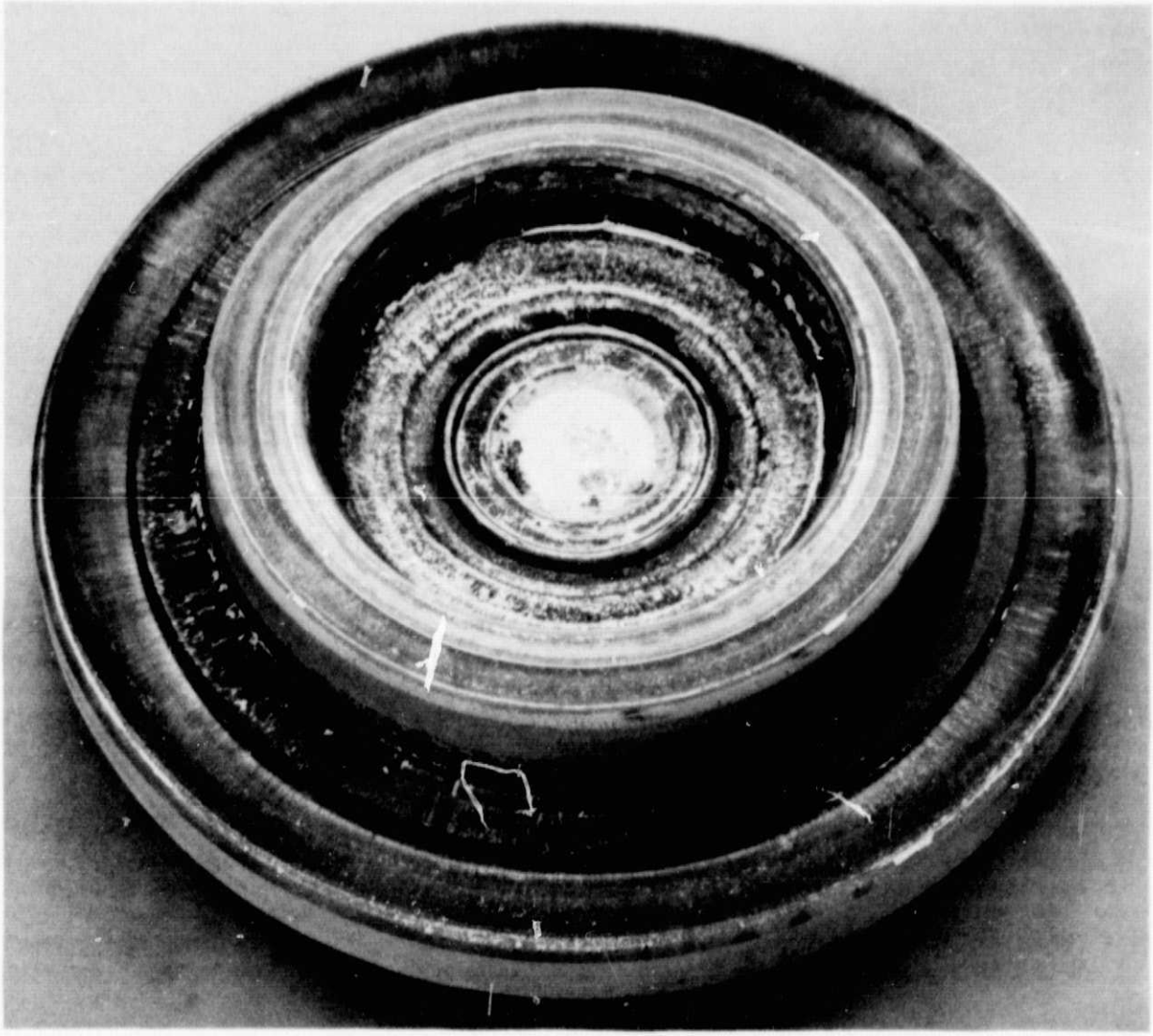

Figure 4.2-9 As-Forged AF2-1DA Full Scale Forging

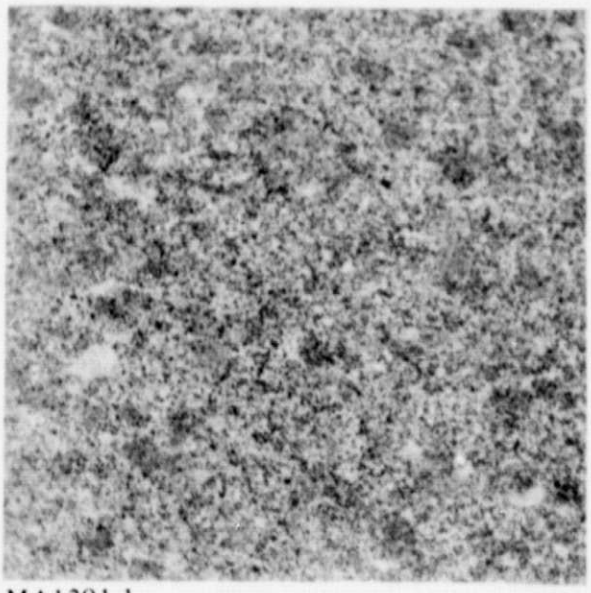

MA1391-1 100X

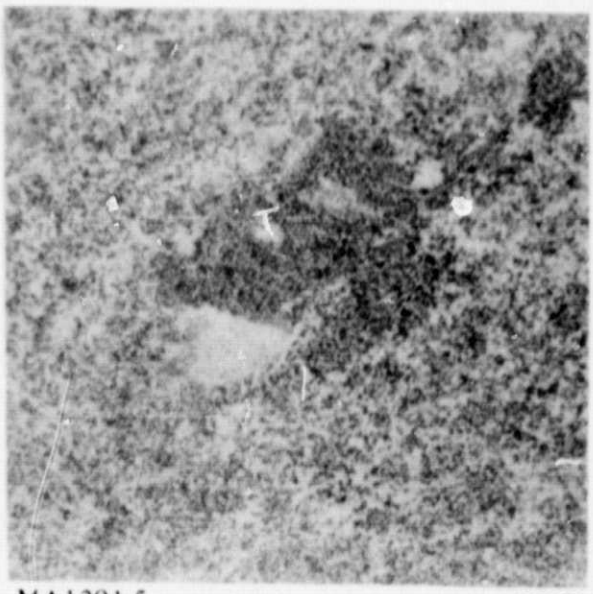

MA1391-5 250X

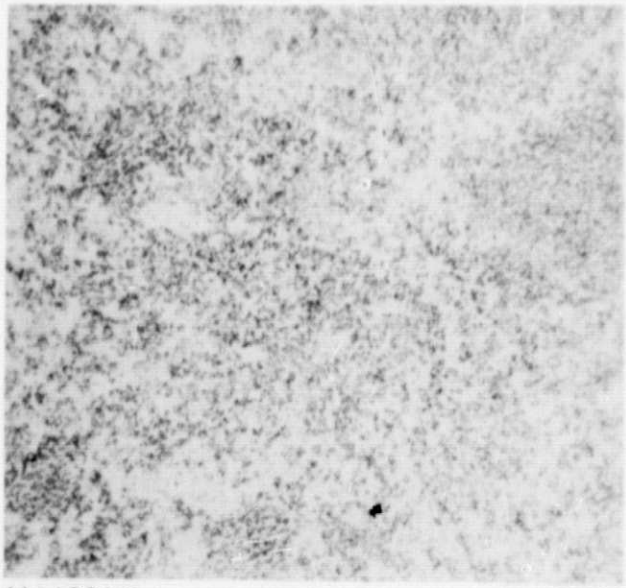

MA1391-6 500X

Figure 4.2-10 Microstructures of As-Forged AF2-1DA
Etchant: Kalling's Reagent

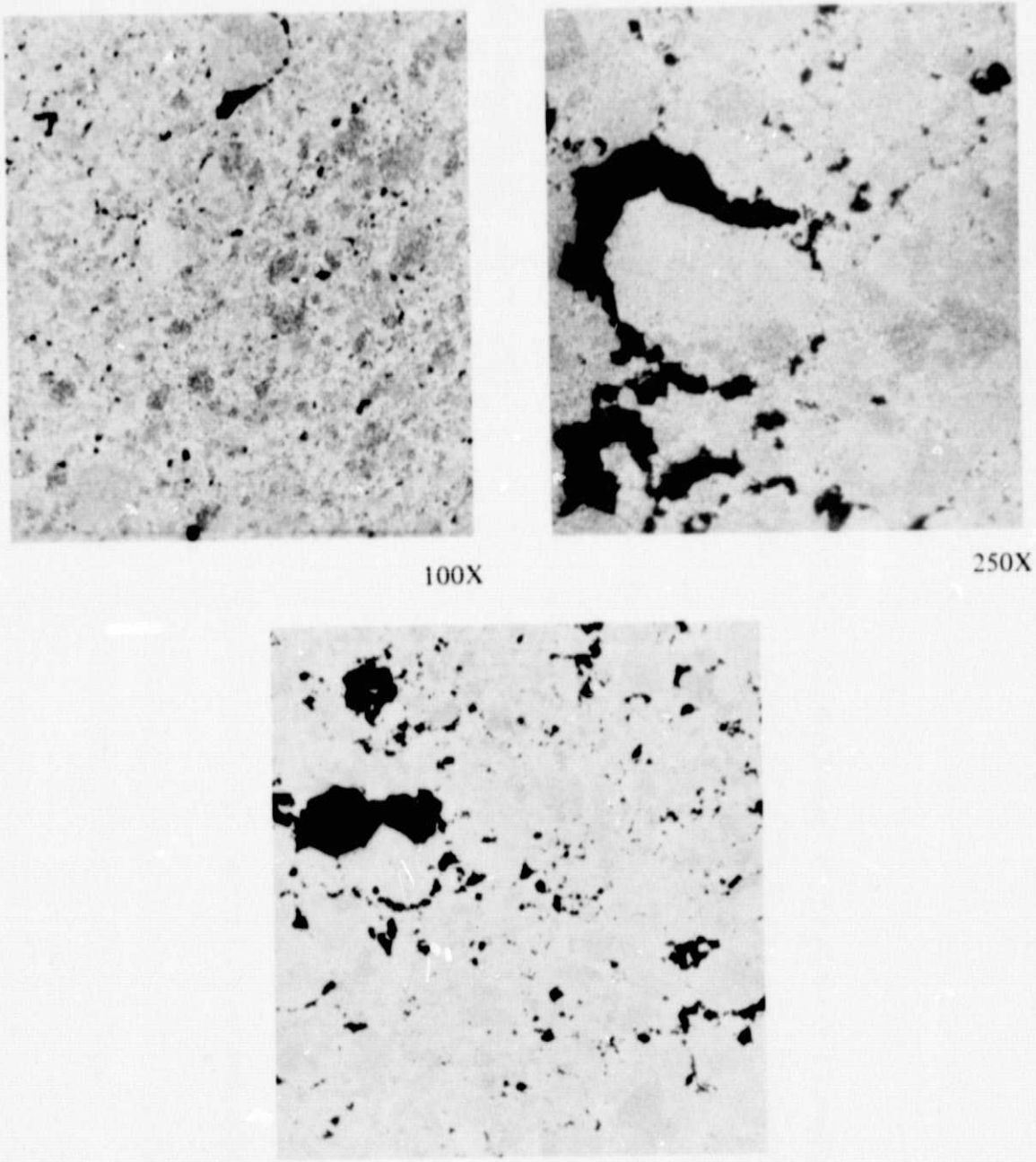

Figure 4.2-11 Microstructures of As-Forged MAR-M432 Showing Decohesion Along Powder Particle Boundaries.

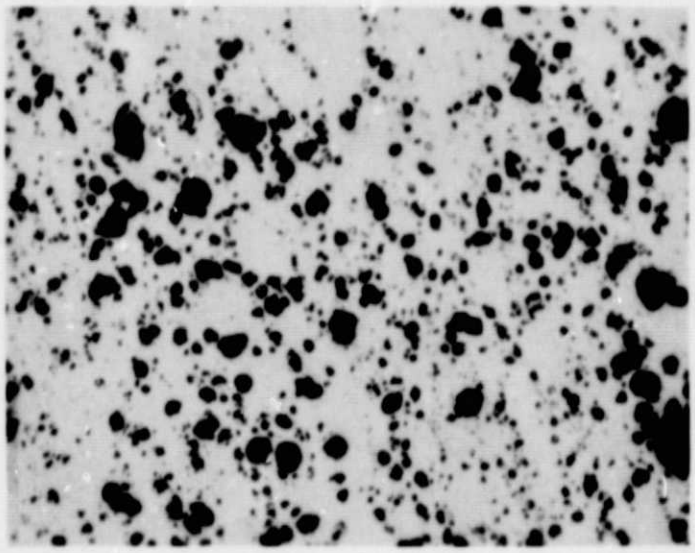

MA1702-2 MAR-M-432 100X

Figure 4.2-12 Microstructure of Fully Processed Mar-M-432 Forging. This figure shows extensive porosity which resulted from an undetected can leak during consolidation.

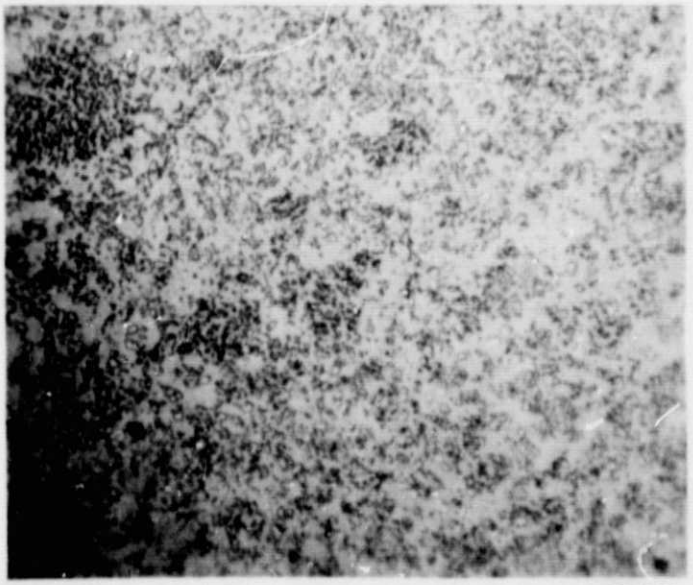

MA1702-1 AF2-1DA 500X
Etchant: 50% HCl in Methanol

Figure 4.2-13 Microstructure of Fully Processed AF2-1DA Disk Forging
Etchant: 50 Percent HCl in Methanol

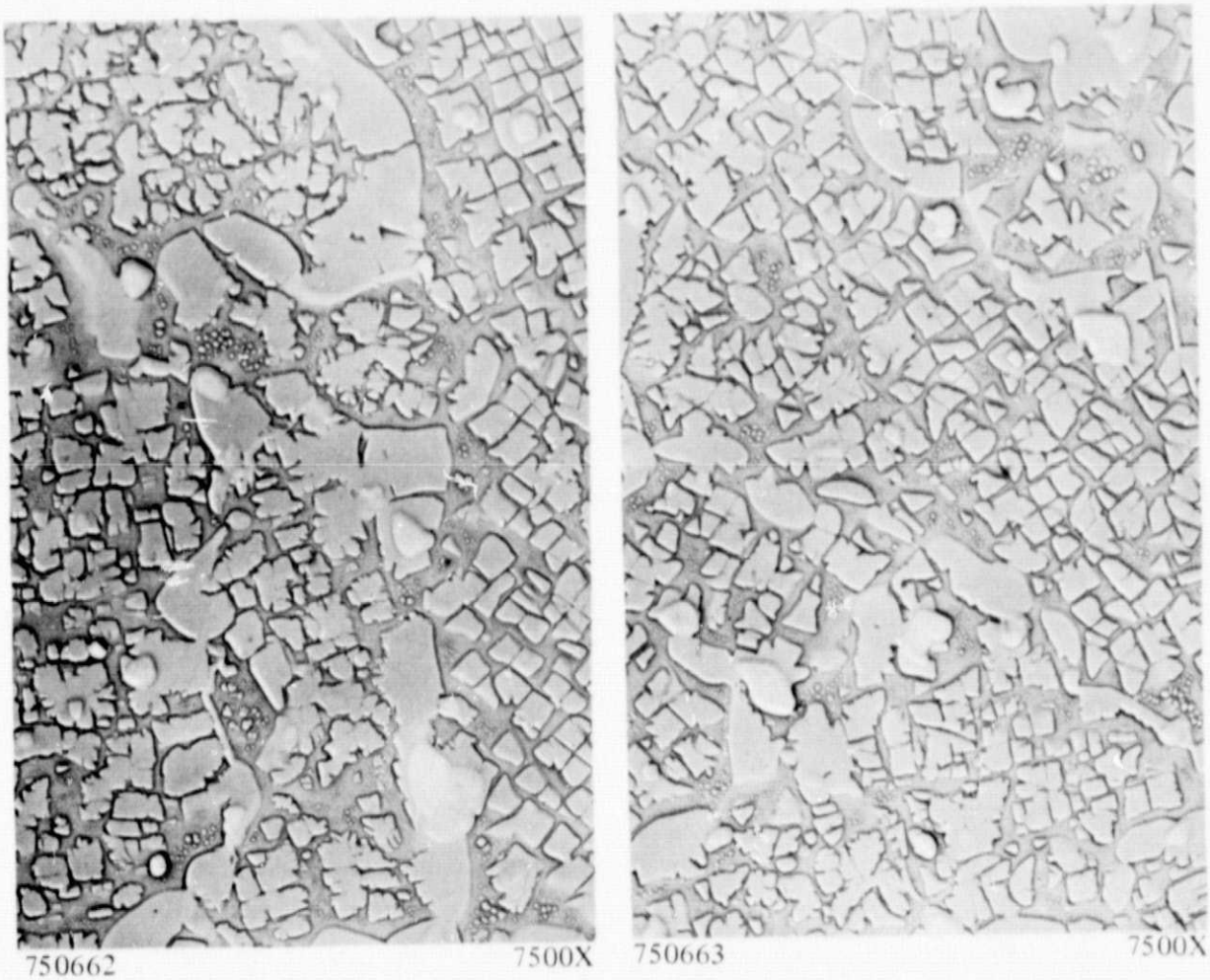

Figure 4.2-14 Microstructures of As-Consolidated AF2-1DA Billet. This figure shows examples of three sizes of gamma prime particles, plus carbides associated with the largest gamma prime.

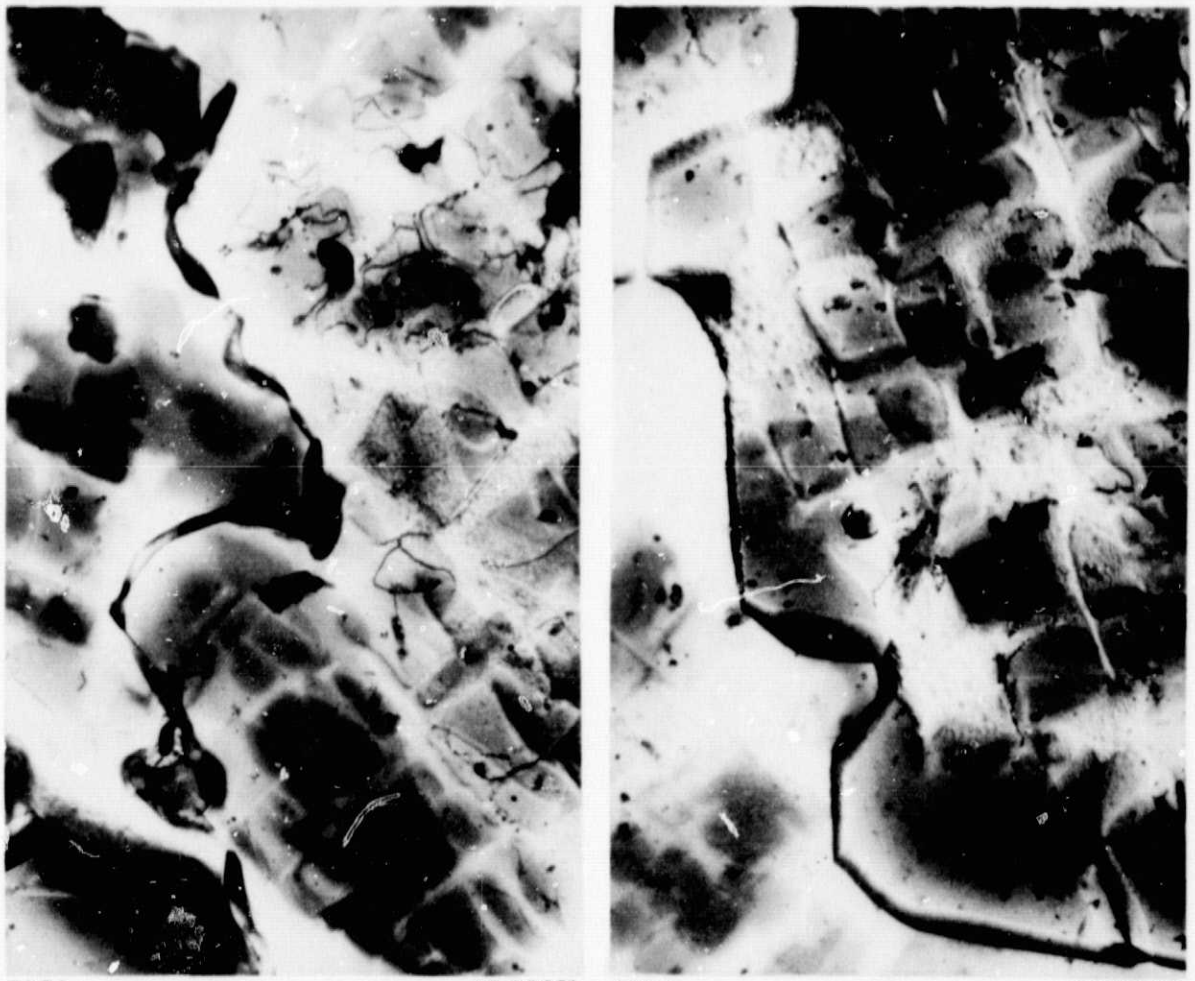

5072 17,800X 5073 17,800X

Figure 4.2-15 Transmission Electron Micrographs of As-Consolidated AF2-1DA. This figure shows examples of generally cuboidal gamma prime with low dislocation density.

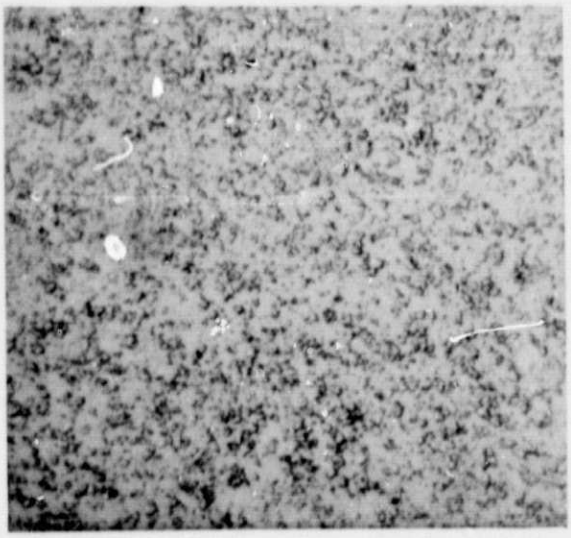

MB577-6 WEB 500X

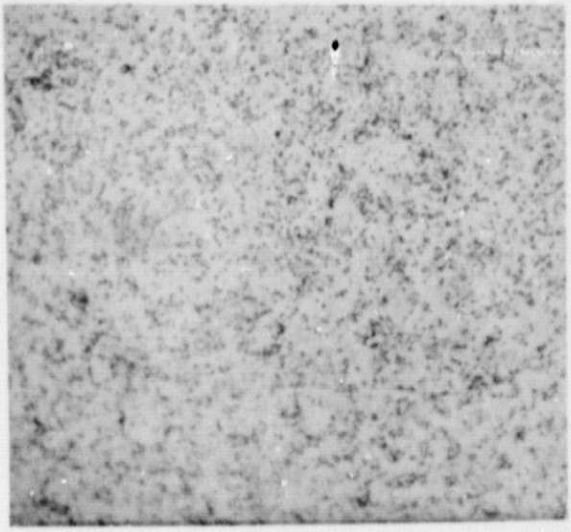

MB577-9 BORE 500X

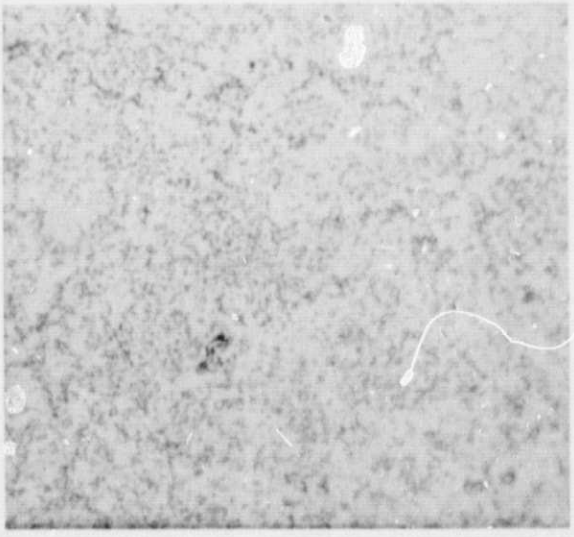

MB577-10 RIM 500X

4.2-16 Microstructures of Fully Processed AF2-1DA Disk Forged at 1135°C (2075°F) and Heat Treated at 1120°C (2075°F), Two Hours, Oil Quench, 760°C (1400°F), Sixteen Hours, Air Cool

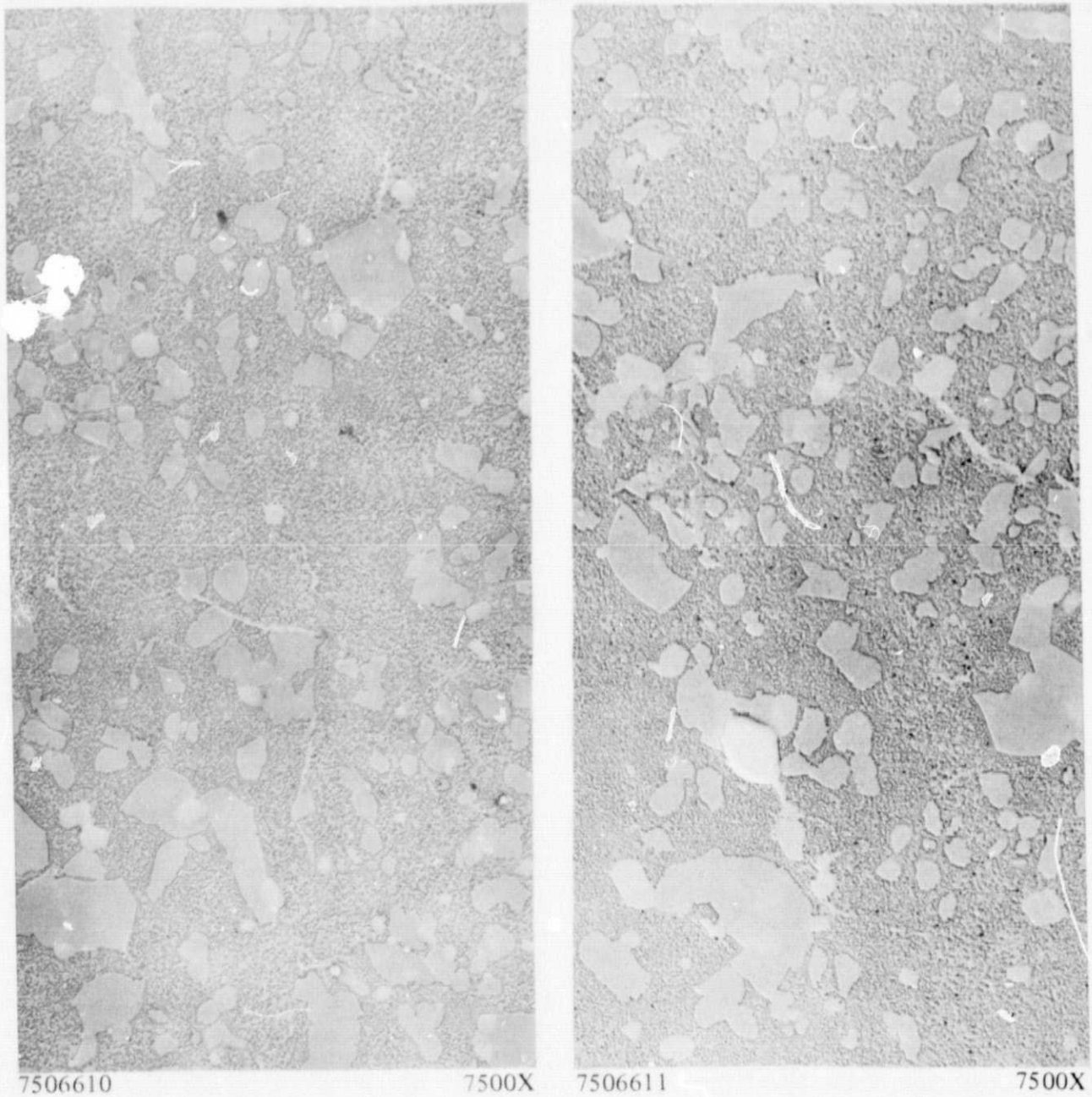

7506610 7500X 7506611 7500X

Figure 4.2-17 Replica Electron Micrographs of Fully Processed AF2-1DA Disk. This figure shows examples of typical microstructures at the disk rim.

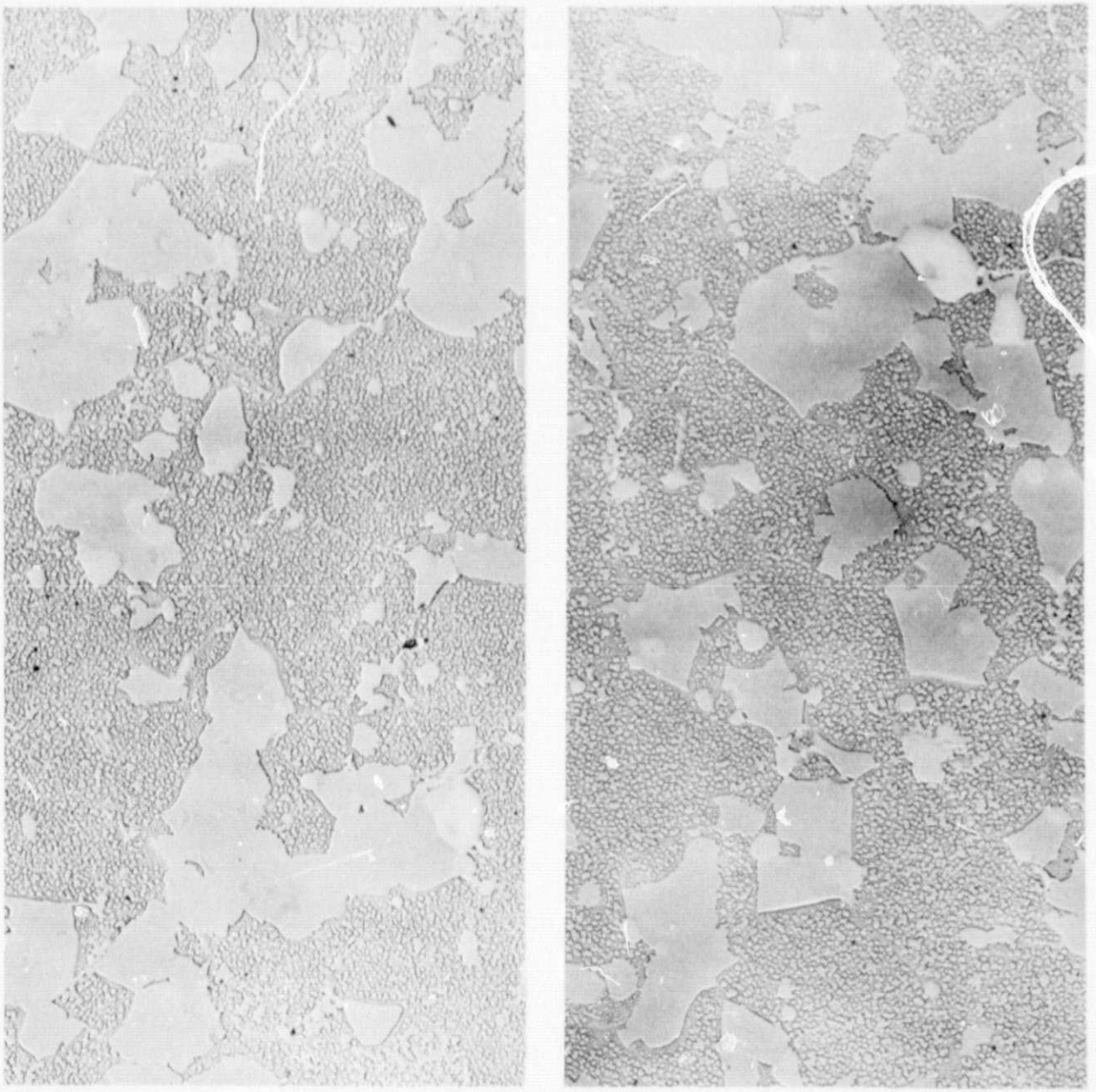

750667 7500X 750669 7500X

Figure 4.2-18 Replica Electron Micrographs of Fully Processed AF2-1DA Disk. This figure shows examples of typical microstructures in the disk web.

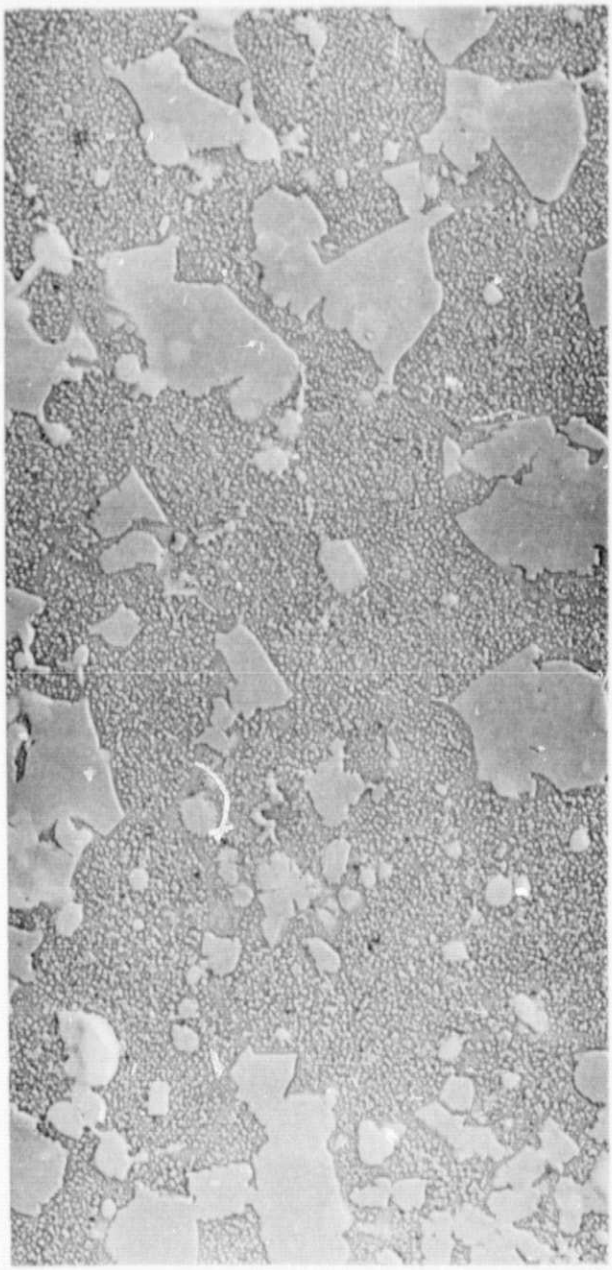

7506614 7500X

7506616 7500X

Figure 4.2-19 Replica Electron Micrographs of Fully Processed AF2-1DA Disk. This figure shows examples of typical microstructures at the disk bore.

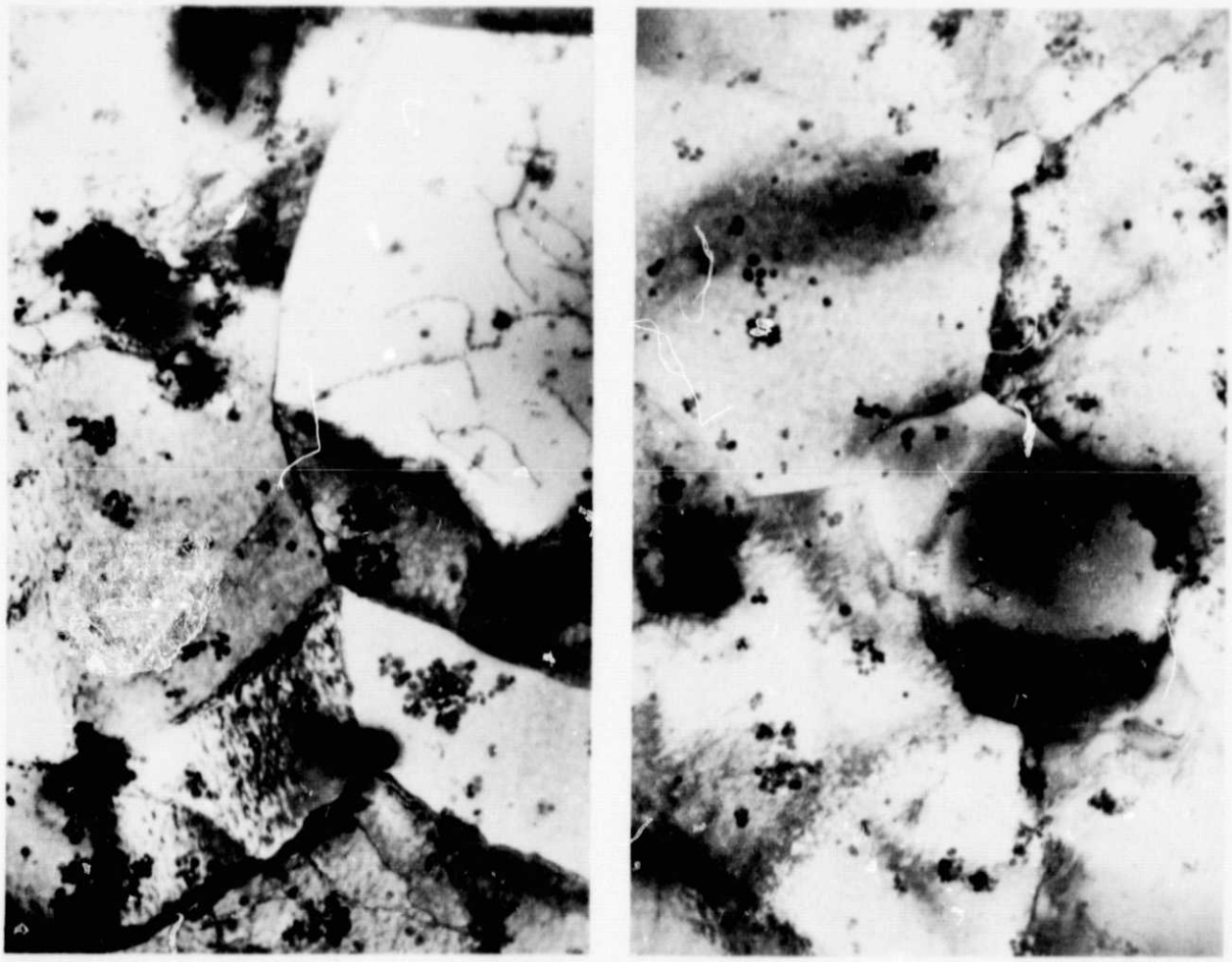

5137 17,800X 5141 17,800X

Figure 4.2-20 Transmission Electron Micrographs of Fully Processed AF2-1DA Disk. This figure shows examples of typical microstructures at the disk rim. Small clusters of particles are artifacts formed by aging gamma prime which re-deposited on the foil.

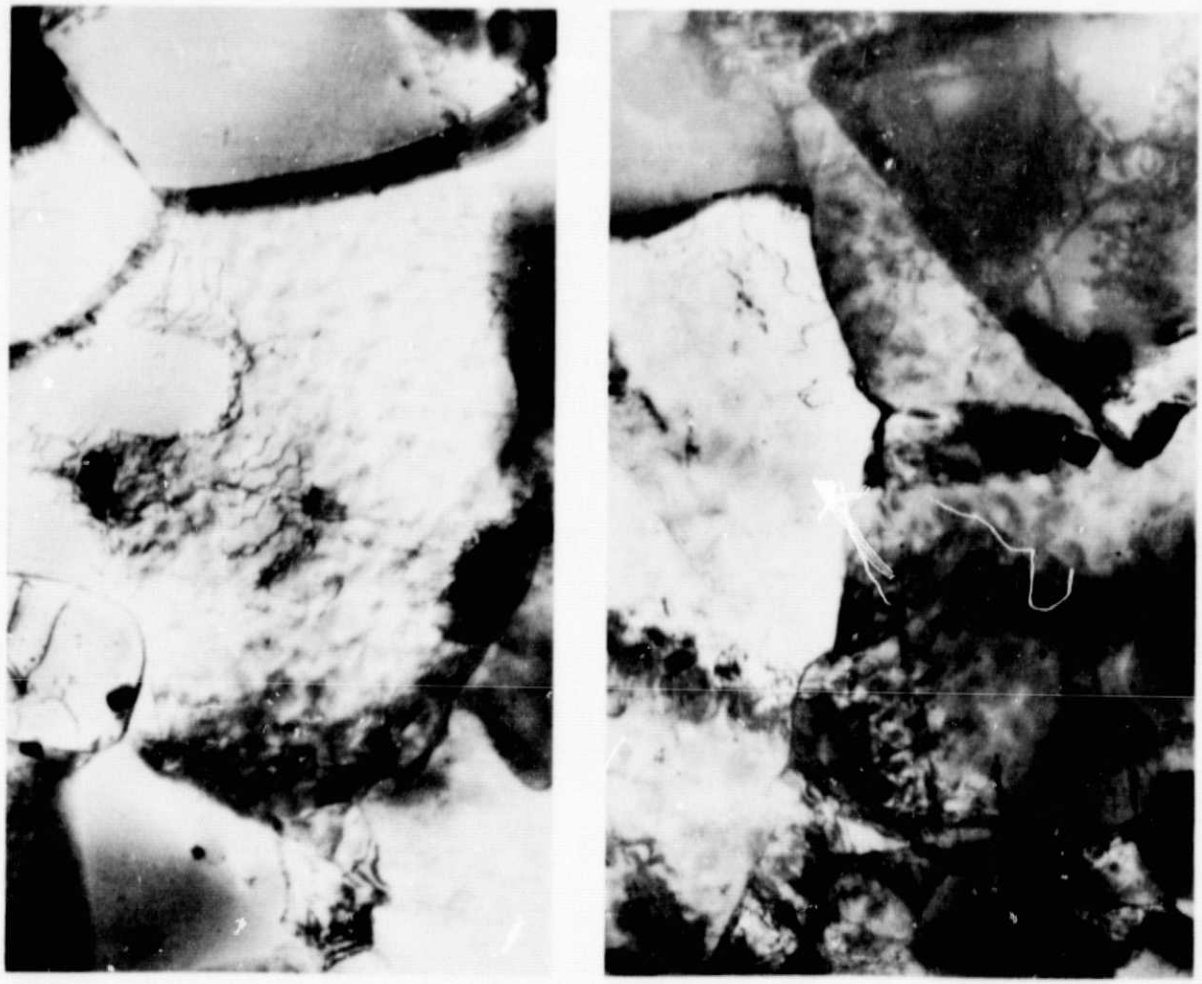

5143 17,800X 5145 17,800X

Figure 4.2-21 Transmission Electron Micrographs of Fully Processed AF2-1DA Disk. This figure shows examples of typical microstructures in the disk web.

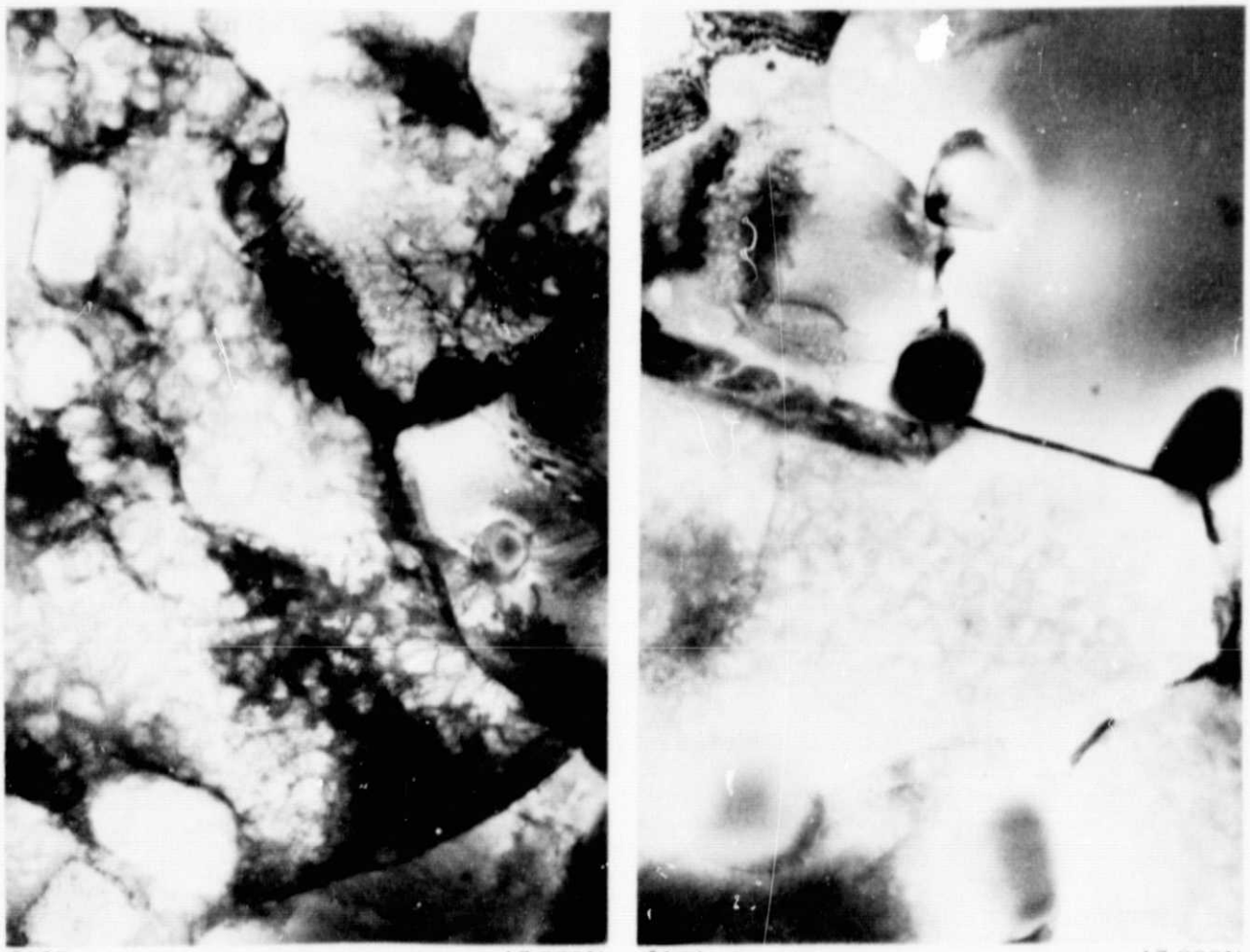

5159 17,800X 5164 17,800X

Figure 4.2-22 Transmission Electron Micrographs of Fully Processed AF2-1DA Disk. This figure shows examples of typical microstructures in the disk bore. Evidence of dislocation build-up at gamma/gamma prime interfaces is seen in micrograph 5159.

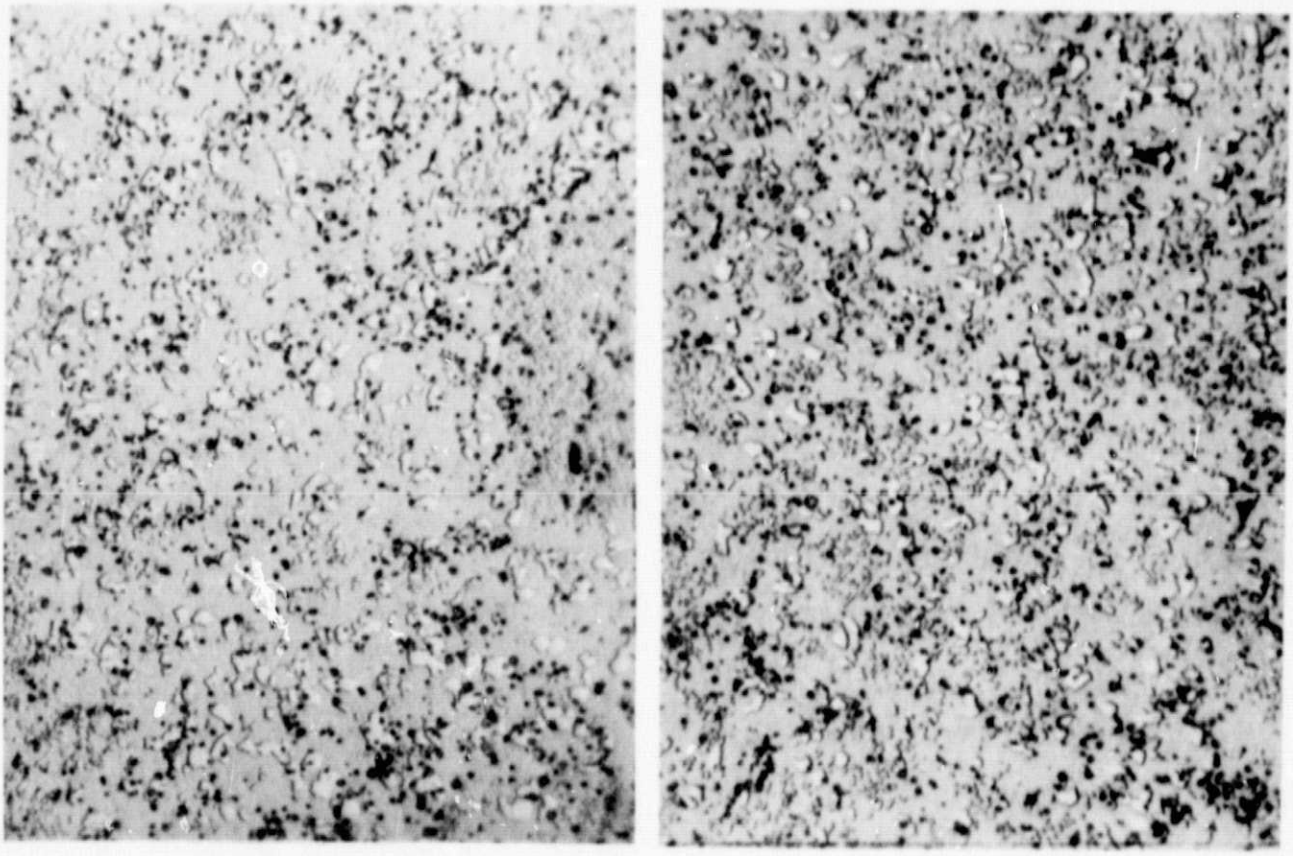

Figure 4.2-23 Optical Microstructures of AF2-1DA Disk Forging After Full Heat Treat Plus 1500 Hour Static Exposure at the Temperatures Indicated

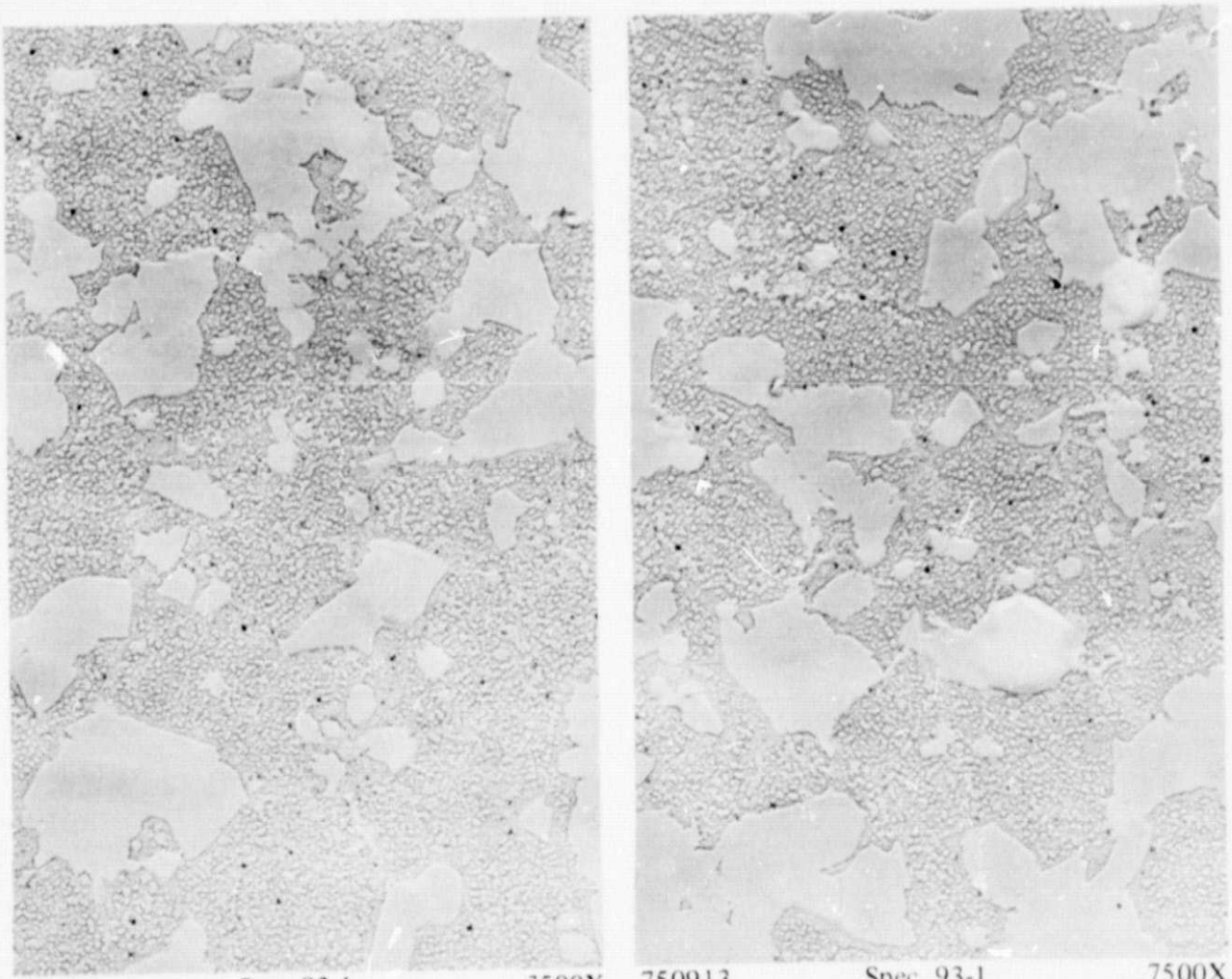

Figure 4.2-24 Replica Electron Micrographs of AF2-1DA Disk Forging After Full Heat Treat Plus Static Exposure at 650°C (1200°F) for 1500 Hours

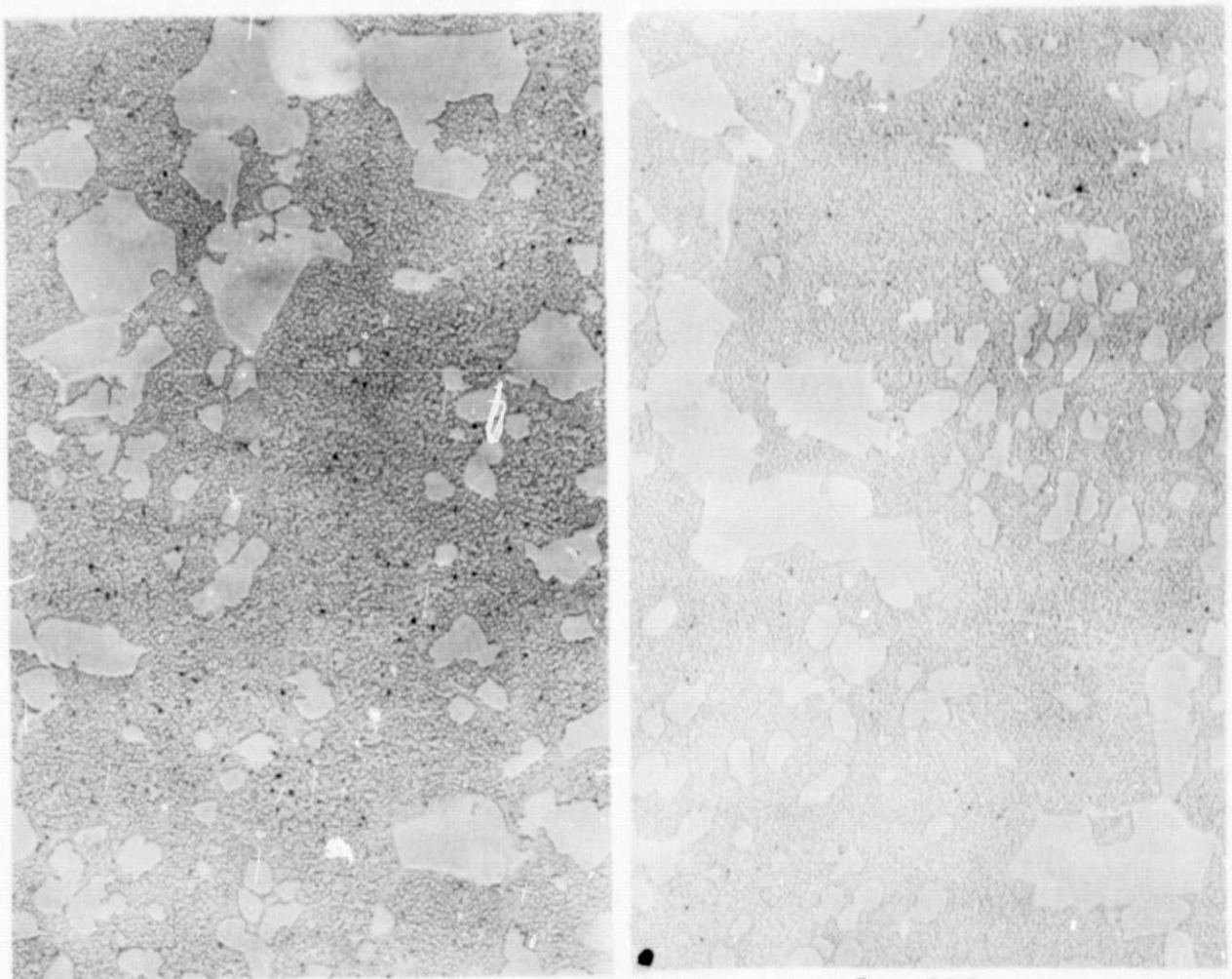

Figure 4.2-25 Replica Electron Micrographs of AF2-1DA Disk Forging After Full Heat Treat Plus Static Exposure at 705°C (1300°F) for 1500 Hours

4.3 TEST RESULTS

Mechanical properties of the full-scale AF2-1DA disk forging were evaluated relative to criteria of importance in design of a disk for an advanced, transport-type gas turbine engine.

The properties evaluated were tensile strength (smooth and notched), creep and stress rupture, low cycle fatigue, and low cycle fatigue crack propagation rate. Test specimens were machined from the fully processed disk, and from sections of the disk after a 1500 hour exposure at 650°C or 705°C (1200°F or 1300°F) temperature.

Location of mechanical test specimens within the disk is shown schematically in Figures 4.3-26 and 4.3-27. Specimen configurations used for mechanical property evaluations are shown in Figures 4.3-28 and 4.3-29.

4.3.1 Tensile, Creep, and Creep-Rupture Tests

Tensile testing was performed on the AF2-1DA disk in the fully processed condition and after 1500 hour exposure at 650 or 705°C (1200 or 1300°F). Smooth bar tests were conducted at room temperature and at 540, 650, and 760°C (1000, 1200, and 1400°F). Notched tensile specimens (K_T = 3.8) were tested at 650 and 760°C (1200 and 1400°F) for fully processed disk material and on material exposed at 650°C (1200°F) for 1500 hours. Results of Task II tensile tests are summarized in Table 4.3-XIV, and comparison is made with the Task I sub-scale disks forged at 0.1 $min.^{-1}$ strain rate.

Comparison of the full scale Task II forging strengths with the sub-scale Task I disk properties indicated improvements in both strength and ductility. Strength improvements were judged to be a result of the partial solution treatment and oil quench given the Task II disk. This treatment should result in more uniform nucleation of gamma prime, with a greater amount of gamma prime available for strengthening during precipitation aging. Metallographic examination of failed tensile specimens indicated an intergranular crack path occurred at both room temperature and 760°C (1400°F). (See Figure 4.3-30).

Creep and creep-rupture testing was conducted under a variety of temperature stress conditions. Specimens machined from the AF2-1DA full scale Task II forging were tested under these conditions:

- 650°C/759 MN/m^2 (1200°F/110 ksi) to rupture
- two temperature/stress conditions selected to produce rupture in a maximum of 300 hours
- nine temperature/stress conditions chosen to achieve 0.5 percent creep elongation within 100-300 hours.

Results of Task II creep and creep-rupture tests are summarized in Table 4.3-XV.

Comparison of 0.1 percent creep and rupture lives with those of Astroloy, a currently-used high temperature turbine disk alloy, is made parametrically in Figures 4.3-31 and 4.3-32.

Results of these tests indicate an improvement in creep life for the AF2-1DA, when compared with Astroloy.

Metallographic examination of failed creep-rupture specimens indicated that, similarly to the tensile specimens, rupture occurred intergranularly. Typical microstructures showing the intergranular crack mode are seen in Figure 4.3-33.

4.3.2 Low Cycle Fatigue and Fatigue Crack Growth Tests

To evaluate the potential capability of the AF2-1DA disk to operate successfully in a high cyclic stress regime, both smooth and notched (K_T = 2.0) axial, Sonntag-type fatigue specimens were machined from the Task II AF2-1DA disk forging. The smooth specimens were cycled to determine failure life only and initiation times to 0.8 mm (1/32-inch) crack plus failure lives were determined for notched specimens. Cyclic rate for all tests was 1800 cycles per minute. Testing was done at 480, 635, and 760°C (900, 1175, and 1400°F) at a steady stress of 275 MN/m^2 (40 ksi) and cyclic stresses of 480 or 620 MN/m^2 (70 or 90 ksi) for K_T = 1.0 specimens and 310 or 415 MN/m^2 (45 or 60 ksi) for notched specimens.

Results of the low cycle fatigue tests, presented in Table 4.3-XVI, indicate a propensity for the smooth specimens to fail in the threaded grip. This phenomenon appears related to the tendency for some of the creep specimens to rupture in the threaded regions of the specimens. The processing conditions for the Task II disk apparently had resulted in a notch-brittle condition. This tendency for notch embrittlement was not evaluated in other mechanical property tests such as stress-rupture.

The low cycle fatigue, crack growth rate of the AF2-1DA Task II forging was measured using center-notched panel specimens cycled at ten cycles per minute. Testing was done at an R ratio (minimum stress/maximum stress) of 0. An elliptical center notch was cut through the 1.8 mm (0.070-inch) thick panel specimen, and a starter crack was produced using 30 Hz, room temperature, low stress cycling. This served to remove the starting crack from the region influenced by the electrical-discharge machined notch. Stress cycling was then conducted, with periodic measurements of the crack length using optical telemetry. From a plot of crack length, a, versus number of cycles, N, the rate of crack growth da/dN was calculated. This rate was then plotted versus the change in stress intensity factor, ΔK, which was calculated using the stress range $\Delta \sigma$ and crack length.

Duplicate testing was conducted at room temperature, and at 425°C and 620°C (800°F and 1150°F). Testing was continued until the crack grew to such an extent that the specimen failed by tensile overload. Examination indicated that several specimens exhibited shear lip formation near the region of rapid tensile fracture. Such a fracture mode indicates a change from a state of plane strain to plane stress, and only data generated under plane strain conditions were used in the analysis.

One half of each tested specimen was examined microscopically after test using scanning electron microscopy. Low magnification photographs were used to document the general fracture appearance, while higher magnifications were used to obtain a more thorough characterization of the fracture mode.

The specimen tested at room temperature exhibited generally a smooth fracture surface and shear lip formation on one side of the fracture occurred early during testing (Figure 4.3-34) at a ΔK of 22 $MN/m^2\sqrt{m}$ (20 $ksi\sqrt{in.}$). The fracture appeared transgranular, primarily Stage II cracking (propagation perpendicular to the stress axis), with frequent short secondary cracks.

At 425°C (800°F), the crack propagation mode was nearly identical to that observed at room temperature. Fatigue striations and small secondary cracks were noted in this specimen also (Figure 4.3-35). At 620°C (1150°F), however, the crack propagation mode changed from transgranular (Stage II) to intergranular (Figure 4.3-36). Some evidence of intergranular secondary cracking was noted, but few fatigue striations were observed despite the fact that the crack growth rate was nearly six times faster than for the specimens tested at 425°C (800°F) (Figure 4.3-37).

Small particles, approximately 0.2μm diameter, presumably carbides, were apparent on the intergranular fracture surfaces of the specimen tested at 620°C (1150°F).